Tehnički institut / Technical Institute of Bijeljina

ZBORNIK RADOVA / BULLETIN OF
Godina / Year XV – No. 29.

DOI: 10.59456 ESCI If 0,1 ISSN 1840-4855
e-ISSN 2233-0046

A R H I V

ZA TEHNIČKE NAUKE

Archives for Technical Sciences

B i j e l j i n a 2023

Tehnički institut / Technical Institute of Bijeljina

ZBORNIK RADOVA / BULLETIN OF
Godina / Year XV – No. 29.

DOI: 10.59456 ESCI If 0,1 ISSN 1840-4855
e-ISSN 2233-0046

Founder and publisher:

Technical Institute of Bijeljina
Republic of Srpska - Bosnia and Herzegovina

Editor in Chief:

Academician Prof. Ph.D. Neđo Đurić
Academy of Sciences and Arts of the Republic of Srpska,
Bosnia and Herzegovina

Technical Editor:

Dr. sci. Dijana Đurić

Lector for English

School of Foreign Languages "Cerovac" Bijeljina

Address:

Technical Institute Bijeljina, Starine Novaka Street 25
76 300 Bijeljina
Republic of Srpska - Bosnia and Herzegovina
Tel./fax +387 (55) 203 – 022, 211 – 701
Mob: +38765511772
E. mail: tehnicki@tehnicki-institut.com
arhiv@arhivzatehnickenauke.com
nedjo@arhivzatehnickenauke.com
www.arhivzatehnickenauke.com

Press:

Mojić d.o.o. Bijeljina

Circulation:

300 copies

Tehnički institut / Technical Institute of Bijeljina

ZBORNIK RADOVA / BULLETIN OF
Godina / Year XV – No. 29.

DOI: 10.59456 ESCI If 0,1 ISSN 1840-4855
e-ISSN 2233-0046

Tehnički institut / Technical Institute of Bijeljina

ZBORNIK RADOVA / BULLETIN OF
Godina / Year XV – No. 29.

DOI: 10.59456 ESCI If 0,1 ISSN 1840-4855
e-ISSN 2233-0046

TABLE OF CONTENTS

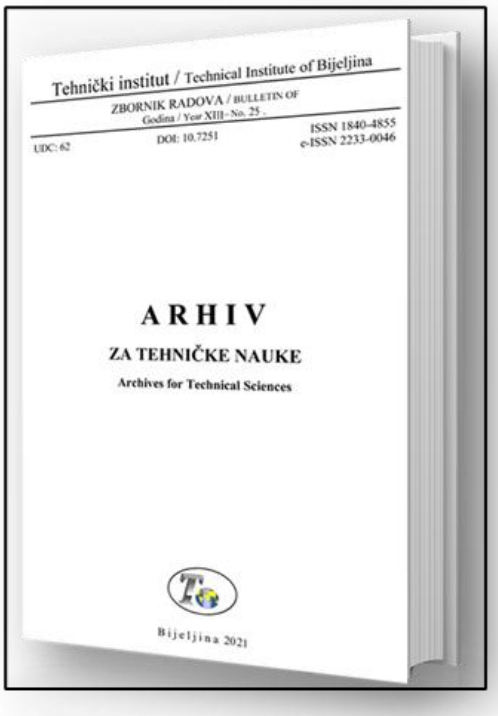

AGRICULTURE

ENVIRONMENT

GEOTECHNICS

Research of marly rocks

Editors

Prof. Ph.D. Dragan Lukić
Prof. Ph.D. Petar Santrač

Review work
http://dx.doi.org/10.59456/afts.2023.1529.001Dj

RESEARCH OF MARLY ROCKS ON THE TERRAIN FORECASTED FOR CONSTRUCTION OF SILOS OBJECTS

Đurić Neđo[1], Đurić Marko[1]

[1]*Technical institute Bijeljina, Bijeljina, Republic of Srpska, Bosnia and Herzegovina,*
e. mail, nedjo@tehnicki-institut.com

ABSTRACT

Complexity of geological terrain built demands different level of research in order to obtain all necessary characteristics for the establishing of connections between the structure of the objects and the terrain. Frequent changes of rocks in vertical profile and their irregular settling related to creasing of the terrain during geological history makes choosing representative parameters harder. Layers of similar characteristics that are interconnected are separated into geological environments by taking medium values of the parameters within that environment.

During the research, for the purpose of constructing of the silos objects, boreholes were drilled in the axis of each silos to a depth of 10.0 m. In a small area, there is a complex structure of the terrain, which, in addition to changes in the lithological composition, is also dictated by tectonic activity. Directly in the hinterland of the research conducted with boreholes, there is an open terrain profile with a height of about 6.0 m. By connecting the layers from the investigation works and the open profile on the terrain, a clearer picture of their position on the narrow part of the terrain was obtained.

Frequent changes of layers of marly rocks and sandstones and their synclinal deposition demanded separation of certain geological environments with layers of the same characteristics. In addition to taking samples for laboratory tests, field tests of the solubility of marly rocks in the void at different temperatures were also conducted. In parallel with the samples from the investigation works, samples from the open terrain profile were examined. The results showed a shorter dissolution time of marly rocks from the open terrain profile compared to the same rocks taken from the core of the borehole.

Key words: *geotechnical environment, rock solubility, physical and mechanical characteristics of rocks*

INTRODUCTION

Terrain research in marl rocks requires a more detailed approach, given that they often alternate with sandstones, which have more favorable geomechanical characteristics. They behave differently in the presence of water and temperature changes. Depending on the type of facilities being built, it is necessary to adjust the type of research and laboratory tests.

The terrain on which the construction of silos type objects is planned is a steep slope that has been eroded over time. A large plateau was created on which smaller facilities have already been built. Terrain investigation works from the plateau are 6.0 m from the natural elevation of the terrain. Observed wider, terrain in the vertical sense is characterized by a folded shape with a synclinal dip of layers around 45^0. Marl rocks of different characteristics alternate with sandstones whose characteristics are also in a wider range.

The slope of the layers, low mightiness, variable characteristics and everything on a small area requires a specific way of connecting the construction of the objects with the construction of the terrain. The degree of cracking of the rocks reduces their characteristics, so that the separated geological environments represent a smaller complex of rocks with similar characteristics. The assessment of the characteristics of each geological environment is given through the RockLab system, where the parameter values are reduced to the natural estimated state. They are significantly lower compared to the results obtained by laboratory tests, but more realistic than the terrain conditions.

TERRAIN CHARACTERISTICS

The complexity of the terrain's morphological characteristics does not represent favorable locations for the construction of objects. That is why the terrain research is very low. The only data is related to the Basic Geological Map 1 : 100 000 and the interpreter accompanying it. Modest data, but still sufficient for an initial familiarization with the terrain, characteristics of object for construction directed research on that part of the terrain.

Earlier researchers for the basic geological map and its interpreter selected sediments that belong to the upper Eocene (E3). They analyzed them in more detail as bank quartz sandstones, conglomerates, friable gray, greenish, sometimes ferruginous sandstones, clays, clayey marls and very rarely clays [1]. Rhythmic sedimentation is also observed, with a pronounced presence of sandstone, and to a lesser extent conglomerate and fine-grained sediments of clays and clayey marls. The slope of the layers is about 25^0.

The characteristics of the lithostratigraphic assemblage classify the terrain and the immediate surroundings as conditionally favorable to favorable terrain. From a geotechnical point of view, terrains with a permissible load > 300 kN/m2 belong to terrains of favorable stability, if other factors such as the disintegration or cracking of rocks, the inclination of the slope and layers are favorable. [2,3,4,5].

Directly at the location of the future objects, the terrain in the vertical profile is characterized by layers of variable characteristics due to the presence of soft marly rocks. [6]. The steep slopes of the layers make it difficult to build foundations in the same layer, which is why it was necessary to separate geological environments with the same or similar characteristics. Marly rocks are present in two levels as the first and second marly layers. They are more easily separated on the terrain in a vertical profile, than in the laboratory during more detailed tests.

METHODOLOGY

For a more detailed study of the terrain, a research methodology was chosen that supplemented the existing knowledge and studied the location itself in detail. The elements of those methodology are:

- Conducting terrain research that will complement the data of the Basic Geological Map,
- Definition of lithological members and their placement by investigative works along the axis of future objects to the depth of the influence of their load,
- Define their behavior in the state when they are extracted from the parent rock [7,8],
- Examination of the solubility of marl rocks in water at a daytime temperature of 36^0C and 19^0C at night temperature [3,6,9,10,11],
- Determination of time of complete solubility of marly rocks in water, evaluation of the state of dissolved material, and consolidation of dissolved particles in water after their mixing and
- With laboratory tests include standard methods for this type of rock in conditions of 18 – 20^0C, which are
    - rock solubility time,
    - volumetric weight,

- uniaxial compressive strength,
- rock strength index and
- dynamic parameters of strength as well as speed of propagation of UV waves.

During the examination, it is necessary to define whether the quasi-homogeneous sediments of the marly layer of the second and third geological environments can be considered as one layer.

RESULTS

Data from the Basic Geological Map and the open profile of the cut located in the hinterland of the plateau provided initial information about the terrain. The arrangement of the exploration boreholes was dictated by the linear arrangement of the three silos. For each silos, one borehole was drilled in its axis, figure 1. The depth of the borehole was determined by the size of the load on the silos, leaving room for it to be changed during drilling depending on the complexity of the geological structure.

During the drilling process, attention was focused on the quality of the core in order to see the natural state of the massif as realistically as possible. Detailed mapping of the core of the inflated material was carried out and samples were taken from the characteristic layers. Along with monitoring of the presence of underground water in the borehole, the behavior of marls was monitored from the time of the extraction from the rock massif to the time of their decomposition on the surface of the terrain.

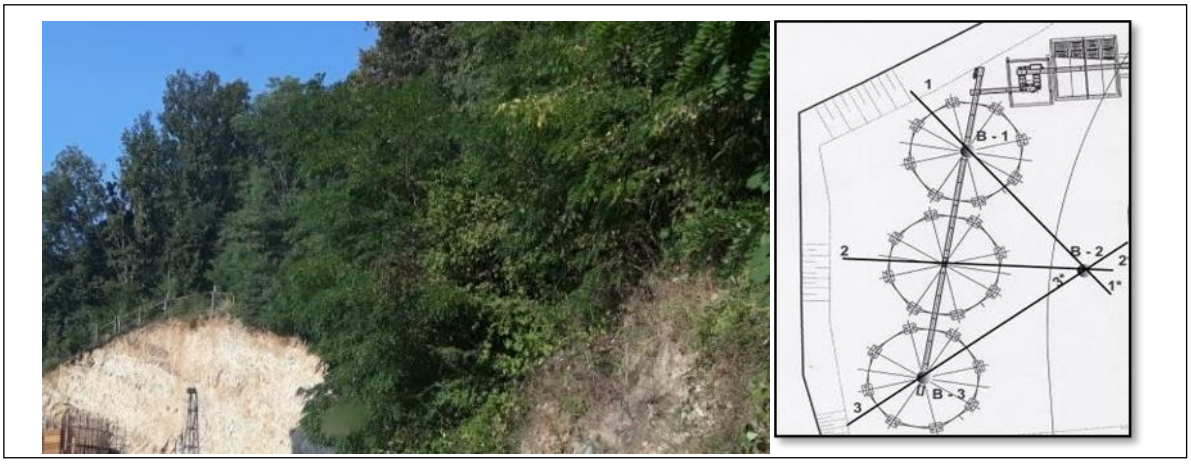

Figure 1. Open cut slope profile with silos at the base

In addition to the "natural decomposition" of marls after their extraction from the rock massif, their solubility in water at a daytime temperature of 36^0C and 19^0 at night temperature was monitored [3,6,9,10,11]. Parallel to the samples from the boreholes, samples from the slope in the immediate vicinity were taken from the same rocks and treated in the same way.

The synclinal deposition of the layers is characterized by their different depths between the exploration boreholes, as well as the open profile of the slope in the hinterland, figure 1. The depths of samplings are different but represent the continuity of the same layers. Correlation of data from the Basic Geological Map and the results of exploratory drilling defined the position of the lithological members in terms of vertical occurrence and horizontal extension. According to the engineering geological classification, the separated layers belong to clastic semi-rocks, classified into three geological environments [3].

Environment 1 represents a complex of layers of fine-grained to medium-grained sandstones in several horizons, of different colors. Sandstone rocks are fine-grained to medium-grained, poorly weathered to hard and well - cemented material, varying in color from light gray to gray with occasional shades of reddish brown. The higher horizon is registered at different depths due to the synclinal alignment of the layers. It starts from a depth of 0.40 m and goes up to maximum of 2.7 m deep.

The lower horizons are at greater depths, although due to the synclinal deposition of the layers, they appear in one part from the surface of the terrain. On the terrain profile (figure 2) the middle is marked with the number 1, and the lithological layers are marked with geomechanical sandstone marks. Those are 1-PŠ^1, 2-PŠ^2, 3-PŠ^1, 5-PŠ^1, 9-PŠ^1. At the bottom of the synclinal part, a layer of well - cemented conglomerate, with a lenticular character, was separated and marked as 7-KG. The values of the parameters move in a smaller range, depending on the horizon from which they were taken, and lower mean values were adopted, table 1.

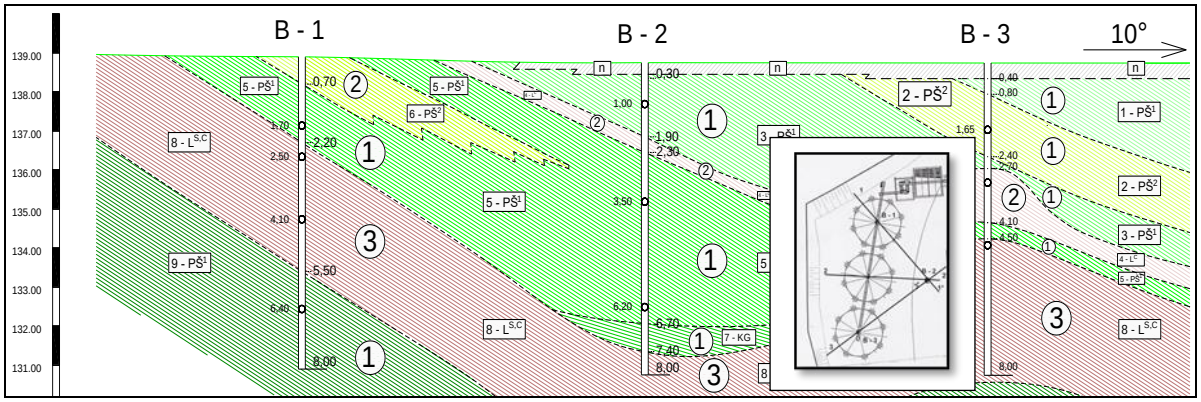

Figure 2. Terrain profile along the axis of the future objects
1,2,3, separated geological environments

Environment 2 has no continuity but is separated as a special one with presence of clayey marl and fine – to medium – grained sandstone. It appears from the surface of the terrain and sinks synclinally up to 4.5 m, with a thickness of about 3.0 – 4.0 m, and in the extreme part of the syncline it decreases to 0.4 m (figure 2). On the terrain profile, it is marked with the number 2 and with geomechanical label of the layer 4-L^C. Values of parameters are given in table 1. The environment is conditionally favorable for objects foundations. In its natural state, it is stable and has a satisfactory load capacity.

Table 1. Parameters for geotechnical environments

Geol. envir.	Profile mark	Lithological type	Physical – mechanical parameters	Adopted environment parameters
1	1-PŠ^1 2-PŠ^2 3-PŠ^1 5-PŠ^1 9-PŠ^1	Fine-grained to medium-grained sandstone, poorly weathered to hard and well-cemented material	γ = 23,66 – 26,30 kN/m³	γ = 24,00 kN/m³
			φ = 27,0 – 32,0^0	φ = 29^0
			c = 2,10 – 2,70 MPa/m^2	c = 2,40 MPa
			σ = 12,80 – 29,97 MPa	σ = 21,00 MPa
			ν = 0,20 – 0,26	ν = 0,23
			E_{din} = 22403 – 36816 MPa	E_{din} = 29000 MPa
	Average RQD 63 – 76%			
2	4-L^C	Clay marl, worn out, brittle	γ = 24,06 kN/m³	γ = 24,00 kN/m³
			φ = 26º	φ = 25^0
			c = 2,10 MPa/m^2	c = 2,0 MPa
			σ = 5,23 MPa	σ = 5,0 MPa
			ν = 0,22	ν = 0,21
			E_{din} = 15782 MPa	E_{din} = 15500 MPa
	Average RQD around 55%			
3	8-L^{SC}	Clay marl, sandy, worn out, brittle	γ = 23,57 – 25,50 kN/m³	γ = 24,50 kN/m³
			φ = 25º	φ = 25^0
			c = 2,30 MPa/m^2	c = 2,2 MPa
			σ = 3,64 – 4,91 MPa	σ = 4,0 MPa
			ν = 0,25 – 0,31	ν = 0,27
			E_{din} = 11552 – 11661 MPa	E_{din} = 11600 MPa
	Average RQD around 69%			

Engineering activities may come into contact with the water from atmospheric precipitation, which can very quickly deteriorate its physical and mechanical characteristics to the limit of soft marly clay. At the same time, it is transformed into an unfavorable environment for the foundation of objects. If the foundation of the objects is carried out in the environment 2, it is necessary to isolate it from the contact with the water.

Environment 3 forms the substrate of the terrain with the characteristics of a quasi - plastic environment, built of fine clastic rocks - marl of clayey, sandy, brittle, dark red-brown color with rare inclusions of gray hard sandstone. It appears from the surface of the terrain and goes to a greater depth from 2.2 m to 7.4 m, that is, it follows the synclinal deposition of contact layers. The center has an average thickness of 2.5 - 3.5 m in the area of the silos facilities (figure 2). On the terrain profile, it is marked with numerical code 3 and geomechanical code of layer 8-L^{SC}.

The values of the parameters are given in table 1. The environment is favorable for the foundation of objects in its natural state. It represents a stable environment, where the rock is weakly compressible to incompressible with a permissible bearing capacity that corresponds to the designed silos facilities. In contact with water, the physical and mechanical characteristics are reduced and it passes into a conditionally favorable environment. During the execution of the works, it is necessary to take measures to protect the rocks from contact with the water.

The layers of lithological members in all environments alternate rhythmically, forming an incomplete flysch sequence with the absence of certain members in the vertical column. They are characterized by frequent changes in thickness as well as lateral changes of lithological members over a short distance.

The solubility of marly rocks in water was carried out on the terrain during exploratory drilling, by hand without previously prepared equipment. It arose from the need to look at the behavior of marly rocks in water at different temperatures. Pieces of marl rock were taken from boreholes and the open terrain profile and submerged in water in different containers. Tests were performed several times at daytime and nighttime air temperatures.

Three samples were taken from the open terrain profile at a distance of about 10.0 m, which is how far the exploration boreholes are from each other. All samples were placed at the same time, under the following conditions:

- samples observed at daytime temperature 36^0C
- initial water temperature 13^0C
- final water temperature 16^0C

The time of complete solubility ranged from 24 to 30 minutes.

- samples observed at night time temperature $19 – 20^0$C
- initial water temperature 12^0C
- final water temperature 12^0C

The time of complete solubility ranged from 52 to 63 minutes.

From each borehole, samples were taken from two layers at different times. Every day, testing was done on a different borehole, which was dictated by the time of exploratory drilling. The samples were observed under the same conditions, given that the day and night temperatures did not change during that period.

The marly layer of geological environment 2 under daytime conditions is characterized by values of complete solubility of 32-41 minutes. The time of complete solubility in night conditions is 58 – 74 minutes.

The marly layer of geological environment 3 under daytime conditions is characterized by values of complete solubility of 35 – 43 minutes. The time of complete solubility in night conditions is 62 – 77 minutes.

Common to the marly layer of geological environments 2 and 3 is that they show slower solubility with depth. There is no direct linear dependence between day and night solubility on all samples, given the partially different characteristics of the samples and terrain test conditions. The results are shown in table 2.

Table 2. Review of the results of the terrain tests of the solubility of marly rocks in water

Place of sampling			Conditions of research	Time of complete solubility (min)	
				Day cond.	Night cond.
Open terrain profile of the slope cut	Sample 1.		Day time temperature 36^0C Initial water temperature 13^0C Final water temperature 16^0C Night time temperature 19 – 20^0C Initial water temperature 12^0C Final water temperature 12^0C	24	57
	Sample 2.			30	63
	Sample 3.			26	52
Boreholes	First layer	B – 1		37	61
		B – 2		32	58
		B – 3		41	74
	Second layer	B – 1		35	67
		B – 2		43	77
		B – 3		37	62

Dissolved marl rocks are of dark grey color, resulting in a grey silty material where the particles float in the water during mixing. It was not possible to monitor the consolidation of floating particles in the water, nor to measure the total sediment in relation to the sample that was immersed in water, as well as the solidification of the sediments in a function of time. Also, the granulometric or mineral composition was not determined, which would be significant for comparison with tests in laboratory conditions.

The geotechnical properties of the terrain were determined from the aspect of the terrain's properties as a working environment in which the objects will be based. For the analysis of the geotechnical conditions for the design and construction of silos facilities, the construction of the terrain was analyzed in detail in relation to the lithological types of rocks, their position within the studied depth of the terrain as well as their mutual position, then their condition, composition, engineering geological and hydrogeological characteristics, and physical - mechanical and resistant - deformable characteristics [10,11,12,13].

Correlation of the data obtained by exploratory drilling was carried out with the data of the open terrain profile in the hinterland located a few meters from the planned objects (figure 1). The subvertical section of the slope shows all the complexity of the geological structure, which is also confirmed by exploratory drilling.

By analyzing rock strength using RocLab, lower parameter values were taken for input data. The degree of reliability of the input data of terrain and laboratory research in the part of investigative works is satisfactory. The data for the rock mass taken from the RocLab program package are quite well chosen [14,15,16,17]. The characteristics of the environments recalculated in RocLab are given in table 3 and in figure 3.

Table 3. Parameters of geotechnical environments recalculated in the RocLab massif

Parameters	Geological environment 1		Geological environment 2		Geological environment 3	
	Intact rock	RocLab massif	Intact rock	RocLab massif	Intact rock	RocLab massif
γ (kN/m³)	24	24	24	24	24,5	25,4
φ = (^{0})	29	37	25	31	25	28
c = (MPa)	2,4	1.343	2,0	0.255	2,2	0.178
σ = (MPa)	21	1.559	5,0	0.268	4,0	0.179

GSI	-	59	-	48	-	45
m_i	-	19	-	12	-	9
σ_{RM}	-	5.418	-	0.911	-	0.594
E_{din} (MPa)	29000	6.510	15500	1.250	11600	1.000
ε_{RM} (MPa)	-	2.518	-	339	-	224

γ – volumetric weight	m_i – constant that depends on the characteristics of the rock
φ – angle of internal friction	σ_{RM} – total strength of the rock mass
c – cohesion	E_{din} – dynamic modulus of elasticity
σ – uniaxial compressive strength	ε_{RM} – modulus of deformation
GSI – geological strength index	

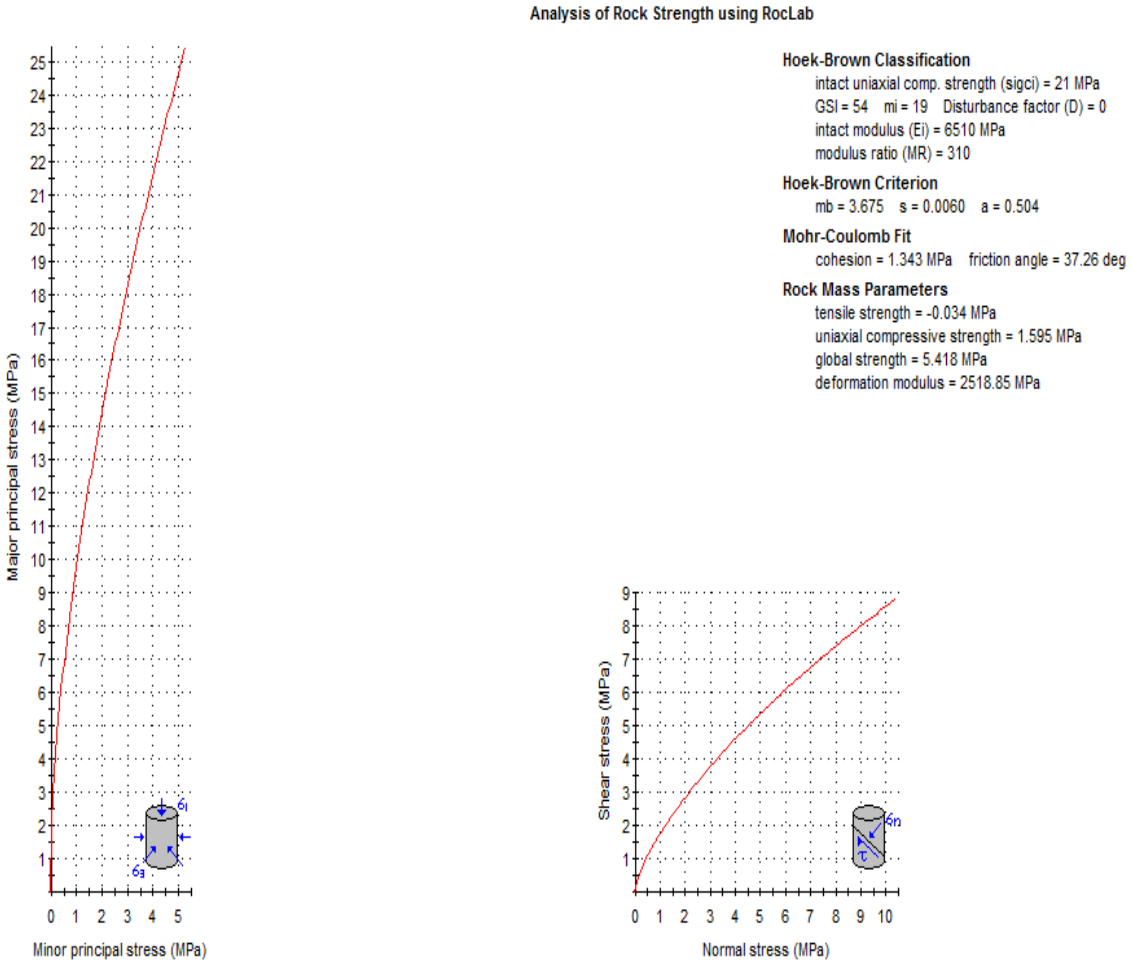

Figure 2. Values obtained by analysis in RocLab for the analyzed environments (example of environment 1)

DISCUSSION

The obtained values of the parameters for the isolated geological environments are in a wider range, and they were adopted on the basis of laboratory tests and evaluation of the quality of the rock during its mapping. Average lower values were taken, which are realistic for monolithic samples [18,19,20]. The rocks in the narrower and wider area do not represent continuity, since there are mechanical discontinuities along which can be a complete absence of cohesion forces. A closer look shows the difference in strength between the monolithic parts of the rock mass and the real rock mass. Conducted terrain research and terrain - laboratory tests show that marly rocks at the location of the future silos are found in the entire range of the group of weak sedimentary rocks [2,17,21,22].

The geotechnical environments that were engaged as working environments with their parameters were selected on the basis of laboratory tests of representative samples of solid rocks. The real properties of the marl complex and the sandstone complex were considered (lithological heterogeneity, structural - textural properties, degree of cracking and characteristics of cracks, degree of surface degradation, presence of groundwater, etc.). Existing correlations between physical - mechanical properties, structural properties and rating of rock mass were analyzed (analysis of Roc/Soil Strength using RocLab). In general, the quasi-homogeneous sediments of the marly layer of the second and third geological environments can be considered as one layer.

The solubility of marly rocks taken from the open profile of the cut terrain is shorter in time compared to the same rocks from boreholes. In the case of rocks on an open terrain profile, their structure has been damaged due to temperature oscillations over the past few years. Over time, the rocks will break down and gradually threaten the stability of the slope in that part. Terrain testing of rock solubility by immersing a sample in water is a handy method for assessing rock characteristics under altered conditions.

The ISO - 1997 standard could not be applied, where the stability of rock material in water can be determined by submerging the sample for one week. The behavior of the sample is determined descriptively in three classes. According to the state of stability in class III, the unstable state of the rock is distinguished, for the complete decomposition of rocks in water. The time of decomposition of marl rocks at the studied location is significantly shorter, which places them in this class [12,14].

The results of the state of stress in the rock massif as a whole and the rocks taken in the exploration works always differ, considering that the exploration works show the real state in the point section along the vertical. It is more or less different from the situation in the immediate surroundings, which depends from the structural - geological characteristics of the terrain.

The values obtained by the analysis in RocLab for the analyzed environments are significantly lower and they reflect the actual situation in the complete block of the rock massif. More detailed research, both in a narrower and wider location, would provide more reliable data for a more realistic view of the massif.

Separated parameters for geotechnical environments provided the starting point for geotechnical calculations for the foundation of silos objects on the investigated site.

CONCLUSION

The complexity of the geological structure of the terrain required a larger scope of research work for silos type objects. By using the data of earlier researchers in the preparation of the Basic Geological Map 1 : 100 000, data from exploratory boreholes and the open profile of the terrain in the hinterland, basic data of its characteristics were obtained. They are not highly reliable, but they represent a starting point for geotechnical calculations.

The alternation of layers in a small area and their synclinal deposition do not give the possibility of choosing a specific layer for the foundation of the building. Layers were grouped into geological environments, taking into account their similar characteristics and lower average parameter values. Three geological environments were separated, which, in addition to the parameters of laboratory tests, were also processed through the RocLab system.

Terrain - laboratory tests using auxiliary methods showed that the rocks from the open profile of the cut terrain have worse characteristics compared to the rocks found in the package of existing rocks at a certain depth. The characteristics of marly rocks change with depth, and their depth is variable due to the folded forms in which the rocks are found.

Received August 2023, accepted September 2023)

LITERATURE

[1] Basic geological map of SFRY, sheet Zvornik, R 1: 100000, and OGK interpreter, Belgrade. Federal Geological Survey, 1980. *[Serbian language]*.

[2] Djukić, D. (2004). "Geotechnical classifications for surface works in mining and construction". Tuzla. Tuzla Mining Institute. *[Serbian language]*.

[3] Đurić, N. (2011). "Hydrogeological and engineering geological research". Subotica, Bijeljina. Faculty of Civil Engineering, Technical Institute. *[Serbian language]*.

[4] Šestanović, S. Engineering–geological characteristics of marl from Eocene flysch in the City of Split. In Proceedings of the Second. International Symposium on Hard Soils–Soft Rocks: The Geotechnics of Hard Soils–Soft Rocks, Naples, Italy, 12–14 October 1998; Evangelista, A., Picarelli, L., Eds.; Balkema: Rotterdam, The Netherlands, 2000; pp. 311–314.

[5] Sabatakakis, N., Koukis, G., Tsiambaos, G., Papanakli, S. (2008). "Index properties and strength variation controlled by microstructure for sedimentary rocks", Engineering Geology, Elsevier, 97, 80-90.

[6] Study on the geomeganical characteristics of the terrain for the need to build a silo within the complex of facilities of the Mill "Molaris", Kozluk near Zvornik, 2019. *[Serbian language]*.

[7] Sonmez, H., Gokceoglu, C., Ulusay, R. (2004). Indirect determination of the modulus of deformation of rock masses based on the GSI system. Int J Rock Mech Min Sci 41(5):849–857.

[8] Zhang, L., Einstein, HH. (2004). Using RQD to estimate the deformation modulus of rock masses. Int J Rock Mech Min Sci 41(2):337–341.

[9] Djuric, N., Besevic, M., Bursac, S., Djuric, D. (2022). Characteristics of lapory rocks at the silos location within the "Molaris" mill complex, in Kozluk near Zvornik in the Republic of Srpska. The 8thInternational Conference "Civil Engineering – science of practice". GNP 2022, Koalšin, Montenegro.

[10] Admassu, Y., Shakoor, A., Wells, N.A. (2012). "Evaluating selected factors affecting the depth of undercutting in rocks subject to differential weathering", Engineering Geology, 124, pp. 1–11.

[11] Stevanic, D., Miscevic, P. (2007). "The Durability Characterization of Selected Marls from Dalmatian Region in Croatia", Proc. of XVIII EYGEC, Ancona (Portonovo), Italy, 17-20.

[12] P. Miscevic, P., Vlastelica, G. (2011). "Durability Characterization of Marls from the Region of Dalmatia, Croatia", Geotechnical and geological engineering, Vol. 29, No. 5, pp. 771-781.

[13] Fookes, P.G., C. S. Gourley, C.S., Ohikere, C. (2008). "Rock weathering in engineering time". Quarterly Journal of Engineering Geology, London, Vol. 21, pp. 33-57.

[14] Kanji, A.M. (2014). "Critical issues in soft rocks", Journal of Rock Mechanics and Geotechnical Engineering, Vol. 6, No. 3, pp. 186-195, 2014. http://dx.doi.org/10.1016/j.jrmge

[15] Bieniawski, Z.T. (1976) Rock Mass Classification in Rock Engineering, In: Exploration for Rock Engineering, Proc. of the Symp.

[16] Bieniawski, Z.T. (1989). Engineering Rock Mass Classification, New York: John Wiley & Sons.

[17] Tziallas, G.P., Tsiambaos, G., Saroglou, H. (2009)."Determination of rock strength and deformability of intact rocks", Electronic Journal of Geotechnical Engineering, 14 G, 1-12.

[18] Hoek, E., Kaiser, P.K., Bawden, W.F. (1995). Support of Underground Excavations in Hard Rock, Rotterdam: A.A. Balkema.

[19] Hoek, E., Carranza-Torres, C.T., Corkum, B. (2002). Hoek Brown failure criterion - 2002 edition. In: Proceedings of the 5th North American Rock Mechanics Symp., Toronto, Canada, pp. 267–73.

[20] Hoek, E., Carter, T.G., Diederichs, M.S. (2013). Quantification of the Geological Strength Index Chart 47th US Rock Mechanics / Geomechanics Symposium, San Francisco.

[21] Najdanović, N. (1979). Soil mechanics and engineering practice. Mining Institute Zemun, Belgrade. *[Serbian language]*.

[22] Maksimović, M. (2005). Soil Mechanics, II Edition. Construction book, Belgrade. *[Serbian language]*.

MINING

Smart mining

Editors

Prof. Ph.D. Božo Kolonja
Prof. Ph.D. Vlado Malbašić

Original scientific article
http://dx.doi.org/10.59456/afts.2023.1529.011T

SMART MINING: JOINT MODEL FOR PARAMETRIZATION OF COAL EXCAVATION PROCESS BASED ON ARTIFICIAL NEURAL NETWORKS

Trivan Jelena[1], Kostić Srđan[2]

[1]*Faculty of Mining Prijedor, University of Banja Luka, Bosnia and Herzegovina, e.mail: jelena.trivan@rf.unibl.org*
[2]*Faculty of Technical Sciences University of Novi Sad, Serbia*

ABSTRACT

In the present paper we propose a new artificial neural network model for the estimation of coal cutting resistance and excavator performance as a nonlinear relationship between the examined input (excavator movement angle in the left and right direction, slice height and thickness, coal unit weight, compressive and shear strength) and output factors (excavator effective capacity, maximum current/power/force/energy consumption, linear and areal cutting resistance). We analyze the dataset collected from three open-pit coal mines in Serbia: Field D, Tamnava Eastern Field and Tamnava Western Field (all part of the Kolubara coal basin). The model is developed using a multilayer feed-forward neural network, with a Levenberg-Marquardt learning algorithm. Results of the preformed analysis indicate satisfying statistical accuracyof the developed model (R>0.9). Additionally, we analyze the individual effects of input factors on the properties of coal cutting resistance and performance of the excavator, by invokling the multiple linear regression. As a result, we single out the statististically significant and physically possible interactions between the individual controlling factors

Keywords: *artificial neural networks, surface coal mining, bucket wheel excavator*

INTRODUCTION

The rapid development of artificial intelligence (AI), its increased availability, and the possibility of use without having demanding processing units leads to the application of AI-based methods in almost every aspect of human activity. The main advantages of involving AI-based methods lie in their convenient use, satisfying accuracy and the essential black-box approach, i.e. one does not need to know all steps leading from input parameters to the outputs, but it is sufficient to repeat "experiments" with different settings of AI-based model in search of the best solution. Results obtained in this way are not always completely accurate, but their accuracy is satisfying for preliminary assessment of the processes or the features being studied. Regarding the mining industry, according to [forbes.com], AI-based methods lead to the so-called ‘’smart mining’’, with the primary aim of reducing the enormous costs in the mining industry [1].

Regarding the mining industry, AI-based methods lead to the so-called ‘’smart mining’’, with the primary aim of reducing the enormous costs in the mining industry [1]. For instance, estimations made by McKinsey [2] are that by 2035 the application of AI in mining will save between $290 billion and $390 billion annually for mineral raw materials producers. AI-based intelligence systems are being widely used by mining companies, helping them: acquire data, convert data, transmit, analyze, and visualize data. Moreover, Karatzoglou points out that future ore exploration will be more complex

since almost entire deposits that are on the surface or relatively easily accessible are nearly exhausted [3]. So, ore bodies that will explore in the future are likely to be deep and hidden by thick overburden, probably interacting with significant geological structures (including faults, and similar). In such cases, AI-based methods could be very useful, since they can ''learn'' from experience. Additionally, it is expected that the use of AI-based methods will increase the safety of the mine workers (by accurately predicting dangerous scenarios) and even lead to the use of autonomous mining vehicles, which could be remotely controlled and operated.

In the last decade, there has been an increased application of artificial intelligence methods in the planning, design, and analysis of processes and parameters related to the coal excavation process. Srivastava and Pradhan [4] reported that mining-related complex operations, computations, and analyses in India have become easier and more accurate with the use of AI-based methods. Wang et al. wrote about the "Chinese mode" of intelligent mining in underground coal mines [5].

The use of AI-based methods and solutions leads to the top-level architecture of 5G+ intelligent coal mine systems that combines intelligent applications such as autonomous intelligent mining, human–machine collaborative rapid tunneling, unmanned auxiliary transportation, closed-loop safety control, and intelligent ecology. Furthermore, according to Azhari et al. in the last five years, deep learning has been implemented to solve a variety of problems related to mine exploration, ore and metal extraction, and reclamation processes [6].

In coal mining, artificial neural networks (ANN) are by far the most used AI-based method in the last 10 years for solving different tasks in engineering practice. Yang and Xiaohong used artificial neural networks (ANN) to develop a quantitative prediction method for mining subsidence and horizontal movement under thin bedrocks and thick unconsolidated layers [7]. Results obtained indicated that the proposed model provides sufficiently accurate data when compared to the measured values, with a relative error in the range of 1.034 – 6.571% for subsidence, and 1.160 – 6.233% for horizontal movement.

Panigrahi and Ray used the ANN approach to develop a new electrochemical method (wet oxidation potential technique) for determining the susceptibility of coal to spontaneous combustion [8]. The model based on the ANN approach provided satisfying statistical accuracy, with R>0.9 and MSE=0.66-2.07 (target values were in the range 0-9). Mlynarczuk and Skiba used pattern recognition techniques and ANN to create an automatic process of classification of maceral groups and mineral components of coal [9]. Results obtained indicate over 97% of correct classifications of maceral groups and mineral components.

Wilkins et al. applied convolutional neural networks to identify microseismic events at the coal mine [10]. The developed model could be used to reveal, classify and locate microseismic events, with satisfying precision. Moreover, their research indicated that the created model was more successful than humans at correctly identifying both true events and false-positive events.

Jiang et al. used graph convolutional networks to develop a multi-point relationship fusion prediction model of mining-induced surface subsidence, based on the surface deformation data obtained from 250 InSAR images [11]. Qi et al. applied a radial basis function neural network for the estimation of the spatial distribution of soil organic carbon in coal mining subsidence areas [12]. Results obtained indicate that the application of neural networks provides statistically more accurate results compared to direct kriging methods (correlation coefficient 0.81 compared to 0.44, respectively).

In the present paper, we apply a three-layer feedforward multiple perceptron neural network, to estimate a series of parameters of the bucket-wheel excavator performance and coal cutting resistance. The model is derived for the case study of three coal basins in Serbia: Tamnava western field, Tamnava eastern field, and Field D (all parts of the Kolubara coal basin). As a result, the model provides an estimation of many excavation and resistance parameters with satisfying accuracy, and it could be used for the first preliminary assessment of excavator consumption and coal resistance to cutting.

The paper is structured as follows. In Section 2 we provide brief information on the data analyzed and applied methodology. In Section 3 results of the performed analysis are presented, including the estimation of the statistical accuracy of the developed model and the explicit mathematical expression. Section 4 is devoted to the conclusions and directions for further research.

DATA ANALYZED AND METHODOLOGY

We analyze the following properties of the excavation process (using a bucket-wheel excavator) recorded at Tamnava Eastern Field, Tamnava Western Field, and Field D (Kolubara coal mine in Serbia):

- Excavator effective capacity Q_{ef} (m^3/h)
- maximum current consumption I_{max} (A)
- maximum power consumption N_{max} (kW)
- maximum force consumption P_{max} (kN)
- maximum energy consumption E_{max} (kWh/m^3)
- excavator movement angle in the left direction φ_L (°)
- excavator movement angle in the right direction φ_D (°)
- slice height h (m)
- slice thickness s (m)

Also, the following properties of coal are examined:

- maximum linear cutting resistance K_{Lmax} (N/cm)
- maximum areal cutting resistance K_{Fmax} (N/cm^2)
- coal unit weight γ (kN/m^3)
- coal compressive strength σ_p (MPa)
- coal cohesion c (MPa)
- coal angle of internal friction φ (°)

Data were collected [13] for the case of coal excavation with a bucket-wheel excavator of the same type SchRs630.

The aforementioned data were further used to develop a prediction model, as a nonlinear function of the following output units: Q_{ef}, I_{max}, N_{max}, P_{max}, E_{max}, $K_{Lmax,}$ and K_{Fmax}, on the following controlling factors: γ, σ_p, c, φ, φ_L, φ_D, h and s. ANN approach included a fast-forward three-layer network with a backpropagation Levenberg-Marquardt (LM) algorithm with a sigmoid activation function. The LM learning algorithm is the fastest method for training moderate-sized feed-forward neural networks. We develop an ANN model with 10 hidden neurons (Figure1).

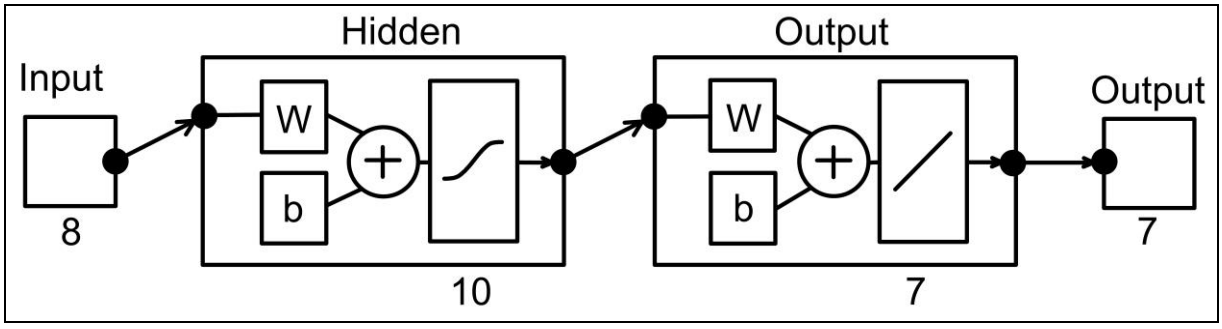

Figure 1. The architecture of the developed ANN model.

The possibility of overfitting was excluded by confirming that any increase in accuracy over the training data set yields a rise in accuracy over a validation data set. In particular, mean-squared error (MSE) should be saturated with the increase of epochs for training and validation data. The total data set has been divided as follows: 65% for training (128 recordings), 20% for validation (40 recordings), and 15% for testing (30 recordings).

DEVELOPMENT OF ANN MODEL

As a result, we developed a unique ANN model, by establishing a nonlinear correlation between the outputs Q_{ef}, I_{max}, N_{max}, P_{max}, E_{max}, K_{Lmax}, and K_{Fmax}, and inputs: γ, σ_p, c, φ, φ_L, φ_D, h and s, in the following general form:

$$[outputs] = tansig\{[a] + [b] \cdot tansig\{[c] + [d] \cdot [input]\} \quad (1)$$

where tansig[N] is a neural transfer function, that takes a matrix of net input vectors, N, and returns the S-by-Q matrix, A, of the elements o N squshed into [-1 1]. It is defined as:

$$tansig\,(N) = \frac{2}{1+e^{-2N}} - 1 \quad (2)$$

and it is mathematically equivalent to tanh(N).

Parameters of Eq. (1) are given as matrices in the present case:

$$[outputs] = \begin{bmatrix} Q_{ef} \\ I_{max} \\ N_{max} \\ P_{max} \\ E_{max} \\ K_{Lmax} \\ K_{Fmax} \end{bmatrix}, \quad [a] = \begin{bmatrix} -1.90 \\ 0.26 \\ -0.53 \\ 0.61 \\ -0.39 \\ 1.25 \\ 0.08 \end{bmatrix}, \quad [c] = \begin{bmatrix} -0.810 \\ 0.067 \\ 1.488 \\ -0.272 \\ 1.342 \\ 0.839 \\ -2.319 \\ 0.961 \\ 2.743 \\ 1.895 \end{bmatrix},$$

$$[b] = \begin{bmatrix} 0.05 & -0.05 & -1.080 & 0.139 & 0.651 & 1.718 & -0.659 & 0.783 & 1.847 & 0.597 \\ -0.06 & 0.018 & 0.033 & 0.337 & 1.775 & -0.150 & -0.291 & -0.608 & 1.227 & -0.105 \\ 0.003 & -0.018 & -0.146 & -0.071 & 0.108 & -0.040 & -0.064 & 0.206 & 0.459 & -0.889 \\ -0.23 & 0.336 & 0.544 & -0.239 & -1.204 & -0.317 & 0.150 & -0.175 & -1.015 & -1.030 \\ 0.41 & 0.048 & -0.079 & 0.587 & -0.306 & -0.113 & -0.380 & -0.324 & 0.334 & -1.035 \\ 0.06 & 0.160 & -0.128 & -0.485 & 1.240 & -0.034 & 0.171 & 0.015 & 0.845 & -1.552 \\ 0.09 & -0.236 & 0.156 & 0.020 & -0.490 & -0.306 & 0.283 & 0.120 & -1.502 & 0.572 \end{bmatrix}, \text{ and}$$

$$[d] = \begin{bmatrix} 2.968 & -0.629 & -1.964 & -1.398 & -0.793 & 1.124 & 0.868 & -1.806 \\ 2.347 & 1.141 & -0.658 & -2.514 & 1.158 & -1.487 & 1.165 & -0.969 \\ -0.499 & -0.225 & 0.966 & -0.922 & -0.487 & 0.289 & 1.272 & -0.254 \\ 0.305 & -0.155 & 1.475 & 0.429 & 1.199 & -1.020 & 1.218 & -1.031 \\ -0.357 & 0.338 & 0.934 & -0.029 & 0.172 & -0.074 & 2.953 & 0.016 \\ -0.309 & -0.333 & -0.131 & -0.522 & -0.621 & 0.966 & 1.611 & 0.015 \\ -0.327 & -0.129 & 0.485 & -0.717 & -0.532 & 0.981 & 1.124 & -2.415 \\ 0.215 & 1.701 & 1.571 & -0.660 & 0.647 & -1.260 & -1.067 & 0.022 \\ 0.852 & -1.023 & 0.539 & -0.115 & 1.322 & 1.149 & -2.729 & 1.871 \\ 0.959 & 2.373 & -1.941 & -0.287 & 0.939 & 0.005 & -1.214 & -0.128 \end{bmatrix}.$$

Developed model (1) provides statistically accurate results, as shown in Figure 2. In all phases of model development, satisfying estimation accuracy was achieved with a correlation coefficient higher than 0.9. The distribution of residuals is given in Figure 3. According to different normality tests, residuals do not follow a normal distribution, Figure 4. Results of the runs test ($p<0.05$) also indicate the absence of randomness in the analyzed data.

The possibility of overfitting was excluded by confirming that any increase in accuracy over the training data set yields a rise in accuracy over a validation data set. In Figure 5. we plot the gradient values, mu, and validation fail. The values of gradient, mu, and val fail were 10^{-7}, 10^{10}, and 6 at 15 epochs, respectively, indicating that the ANN model was well-trained.

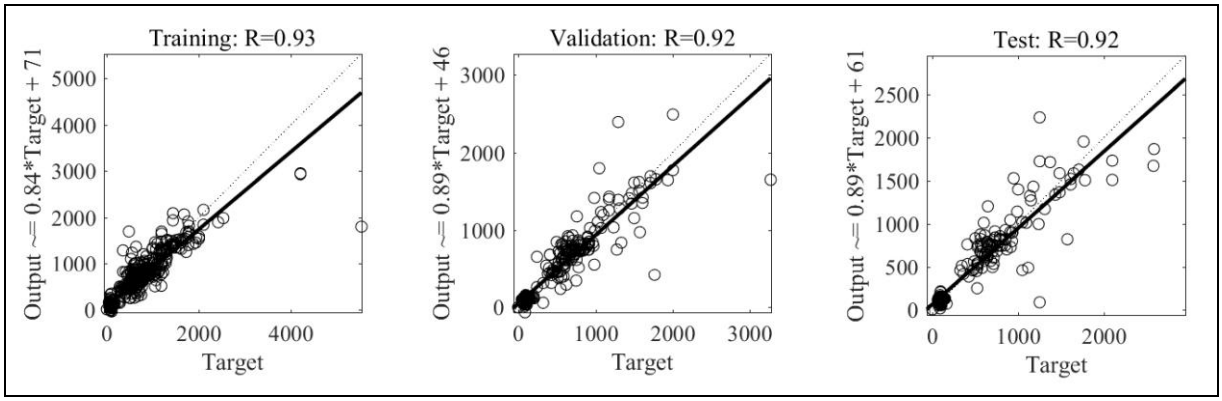

Figure 2. Regression plots for model (1): (left) training set, (middle) validation set, (right) testing set.

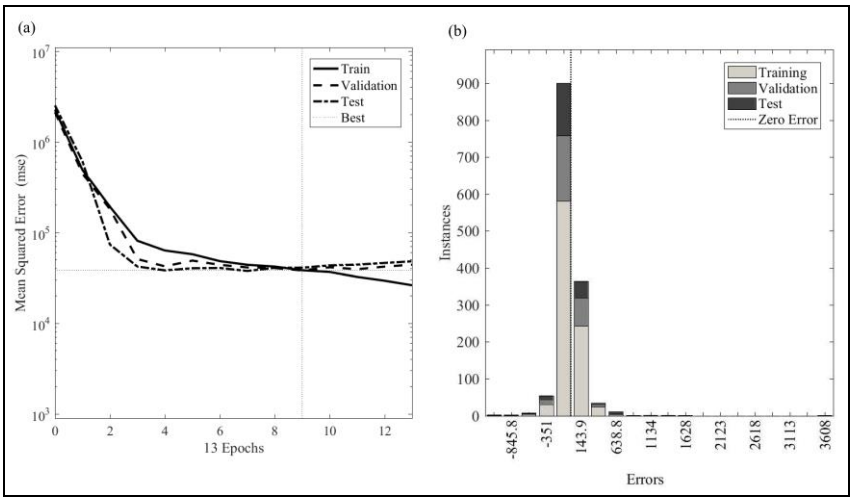

Figure 3. (a) Training evaluation for development of model (1), (b) distribution of residuals of model (1).

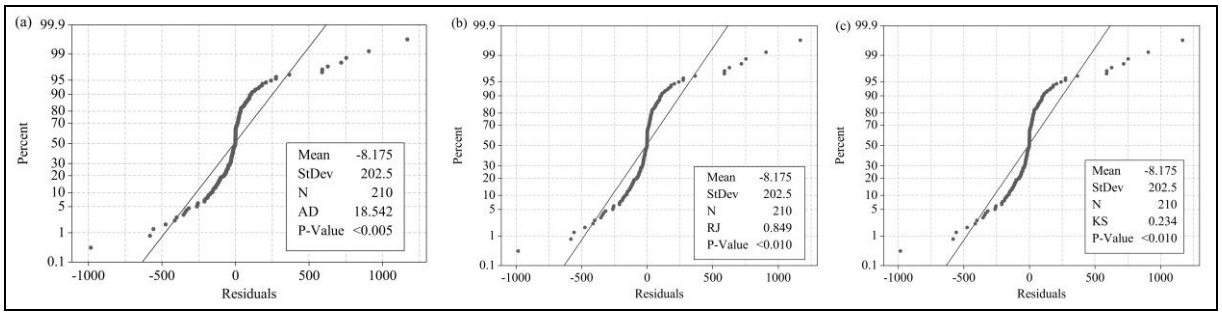

Figure 4. Results of normality tests for residuals: (a) Anderson-Darling test,
(b) Ryan-Joiner test, (c) Kolomogorov-Smirnov test.

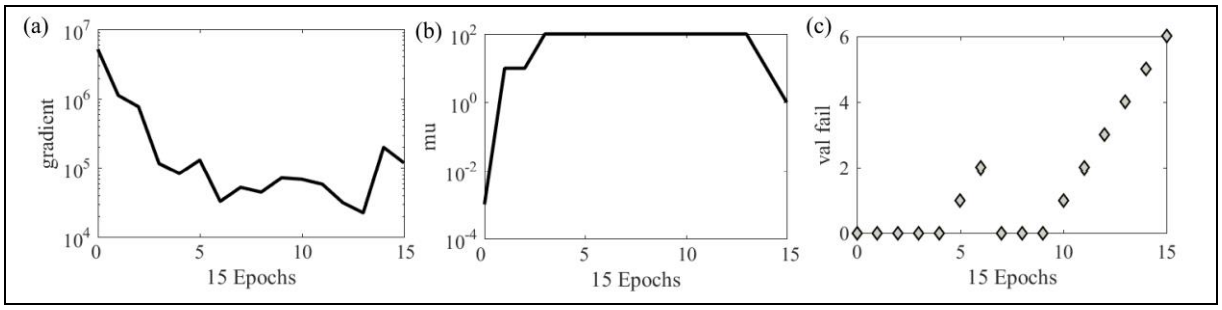

Figure 5. (a) Gradient values, (b) mu and (c) validation fail for the trained ANN model.

INDIVIDUAL EFFECTS OF INPUT FACTORS

The effect of input factors on each output unit is assessed by invoking the multiple linear regression method. Explicit mathematical expressions are provided in Tables 1-2.

Table 1. Statistically significant individual factors and two-factor interactions on Q_{ef}, N_{max}, P_{max}, and E_{max}.

ln (Q_{ef})		1/(N_{max})		Sqrt (P_{max})		ln (E_{max})	
0.008	γ	-3.6E-05	γ	0.29	γ	-0.05	γ
-7.52	σ_p	0.000237	σ_p	-31.69	σ_p	0.039	σ_p
-0.26	φ	-0.00308	c	54.36	c	-3.5	c
-0.12	φ_L	-1.8E-05	φ_L	0.26	φ_L	-0.004	φ
0.0007	φ_D	4.37E-05	φ_D	-0.31	φ_D	0.026	φ_L
-0.81	h	-0.00177	s	18.7	h	-0.022	φ_D
5.05	s	-0.00064	σ_p x s	-7.65	s	0.132	h
0.14	σ_p x φ	0.00046	c x h	-0.037	σ_p x φ_L	0.167	γ x s
0.019	σ_p x φ_L	4.57E-05	φ x s	0.041	σ_p x φ_D	-0.379	σ_p x s
-0.363	σ_p x φ_D	5.85E-08	φ_L x φ_D	2.18	σ_p x s	0.0002	φ_L x φ_D
-0.037	c x φ_L	1.03E-05	φ_D x s	0.02	φ_L x h	-0.008	φ_D x s
0.0014	φ x φ_L			-0.015	φ_D x h	0.52	* h * s
-0.0002	φ_L x φ_D			4.15	σ_p^2		
				0.45	s^2		

Table 2. Statistically significant individual factors and two-factor interactions on I_{max}, K_{Lmax}, and K_{Fmax}.

ln (I_{max})		ln(K_{Lmax})		ln (K_{Fmax})	
2.66	γ	0.39	γ	0.39	γ
-3.06	σ_p	5.99	c	-0.126	φ
-0.29	c	0.073	φ_L	0.07	φ_L
1.81	φ	-0.052	φ_D	-0.026	φ_D
-0.05	φ_L	-2.15	s	1.27	h
0.05	φ_D	-0.001	σ_p x φ_L	-0.013	σ_p x φ_L
3.45	s	0.0086	σ_p x φ_D	0.01	σ_p x φ_D
-1.43	γ x c	-0.53	c x h	-2.40	c x s
0.01	σ_p x φ_L	0.0039	φ_L x h	0.005	* Fi L * h
-0.01	σ_p x φ_D	-0.0045	φ_D x h	-0.007	* Fi D * h
1.11	c x h	-0.005	φ_D x s	-0.007	* Fi D * s
-0.09	φ x h	0.26	* h * s	0.447	* h * s
-0.18	h x s	0.26	σ_p^2	-0.161	h^2
0.33	σ_p^2	0.16	s^2		
5.68	c^2				
-0.019	φ^2				
-0.00005	φ_L^2				
-0.18	s^2				

Statistically significant individual factors affecting Q_{ef} are presented in Figure 6. One can clearly single out two groups of parameters (input factors) that have different effects on Q_{ef},Figure 6:

- slice thickness has the most significant predominant influence on Q_{ef}. It is expected that the increase in slice height will lead to an increase in Q_{ef}.
- minor effect comes from the following group of parameters:
  - unit weight, compression strength, and cohesion have qualitatively the same effect, which could be described as a minor positive (increasing) influence, meaning that the increase of these parameters leads to the increase of Q_{ef}.

- Slice height and excavator movement angle in right and left directions have minor, but negative (decreasing) effects on Q_{ef}, meaning that the increase of these parameters leads to a decrease in Q_{ef}.

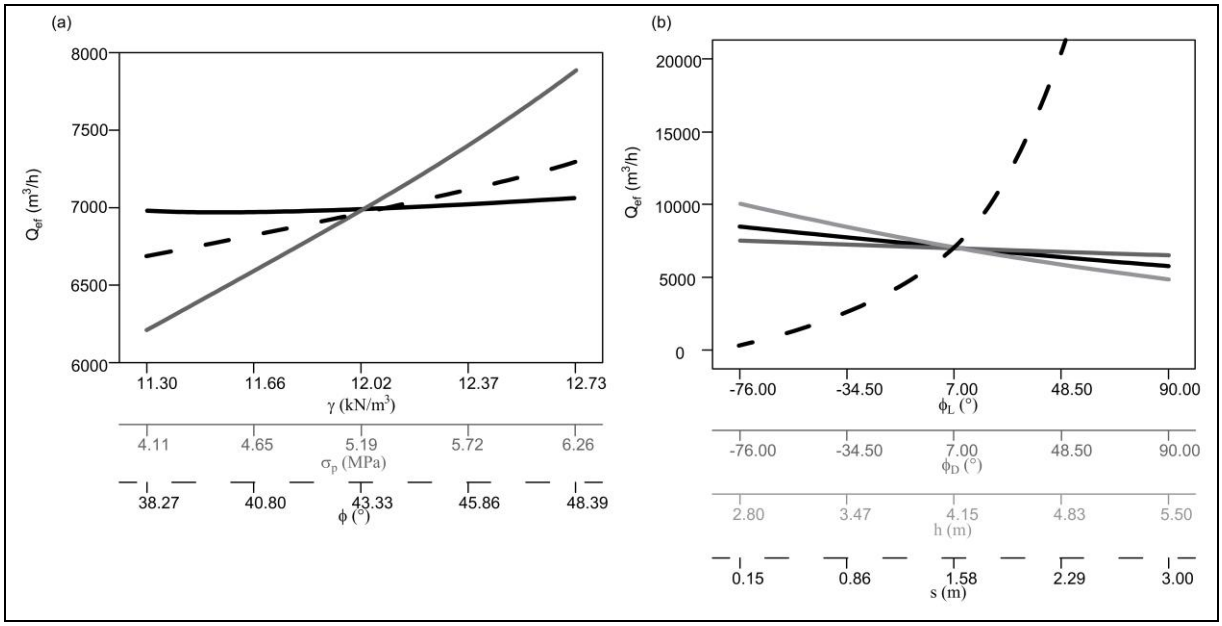

Figure 6. Effect of individual factors on Q_{ef}: (a) Q_{ef} as a function of γ, σp and φ; (b) Q_{ef} as a function of φ_L, φ_D, s and h. While a single parameter is varied, others are held at constant moderate values: $\gamma = 12.02$ kN/m^3, $c = 1.25$ MPa, $\varphi_L = 7°$, $\varphi_D = 7°$, $h = 4.15$m, $s = 1.58$m, $\sigma_p = 5.19$ MPa, $\varphi = 43.33°$.

Regarding the individual effects of input factors on I_{max}, three groups of parameters could be singled out, Figure7:

- Parameters with significant predominant positive (increasing) influence on I_{max}: σp and c.
- Parameters with minor negative (decreasing) influence on Imax: γ, φ_D.
- Parameter with minor positive (increasing) influence on Imax: s, φ_L, φ

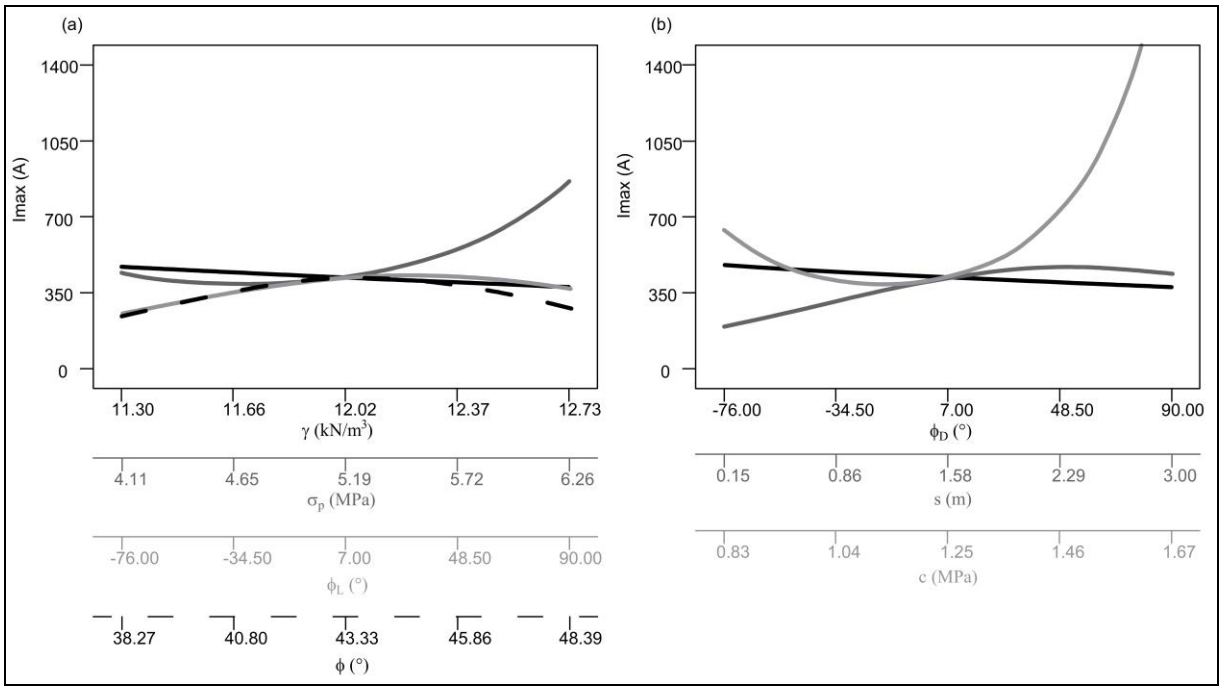

Figure 7. Effect of individual factors on I_{max}: (a) I_{max} as a function of γ, σ_p, φ_L, and φ; (b) I_{max} as a function of φ_D, s, c, and h. While a single parameter is varied, others are held at constant moderate values: $\gamma = 12.02$ kN/m^3, $c = 1.25$ MPa, $\varphi_L = 7°$, $\varphi_D = 7°$, $h = 4.15$m, $s = 1.58$m, $\sigma_p = 5.19$ MPa, $\varphi = 43.33°$.

The examined input factors have the following effects on N_{max}, Figure 8:

- Unit weight has almost no effect on N_{max}.
- Compression strength and cohesion have a significant positive (increasing) effect on N_{max}.

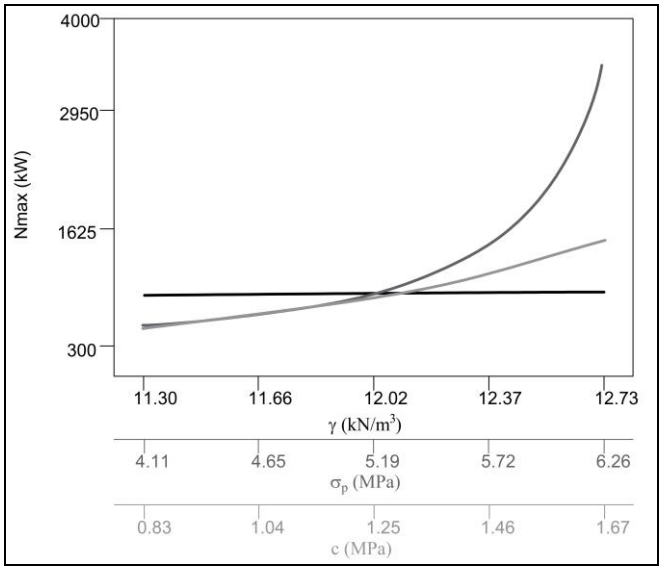

Figure 8. Effect of individual factors on N_{max}: γ, σ_p, and c. While a single parameter is varied, others are held at constant moderate values: γ = 12.02 kN/m^3, *c* = 1.25 MPa, φ_L = 7°, φ_D = 7°, *h* = 4.15m, *s* = 1.58m, σ_p = 5.19 MPa, φ = 43.33°.

Regarding the dependence of P_{max} on the analyzed input factors, the results of the analysis indicate the following, Figure 9:

- Slice height and coal unit weight have a minor positive effect on P_{max}.
- Slice thickness s and angle of the excavator movement in the left direction have a strong positive (increasing) effect on P_{max}.
- Excavator movement angle in the right direction has a strong negative (decreasing) effect on P_{max}.
- Compression strength and coal cohesion have negative effects for the lower range of values. For the upper range of values, they have a positive (increasing) effect.

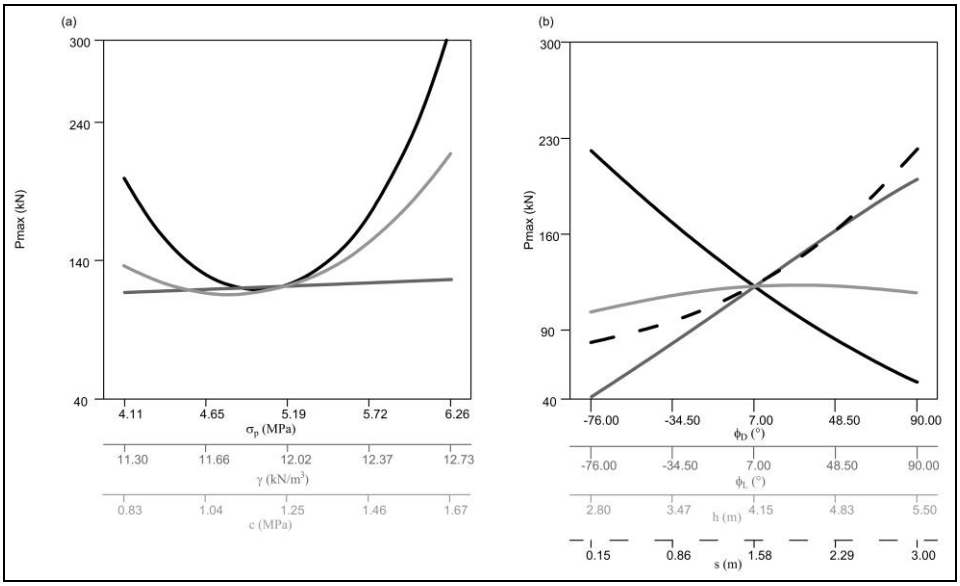

Figure 9. Effect of individual factors on P_{max}: (a) P_{max} as a function of γ, σ_p, and c; (b) P_{max} as a function of φ_D, φ_L, h, and s. While a single parameter is varied, others are held at constant moderate values: γ = 12.02 kN/m^3, *c* = 1.25 MPa, φ_L = 7°, φ_D = 7°, *h* = 4.15m, *s* = 1.58m, σ_p = 5.19 MPa, φ = 43.33°.

Results of the performed analyses indicate the following influence of the input factors on $E_{max,}$ Figure 10:

- Coal unit weight, compression strength, cohesion, and friction angle have almost no effect on E_{max};
- Excavator movement in the left direction and slice height have a slight positive (increasing) effect on E_{max};
- Excavator movement in the right direction has a slight negative (decreasing) effect on E_{max}.

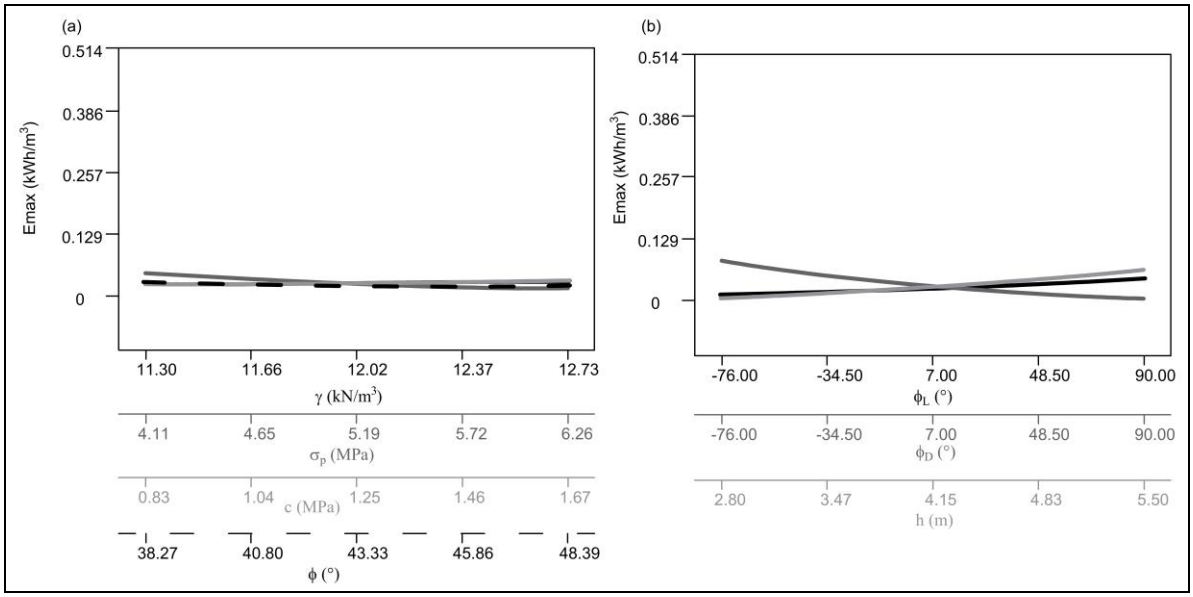

Figure 10. Effect of individual factors on E_{max}: (a) E_{max} as a function of γ, σ_p, c and φ; (b) Emax as a function of φ_D, φ_L, and h. While a single parameter is varied, others are held at constant moderate values: γ = 12.02 kN/m^3, *c* = 1.25 MPa, φ_L = 7°, φ_D = 7°, *h* = 4.15m, *s* = 1.58m, σ_p = 5.19 MPa, φ = 43.33°.

The dependence of K_{Lmax} on the input factors is the following, Figure11:

- Coal unit weight, cohesion, excavator movement angle in the left direction, and slice height have a slight positive (increasing) effect on K_{Lmax};
- Excavator movement in the right direction has a significant negative (decreasing) effect on K_{Lmax};

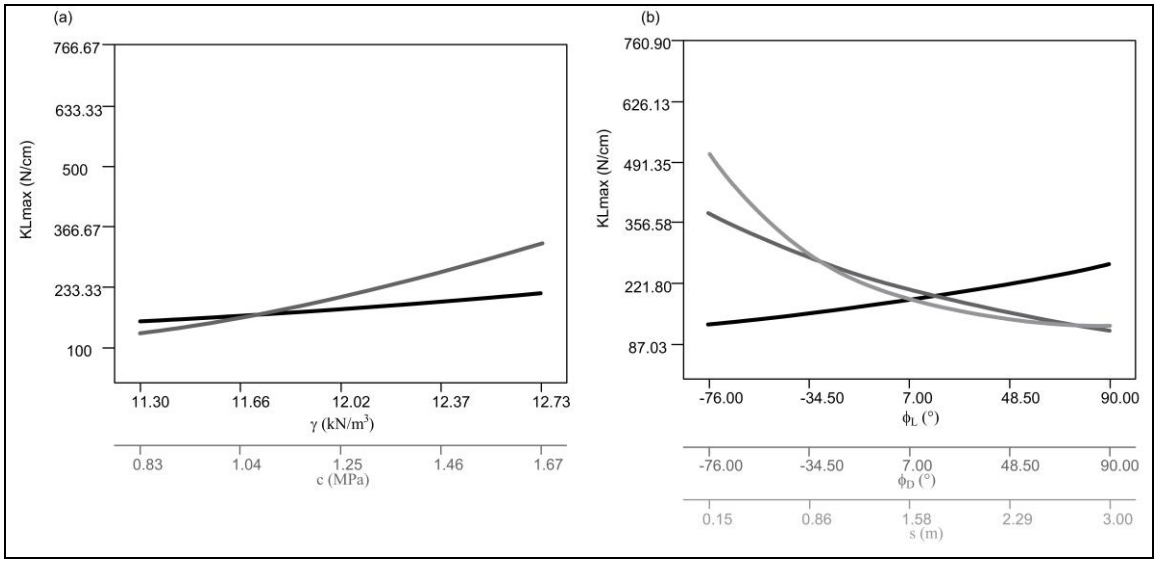

Figure 11. Effect of individual factors on K_{Lmax}: (a) K_{Lmax} as a function of γ and c; (b) K_{Lmax} as a function of φ_D, φ_L, and s. While a single parameter is varied, others are held at constant moderate values: γ = 12.02 kN/m^3, *c* = 1.25 MPa, φ_L = 7°, φ_D = 7°, *h* = 4.15m, *s* = 1.58m, σ_p = 5.19 MPa, φ = 43.33°.

Obtained results indicate the following effect of the examined input factors on $K_{Fmax,}$ Figure 12:

- Excavator movement angle in either direction and coal friction angle have almost no effect on K_{Fmax};
- Coal unit weight has a minor positive (increasing) effect on K_{Fmax}, which is the expected impact;
- Slice height has a significant positive (increasing) effect on K_{Fmax}, which is also expected;

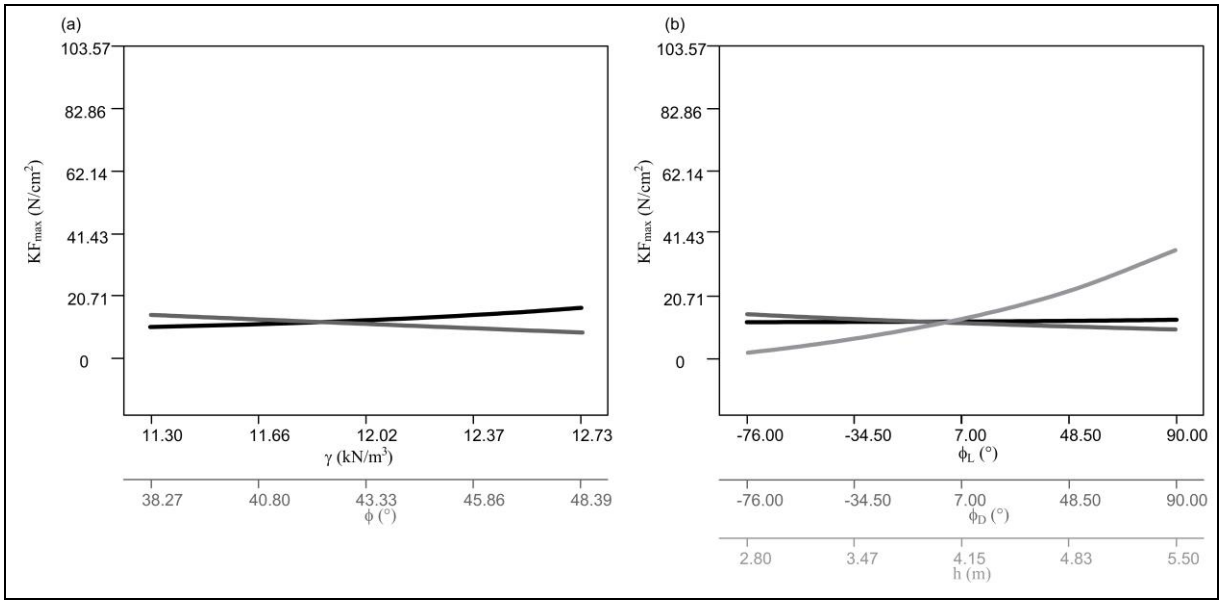

Figure 12. Effect of individual factors on K_{Fmax}: (a) K_{Fmax} as a function of γ and φ; (b) K_{Fmax} as a function of φ_D, φ_L and h. While a single parameter is varied, others are held at constant moderate values: γ = 12.02 kN/m^3, *c* = 1.25 MPa, φ_L = 7°, φ_D = 7°, *h* = 4.15m, *s* = 1.58m, σ_p = 5.19 MPa, φ = 43.33°.

CONCLUSIONS

In the present paper, we propose a new model for the estimation of coal cutting resistance and excavator performance based on the application of artificial neural networks. The developed model includes the following input parameters: slice height h (m), slice thickness s (m), coal unit weight γ (kN/m^3), coal compressive strength σ_p (MPa), coal cohesion c (MPa), and coal angle of internal friction φ (°), and the following output parameters: excavator effective capacity Q_{ef} (m^3/h), maximum current consumption I_{max} (A), maximum power consumption N_{max} (kW), maximum force consumption P_{max} (kN), maximum energy consumption E_{max} (kWh/m^3), excavator movement angle in the left direction φ_L(°), and excavator movement angle in the right direction φ_D (°), maximum linear cutting resistance K_{Lmax} (N/cm) and maximum areal cutting resistance K_{Fmax} (N/cm^2).

Statistical analysis of the obtained results indicates high statistical reliability of the developed model, with R>0.92. In contrast to our previous research [13], where we invoked the deep neural network approach, here we apply a multilayer perceptron feed-forward neural network, which results in the explicit mathematical expression for estimation of coal cutting resistance and excavator performance that could be further used in engineering practice.

Additionally, in the present paper, we provide a detailed analysis of the effect of statistically significant and physically possible individual factors on the examined output factors. In particular, the results of our analysis indicate the following:

- Effect of slice height h:
  - minor, but negative (decreasing) effect on Q_{ef},
  - minor positive effect on P_{max},
  - a slight positive (increasing) effect on E_{max},
  - a slight positive (increasing) effect on K_{Lmax};
  - a significant positive (increasing) effect on K_{Fmax}.

- Effect of slice thickness s:
  - the most significant predominant influence on Q_{ef},
  - a strong positive (increasing) effect on P_{max}.
- Effect of excavator movement angle in the left direction φ_L (°)
  - minor, but negative (decreasing) effect on Q_{ef},
  - a strong positive (increasing) effect on P_{max},
  - a slight positive (increasing) effect on E_{max};
  - a slight positive (increasing) effect on K_{Lmax},
  - almost no effect on Kfmax.
- Effect of excavator movement angle in the right direction φ_D (°)
  - minor, but negative (decreasing) effect on Q_{ef},
  - a strong negative (decreasing) effect on P_{max},
  - a slight negative (decreasing) effect on E_{max},
  - a significant negative (decreasing) effect on K_{Lmax}.
- Effect of coal unit weight γ (kN/m^3)
  - minor positive (increasing) influence on Q_{ef},
  - almost no effect on N_{max},
  - minor positive effect on P_{max},
  - almost no effect on E_{max},
  - a slight positive (increasing) effect on K_{Lmax},
  - a minor positive (increasing) effect on K_{Fmax}.
- coal compressive strength σ_p (MPa)
  - minor positive (increasing) influence on Q_{ef},
  - significant positive (increasing) effect on N_{max},
  - negative effect on Pmax for the lower range of values; for the upper range of values there is a positive (increasing) effect on P_{max},
  - almost no effect on E_{max}.
- coal cohesion c (MPa)
  - minor positive (increasing) influence on Q_{ef},
  - significant positive (increasing) effect on N_{max},
  - negative effect on Pmax for the lower range of values; for the upper range of values there is a positive (increasing) effect on P_{max},
  - almost no effect on E_{max},
  - a slight positive (increasing) effect on K_{Lmax}.

The coal friction angle has almost no influence on any of the examined output factors.

The presented approach and developed model could be further utilized for smart planning of open-pit coal mining and optimization of the excavation process. The performance of the developed model could be improved and made for general use if a larger dataset is examined in the succeeding studies.

Received September 2023, accepted November 2023)

REFERENCES

[1] https://www.forbes.com/sites/cindygordon/2021/07/31/ai-innovations-in-mining/?sh=72466dee4ec0
[2] https://www.prescouter.com/2020/08/smart-mining-how-artificial-intelligence-can-benefit-the-mining-industry/
[3] Bui, X., Bui, H., Nguyen, H. (2020). A Review of Artificial Intelligence Applications in Mining and Geological Engineering. Proceedings of the International Conference on Innovations for Sustainable and Responsible Mining. Part of the Lecture Notes in Civil Engineering book series (LNCE, volume 109)
[4] Shrivastava P., Pradhan, G.K. (2022). Use of Artificial Intelligence in Mining: An Indian Overview. International Congress and Workshop on Industrial AI 2021. Part of the Lecture Notes in Mechanical Engineering book series (LNME).
[5] Wang, G., Ren, H., Zhao, G., Zhang, D., Wen, Z., Meng, L., Gong, S. (2022). Research and practice of intelligent coal mine technology systems in China. International Journal of Coal Science & Technology 9:24.

[6] Azhari, F., Sennersten, C., Lindley, C., Sellers, E. 2023. Deep learning implementations in mining applications: a compact critical review. Artifcial Intelligence Review https://doi.org/10.1007/s10462-02310500-9

[7] Yang, W., Xiaohong, X. (2013). Prediction of mining subsidence under thin bedrocks and thick unconsolidated layers based on field measurement and artificial neural networks. Computers and Geosciences, 52, 199 – 203.

[8] Panigrahi, D.C., Ray, S.K. (2014). Assessment of self-heating susceptibility of indian coal seams - A neural network approach. Archives of Mining Sciences 59, 4, 1061 – 10761.

[9] Mlynarczuk, M., Skiba, M. (2017). The application of artificial intelligence for the identification of the maceral groups and mineral components of coal. Computers and Geosciences, 103, 133 – 141.

[10] Wilkins, A., Strange, A., Duan, Y., Luo, X. (2020). Identifying microseismic events in a mining scenario using a convolutional neural network. Computers and Geosciences, 137, 104418.

[11] Jiang, B., Zhang, K., Liu, X., Lu, Y. (2023). Prediction model with multi-point relationship fusion via graph convolutional network: A case study on mining-induced surface subsidence. PLoS ONE, 18, 8, e0289846.

[12] Qi, Q., Yue, X., Duo, X., Xu, Z., Li, Z. (2023). Spatial prediction of soil organic carbon in coal mining subsidence areas based on RBF neural network. International Journal of Coal Science and Technology, 10, 1, 30.

[13] Ignjatović, D. (2003). Study on optimization of the construction of buckets of the buecket-wheel excavator in order to increase the capacity of the excavator. University of Belgrade Faculty of Mining and Geology (In Serbian), pp. 218. doi: 10.1371/journal.pone.0289846

[14] Kostić, S., Stojković, M., Ilić, V., Trivan, J. (2023). Deep Neural Network Model for Determination of Coal Cutting Resistance and Performance of Bucket-Wheel Excavator Based on the Environmental Properties and Excavation Parameters. Processes 11, 3067. https://doi.org/10.3390/pr11113067

CONSTRUCTION

Deformations of the brige
reinforced concrete slab strengthening

Editors

Prof. Ph.D. Dragan Lukić
Prof. Ph.D. Miroslav Bešević

Original Scientific article
http://dx.doi.org/10.59456/afts.2023.1529.023C

TIME DEPENDENT DEFORMATIONS OF A COUPLED BRIDGE: A CASE STUDY

Cumbo Anđelko[1], Folić Radomir[2]

[1]*Faculty of Architecture, Civil Engineering and Geodesy, University of Banjaluka, Republic of Srpska, Bosnia and Herzegovina, e-mail: andjelko.cumbo@aggf.unibl.org*
[2]*Department of Civil Engineering and Geodesy, Faculty of Technical Sciences, University of Novi Sad, Serbia*

ABSTRACT

The bridge's span structure comprises a connected beam designed to support a concrete slab poured over parallel steel supports. Simultaneously, segmental construction, shrinkage, and the flow of concrete play a significant role in stress redistribution over time. The span construction is statically indeterminate due to its connections with the abutments, and temporal deformations occur under additional complex conditions. In this analysis, we employed a calculation model based on the layered finite elements method developed by the authors. This model can be utilized to analyse both statically indeterminate supports and the predicted phased construction method. It accounts for changes in the static system and loading, as well as variations in the layers within the coupled section and the viscous properties of the concrete over time. The calculation analysis results reveal that viscous concrete deformations, combined with different moments of activation of individual segments, have a significant impact on stress redistribution over time. Such intricate analyses are indispensable for ensuring the required safety and cost-effectiveness of the bridge span construction.

Key words: *composite bridges, creep and shrinkage of concrete, phased construction, effective width, finite element method.*

INTRODUCTRION AND SUMMARY OF LITERATURE

Coupled steel-concrete (CS-C) structures are commonly employed in both buildings and bridges. In bridges, it is typical to utilize span-jointed beams, which are created by pouring a concrete slab over parallel steel girders. Simultaneously, the connection between the steel supports and the concrete slab is established using tie rods. This approach results in the formation of a rational and cost-effective configuration for the span beam, leveraging the advantages of the high tensile load capacity of the steel support and the high compressive strength of the concrete [1]. This construction method yields beams characterized by significant load-bearing capacity and substantial rigidity [2]. The benefits of employing such structures manifest in terms of cost-effectiveness, construction speed, and safety. The composite cross-section consists of two distinct materials: steel, exhibiting elastic behaviour, and concrete, which displays viscous properties due to shrinkage and flow. These rheological phenomena in concrete induce alterations in internal forces, deflections, and their redistribution under the working loads applied to the coupled beam. This holds true for both statically determinate and statically indeterminate systems.

The international code provisions are used for the designing of composite bridges. In the USA it is [3], and in Europe those are, primarily, Eurocode [4] and [5], and in New Zealand, the reference [6] is used. Prediction and inclusion of the shrinkage and creep of concrete uses the provisions of [4]

documents [7] and [8], and in the USA [9], as well as the reference [10]. The comparative analysis of European and US codes is the subject matter of [10], for the creep function is suggested by the ACI [9]. Particularly important are the guidelines for the application of Eurocodes provided in [12] and [13]. A status review related to the conceptual designing of composite bridges (CB) is discussed in [14], and designing and analysis in [15].

The subject matter of the paper [1] is the review of the time-dependent behaviour of CS-C bridges, and the general design approach, along with the analysis of the construction phases were described in [16]. Effects of time-dependent behaviour of concrete based on the coupling of the FEM with a numerical solution of the hereditary Volterra integral equations were discussed. A similar paper is also [17] in which the effects temperature changing and concrete creep CS-C bridges and behaviour during construction and operation periods were discussed. The master theses [18] are also worth mentioning, as they provide general consideration on the designing of CS-C bridges, and in [19] are present the analysis of the effects of shrinkage and creep of concrete in S-C composite beams, mainly based on the use of Eurocodes. In the paper [20] are considered the effects of redistribution in the linear elastic analysis of a continuous composite beam according to Eurocode 4, and in the paper [21] there is a non-linear analysis of the time-dependent behaviour of a composite beam. A mixed FE model for nonlinear analysis with partial shear connection was used and it was shown that the interaction between cracking and time effects significantly increases the deformation. The factors affecting the shrinkage and creep of concrete and the guidelines for their modelling were described in [22], and there are also useful data in the Proceedings of the workshop [23].

In the analysis of the composite steel-concrete bridges is used the effective width of the slab in order to employ the linear elements in the bridge analysis. It was stipulated in the provisions of Eurocode 4, and a more accurate analysis was presented in the papers [24,25,26]. In [25] it was indicated that the results calculated according to EN 1994 are not always sufficiently conservative, so significant structures require an in-detail analysis, most often created using the Finite Element Method. A comparative analysis of the expressions for determining the effective width recommended in the AASHTO, EC54, and norms of Brazil and China is presented in [30]. Also, it is recommended to use the reference [8] for the assessment of creep and shrinkage rate, and the use of the ACI model predicted the highest concrete shrinkage.

The results of the extensive research from Australia, about the time-dependent behaviour of a composite simple beam were described in the Report [27]. Similar results were presented in the paper [28]. The effects of time-dependent deformations for the perfect connection of the steel beam and the concrete slab were described in [29]. Results of the finite element method analysis for the ultimate limit state, and time-dependent behaviour were presented in [30]. The results of the analysis of simulation methods using the finite element method are the subject of the paper [31]. In the paper [32] the simplified analysis methodology was described, and the accuracy aspect of the results was discussed. In the paper [33] a simplified algorithm for the simple composite beam was developed, and in the paper [34] the experimental results for the negative zone of bending moments of the specially reinforced road deck were described. The subject of the paper [35] is studying the impact of the shear creep for the analysis of long-term deformations of a long span concrete beam. A special case of formation of composite beams, Preflex and Flexstress beams, with different phases of formation of composite beams and their analysis were provided in the paper [36]. Steel I beams, in addition to the top reinforced concrete slab also have a bottom slab, i.e., concreted bottom flange.

One of the composite bridges is the subject of this paper, and it is the new road bridge across the Vrbas river on the approach to the city of Banjaluka (B and H) which was in accordance with the local prescribed requirements, technical norms and professional rules (Figure 1). The bridge is located perpendicular to the river, having a static span of 6.0+50.0+6.0 m, with a two-way traffic, and the total width of 11.0 m. The shallow foundations of caisson abutments lie on the soil having sound engineering and geological properties. The spanning structure is a continuous steel-concrete composite beam (two steel I beams of variable height 160-250 cm, with transverse beams and stiffeners; the 25-35 cm thick reinforced concrete (RC) road deck was concreted on top of this structure. The spanning structure is in fact an elastically restrained beam. The length of the medium span is considerably higher than the end spans, which forms a couple reactions in the abutments. These reactions are

absorbed by the massive caisson abutments which act as counterweights during the console construction of the bridge, but also in operation. The position, symmetrical proportions and appearance of the bridge make it fit well into the natural environment of the location.

Figure 1. Road bridge over the Vrbas river, Banjaluka

During the development of the project, the authors performed a control calculation analysis of the stress-deformation state of the coupled span structure of the bridge. All relevant phases which included the segmental procedure of construction with a special emphasis on shrinkage and creep of concrete were analysed.

In this paper, in addition to a brief review of the literature, the theoretical bases for the analysis, which were previously developed by the author, are briefly presented [37,38]. The necessary input data for the analysis were listed, as well as the results of calculation for the composite spanning structure – beam. The results for all the phases of analysis were discussed, and based on them the appropriate conclusions were drawn.

ANALYSIIS METHODOLOGY

Theoretical Basis for Calculating the Effects of Shrinkage and Flow of Concrete

Bridges are often constructed in phases using coupled steel-concrete span structures. These phases involve changes in the geometry of the elements, the static system, and the loads at various time intervals, resulting in alterations in the state of stress and deformation within the elements. The shrinkage and flow of concrete, along with the emergence of cracks in the tensioned zone, lead to a redistribution of stresses and deformations in the coupled structure. This necessitates the introduction of varying time intervals for the inclusion or exclusion of individual elements or their layers in tension activities, taking into account all their viscoelastic material properties. This is crucial due to the phased construction process and, additionally, the static indeterminacy of the structure, which can lead to changes in forces within the structure without altering the external load.

To address these challenges, the authors developed a computational algorithm utilizing layered finite elements (FE) [37] and [38]. Through appropriately defined layers, the rheological properties of concrete are incorporated in the form of a fictitious load, enabling the analysis of statically indeterminate coupled structures. Incremental forms of the stress-strain relationship were applied to all different materials. The computational algorithm accommodates both discontinuous and continuous changes (in the static system, geometry, load, and rheology) across fictitious $(\Delta t_k = 0)$ and finite $(\Delta t_k \neq 0)$ time intervals. The solution is obtained by solving a system of algebraic equations in matrix form using the finite element method (FEM). This computational algorithm has been validated against a substantial number of examples from the literature, confirming a very good agreement of the results.

In general, the calculation model comprises rigidly coupled layered elements and assumes a linear stress-strain relationship for concrete $(\sigma_c \leq 0.4 f_{ck})$, adhering to the hypothesis of flat sections and the linear theory of concrete flow.

In the expressions presented here, symbols are introduced for common materials constituting the coupled elements (a-structural steel, c-concrete, s-reinforcement), Therefore, the deformation of the observed fiber within the coupled cross-section during the current time interval (Δt_k) is valid for the incremental equation (in matrix form):

$$\Delta\varepsilon_k = [\Delta\varepsilon_r \quad \Delta\kappa]_k \cdot \begin{vmatrix} 1 \\ y \end{vmatrix}_k \tag{1}$$

Here:

$\Delta\varepsilon_k$ – Deformation of the observed fiber cross-section,

$\Delta\varepsilon_{r,k}$ – Expansion of the fiber at the level of the reference axis of the cross-section ($y = 0$),

$\Delta\kappa_k$ – Curvature of the cross-section,

y – Distance of the observed fiber from the reference axis r.

For the adopted linear relationship between stress parameters ($\Delta\alpha_{r,k}$ and $\Delta\beta_k$) and deformation ($\Delta\varepsilon_{r,k}$ and $\Delta\kappa_k$), the constitutive relationship for structural steel and reinforcement (both elastic materials) is as follows:

$$\begin{vmatrix} \Delta\alpha_r \\ \Delta\beta \end{vmatrix}_{a,k} = E_a \cdot \begin{vmatrix} \Delta\varepsilon_r \\ \Delta\kappa \end{vmatrix}_{a,k} \quad ; \quad \begin{vmatrix} \Delta\alpha_r \\ \Delta\beta \end{vmatrix}_{s,k} = E_s \cdot \begin{vmatrix} \Delta\varepsilon_r \\ \Delta\kappa \end{vmatrix}_{s,k} \tag{2}$$

The constitutive relationship for concrete (a viscous material) takes the following form:

$$\begin{vmatrix} \Delta\alpha_r \\ \Delta\beta \end{vmatrix}_{c,k} = E_{c(k,k-1)} \cdot \left(\begin{vmatrix} \Delta\varepsilon_r \\ \Delta\kappa \end{vmatrix} - \begin{vmatrix} \Delta\varepsilon_r^* \\ \Delta\kappa^* \end{vmatrix} \right)_{c,k} \tag{3}$$

In contrast to structural and reinforcing steel, which are assumed to exhibit elastic stress-strain relationships, concrete, as a viscous material, introduces an additional deformation known as “free deformation.” This accounts for viscous time-dependent deformations as follows:

$$\begin{vmatrix} \Delta\varepsilon_r^* \\ \Delta\kappa^* \end{vmatrix}_{c,k} = \sum_{i=1}^{k-1} \frac{1}{E^*_{c(k,i-1)}} \cdot \begin{vmatrix} \Delta\alpha_r \\ \Delta\beta \end{vmatrix}_{c,i} + \begin{vmatrix} \Delta\varepsilon_{cs} \\ 0 \end{vmatrix}_k \tag{4}$$

Here:

$E_{c(k,k-1)}$ – Effective generalized concrete deformation modulus.,

$E^*_{c(k,i-1)}$ – Effective derived concrete deformation modulus,

$\Delta\varepsilon_{cs,k}$ – Deformation due to shrinkage of concrete (constant for the height of the cross-section).

The deformation moduli depend on the concrete yield function applied and the type of numerical integration, following the relationship:

$$\frac{1}{E^*_{c(k,i-1)}} = \frac{1}{E_{c(k,i-1)}} - \frac{1}{E_{c(k-1,i-1)}} \quad ; \quad i = 1,2,\dots,k-1 \tag{5}$$

The generalized form of the constitutive stress-strain relation (3) allows for the application of various concrete flow function forms. The AAEM method [10] is implemented as follows:

$$\frac{1}{E_{c(k,i-1)}} = 1 + \chi_{(k,i-1)} \cdot \varphi_{(k,i-1)} \quad ; \quad i = 1,2,\dots,k \tag{6}$$

Here:

$\chi_{(k,i-1)}$ – Correction coefficient of concrete flow (aging coefficient),

$\varphi_{(k,i-1)}$ – Flow coefficient of concrete, ($i = 1,2,\dots,k$).

Expression (4) calculates the “free deformations” of the concrete within the k-th interval, considering stress from all previous intervals Δt_i, ($i = 1,2,\dots,k-1$), and the deformations from the shrinkage of

concrete that takes place in the current interval (Δt_k). This approach unifies calculations across all fictitious and finite time intervals, accounting for varying geometric and material properties and external influences.

The incremental relationship between deformation and forces in the cross-section can be expressed as follows:

$$\mathbf{K}_k \cdot \left|\begin{matrix}\Delta\varepsilon_r \\ \Delta\kappa\end{matrix}\right|_k = \left|\begin{matrix}\Delta N \\ \Delta M\end{matrix}\right|_k - \left|\begin{matrix}\Delta N^* \\ \Delta M^*\end{matrix}\right|_{c,k} \tag{7}$$

Here:

K_k – Matrix of stiffness for the coupled cross-section (the sum of contributions from steel, reinforcement, and concrete),

ΔN_k , ΔM_k – Normal force and bending moment in the cross-section due to external loads,

$\Delta N^*_{c,k}$, $\Delta M^*_{c,k}$ – Fictitious normal force and fictitious bending moment in the cross-section resulting from shrinkage and flow of concrete.

For statically determined supports, it would be sufficient to use expression (7) because it allows for the determination of deformations and normal stresses in the cross-section. However, in the case of statically undetermined constructions, forces within the cross-sections change due to the rheological properties of the concrete, even when there is no change in the external load. In such cases, calculations of the state within the cross-section may not yield authoritative results. Therefore, there is a need to develop a complete construction algorithm, and for this purpose, the finite element method (FEM) is highly suitable.

In accordance with FEM principles, all parameters are associated with nodal points (e.g., displacements: $\Delta u, \Delta v, \Delta\varphi$, forces: $\Delta N, \Delta T, \Delta M$). For a single finite element (FE), the incremental relationship between the deformation magnitudes at the field points of the element ($\Delta\varepsilon_r$ and $\Delta\kappa$) and the displacement vector of its nodes ($\mathbf{\Delta q}_r$) is expressed as follows:

$$\left|\begin{matrix}\Delta\varepsilon_r \\ \Delta\kappa\end{matrix}\right|_k = \mathbf{B}_{r,k} \cdot \mathbf{\Delta q}_{r,k} \tag{8}$$

Here, $B_{r,k}$ represents the shape function, which is the element field matrix for the reference axis r.

By applying the established theoretical principles upon which the FEM is founded, we derive the fundamental equation for the coupled viscous FE in the following form:

$$\mathbf{K}_k \cdot \mathbf{\Delta q}_{r,k} = \mathbf{\Delta Q}_k - \mathbf{\Delta Q}^*_{c,k} \tag{9}$$

Where:

K_k – Stiffness matrix of the coupled finite element (sum of contributions from all layers),

$\Delta q_{r,k}$ – Displacement vector of FE nodes for reference axis r $(\Delta u, \Delta v, \Delta\varphi)$,

ΔQ_k – Vector of external forces at FE nodes $(\Delta N, \Delta T, \Delta M)$,

$\Delta Q^*_{c,k}$ – Vector of fictitious forces at FE nodes $(\Delta N^*, \Delta T^*, \Delta M^*)$ arising from concrete flow and shrinkage.

To model the entire construction system, it is essential to establish a FE network. In such a network, the stiffness matrix and force vectors (9) of all FEs are combined in accordance with the principles of FEM (finite element method), connecting nodes within the overall network of FEs. By solving the system of algebraic equations, we can determine the global displacement vector of the nodes, subsequently allowing for the analysis of the required deformation components for each FE within their local systems:

$$\left|\begin{matrix}\Delta\varepsilon_r \\ \Delta\kappa\end{matrix}\right|_k = \mathbf{B}_{r,k} \cdot \mathbf{\Delta q}_{r,k} + \left|\begin{matrix}\Delta\varepsilon_N \\ -\Delta\kappa_M\end{matrix}\right|_k \tag{10}$$

Where:

$\Delta\varepsilon_{N,k}$ – Part of the deformation resulting from the averaging of fictitious normal forces of the observed FE,

$\Delta\kappa_{M,k}$ – Part of the curvature originating from the external distributed load in the element's field, transformed into nodes.

The total stresses and strains for a discrete moment in time are determined through a step-by-step superposition process [38].

Settings for the Coupled Beam Analysis

Based on the longitudinal and transverse cross-section of the bridge (Figure 2), it was assumed for the static calculation that the continuous span beam consists of a steel beam (SB) of varying cross-section and a subsequently cast concrete slab, which forms a composite T-section (Figure 3). Simultaneously, SB is longitudinally extended using a system of segmental cantilever construction in three phases, symmetrically on both sides of the bridge (Figure 4). After that, the slab is reinforced and cast, also symmetrically by segments in three phases (Figure 4), starting with the central segment and then the segments towards the ends of the bridge, every 10 days. The paving and other finishing works complete the construction of the bridge, which introduces an additional permanent (dead) and moving (live) load (Figure 4). All the aforementioned phases of construction define a possible change in the static system and in the geometry of the elements, as well as a change in the load and rheology of concrete.

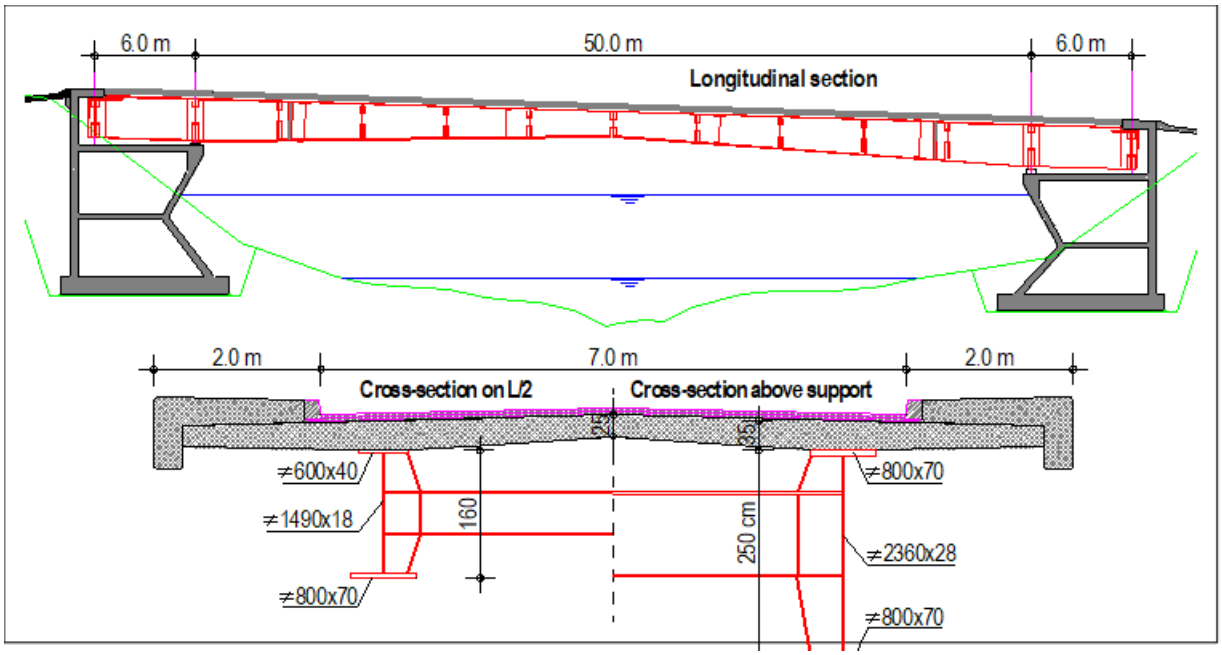

Figure 2. Longitudinal and transverse cross-sections of the bridge (mid-span and above the point of support)

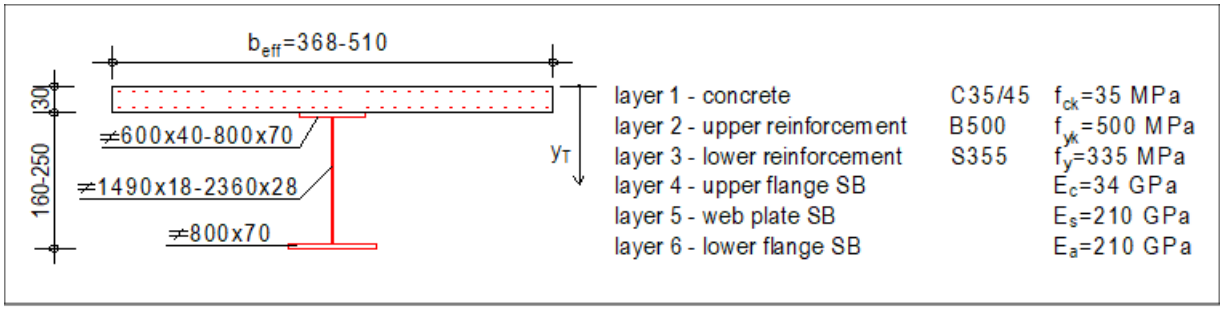

Figure 3. Alternative cross – sections of the composite beam

The data necessary for the analysis (material characteristics, phased loads, and element geometry) are given in the figures. Figure 4 illustrates the static systems and loads across different time intervals. The activation of the load and the adjustment of the FE stiffness align with the actual conditions during the phased segmental construction and bridge operation.

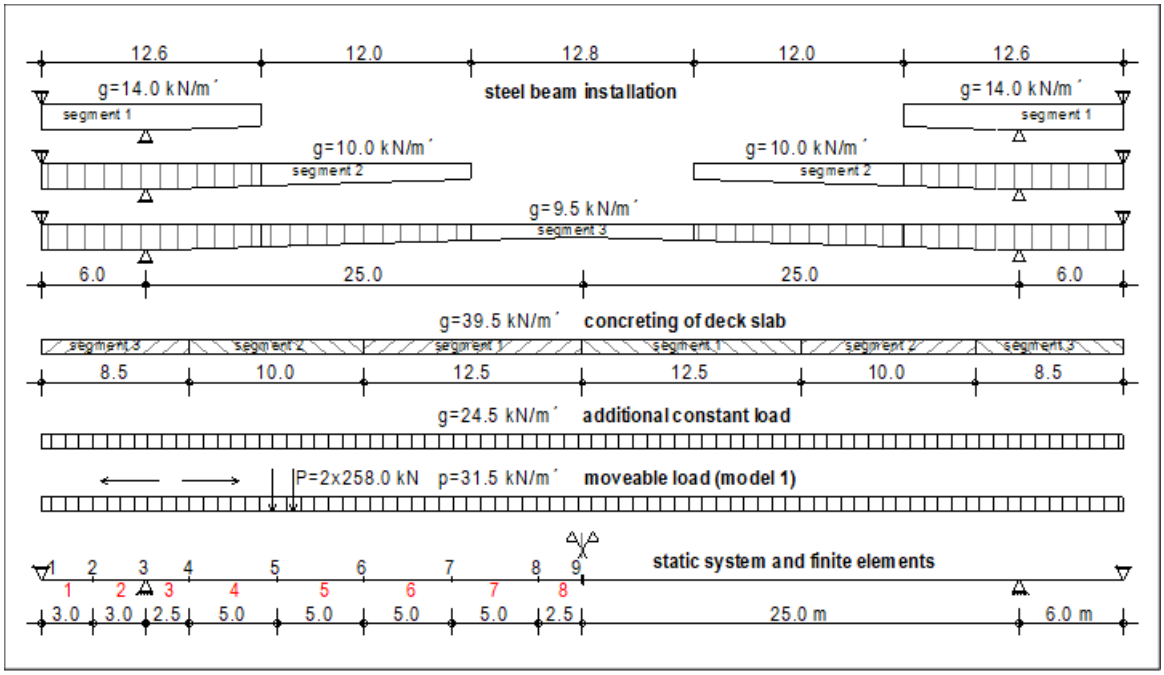

Figure 4. Phases of steel beam installation and slab casting,
additional dead and live loads, static system, and finite elements

The analysis of the span structure of the bridge with the introduced rheological properties (rheology) of concrete was carried out for the period from the beginning of construction up to 10,000 elapsed days, and for different states of stiffness of the concrete slab (non-cracked and cracked zone of tensioned concrete). In doing so, the total time period was divided into 14 intervals in accordance with the adopted construction technology and the load on the span structure of the bridge (Table 1). The finite elements (FE) mesh was formed for half of the symmetrical beam, and the corresponding geometric characteristics of the elements were calculated for them (Figures 3 and 4).

Table 1. Flow of calculation analysis of the characteristic construction phases

Time		Flow of activities	FE/layer
$\Delta t_1=0$	$t_1=0$	Fitting of SB – segment 1	(1-4)/(4-6)
$\Delta t_2=0$	$t_2=0$	Fitting of SB – segment 2	(1-6)/(4-6)
$\Delta t_3=0$	$t_3=0$	Fitting of SB – segment 3	(1-8)/(4-6)
$\Delta t_4=0$	$t_4=10$	Concreting – segment 1	(1-8)/(4-6)
$\Delta t_5=10$	$t_5=20$	Concrete Rheology (time-dependent changes)- segment 1	(1-5)/(4-6) (6-8)/(1-6)
$\Delta t_6=0$	$t_6=20$	Concreting – segment 2	(1-5)/(4-6) (6-8)/(1-6)
$\Delta t_7=10$	$t_7=30$	Concrete Rheology (time-dependent changes)- segment 1+2	(1-3)/(4-6) (4-8)/(1-6)
$\Delta t_8=0$	$t_8=30$	Concreting – segment 3	(1-3)/(4-6) (4-8)/(1-6)
$\Delta t_9=25$	$t_9=25$	Concrete Rheology (time-dependent changes)- segment 1+2+3	(1-8)/(1-6)
$\Delta t_{10}=0$	$t_{10}=25$	Additional dead load	(1-8)/(1-6)
$\Delta t_{11}=310$	$t_{11}=365$	Concrete Rheology (time-dependent changes)	(1-8)/(1-6)
$\Delta t_{12}=635$	$t_{12}=1000$	Concrete Rheology (time-dependent changes)	(1-8)/(1-6)
$\Delta t_{13}=9000$	$t_{13}=10000$	Concrete Rheology (time-dependent changes)	(1-8)/(1-6)
$\Delta t_{14}=0$	$t_{14}=10000$	Live load	(1-8)/(1-6)

The rheological characteristics of the beam concrete were calculated in accordance with EC2. In this case, for RH=80%, the maximum values of the coefficient of creep and shrinkage were assumed to be $\varphi_{(\infty,10)} = 1.75$ and $\varepsilon_{cs(\infty,10)} = 0.24$ ‰ respectively. All intermediate values, for the relative time relations between discrete moments, are calculated as increments. The calculation analysis was carried out using the established computer algorithm.

The concrete slab with creep and shrinkage properties was calculated assuming different ages of concrete and non-cracked and cracked variants.

ANALYSIS OF CALCULATION RESULTS

After the analysis, the results are provided in the form of deflection diagrams along the beam and stress diagrams in relevant cross-sections (mid-span and support cross-section) for cracked and non-cracked concrete in the tensioned support zone (Figures 5-9).

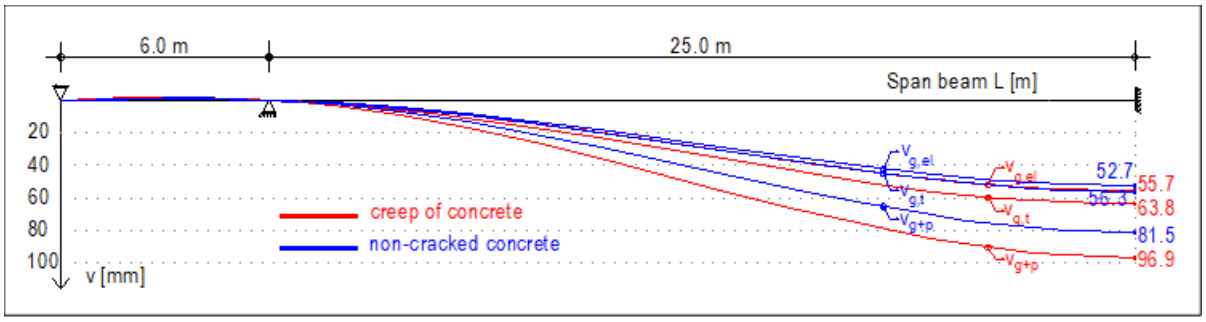

Figure 5. Deflections along the composite beam

Deflections along the beam, with all discrete intervals summed up (Δt_1+ Δt_2+ Δt_3+ Δt_4+ Δt_6+ Δt_8+ Δt_{10}) which include the elastic discontinuous effects of the dead load, have the expected values. In the middle of the range for sprayed concrete (Figure 5), this deflection is $v_{g,el}$=55.7 mm, which corresponds to approximately L/900. The effects of shrinkage and flow in the pressed concrete contributed to an increase in deflection of 14.5%, resulting in a value of $v_{g,t}$=63.8 mm.

When considering the impact of a moving load, the total deflection at L/2 is v_{g+p}=96.9 mm (approximately L/500). This deflection needs to be elevated with the camber level in the phase of fitting the segments of the plate supports. In the case of the non-cracked concrete, the deflections are lower, so in L/2, this deflection is v_{g+p}=81.5 mm, which is a decline of 16% compared to the state of the cracked concrete (Figure 5).

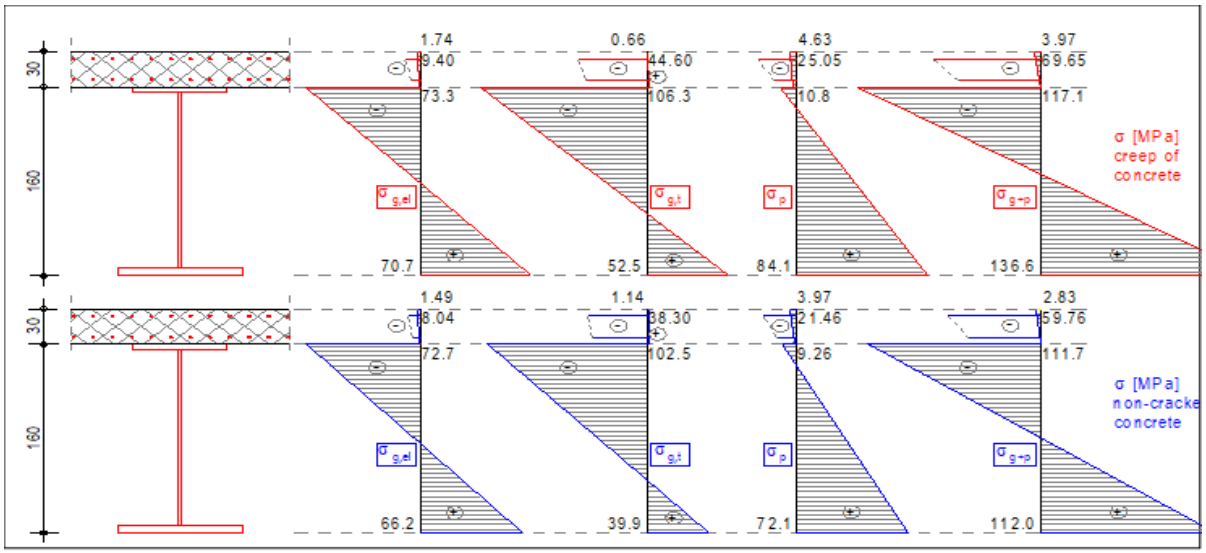

Figure 6. Stresses in the cross-section of the composite beam at L/2

When it comes to the normal stresses in the mid-span cross-section of the cracked tensioned concrete (Figure 6), a significant influence of the viscous behaviour of concrete on the change of these stresses in all layers of the section is visible.

The concrete layer was unloaded to such an extent that it went from a slightly compressed state to a tensile state (from -1.74 to +0.66 MPa), and due to this redistribution of the stress, the reinforcement in the concrete and the top flange LN suffered a significant increase in compressive stress (reinforcement from -9.40 to - 44.60 MPa which is an increase of 4.7 times, the top flange from -73.3 to -106.3 MPa, which is an increase of 45%). At the same time, the tensile stresses on the bottom flange LN decreased (from +70.7 to +52.5 MPa, which is a decrease of 25.7%).

These stresses, summed up with the contribution of the live load, indicate a sufficient reserve in terms of the utilization of individual layers/materials for normal stresses. For non-cracked concrete, the stresses in all layers are lower compared to the condition of the cracked tensioned concrete (Figure 6).

When it comes to the redistribution of stresses in L/2 over time (Figure 7) it is visible that the changes are more intensive in the initial intervals, when the concrete is less aged, in contrast to the slower increase of the aged concrete, for example, after 3 years.

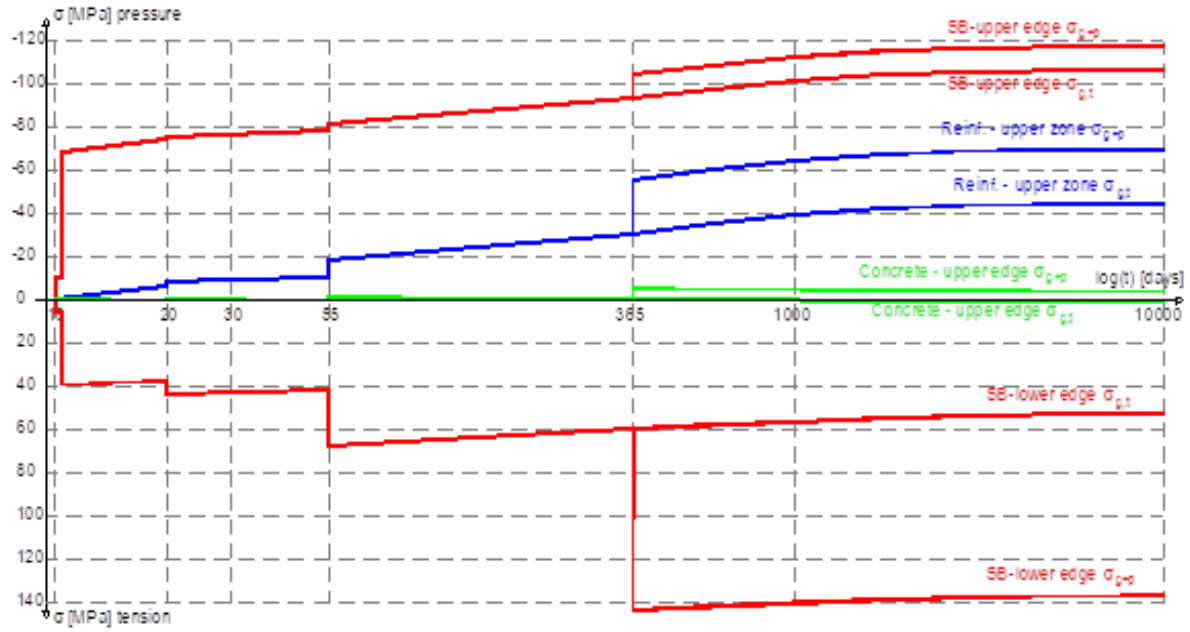

Figure 7. Stresses in the cross-section in L/2 over time, cracked tensioned concrete

In the case of normal stresses of the cross-section of the support (Figure 8), a slightly smaller influence of the viscous behaviour of concrete on the change of these stresses was recorded compared to the cross-section in L/2. This is somewhat expected considering that the tensioned cracked layer, which is excluded from the bearing capacity, is located directly above the observed support cross-section. In all other active layers, the normal stresses increased (reinforcement from +27.9 to +40.3 MPa, which is an increase of 44.4%, top flange from +97.2 to +109.7 MPa, which is an increase of 12.9%, bottom flange from -103.4 to -118.7 MPa, which is an increase of 14.8%).

These stresses, summed up with the contribution of the live load, indicate the efficient utilisation of individual layers/materials for normal stresses. For non-cracked tensioned concrete, the stresses in all layers are lower compared to the state of the cracked concrete (Figure 8). This especially applies to the upper layers closer to the active concrete (reinforcement and top flange LN), which is why the neutral axis is significantly shifted upwards.

When it comes to the redistribution of stresses in the support cross-section over time (Figure 9), as in the L/2 cross-section, the changes are more intensive when the concrete is less aged, in contrast to the slower increase of the aged concrete, e.g., after 2-3 years

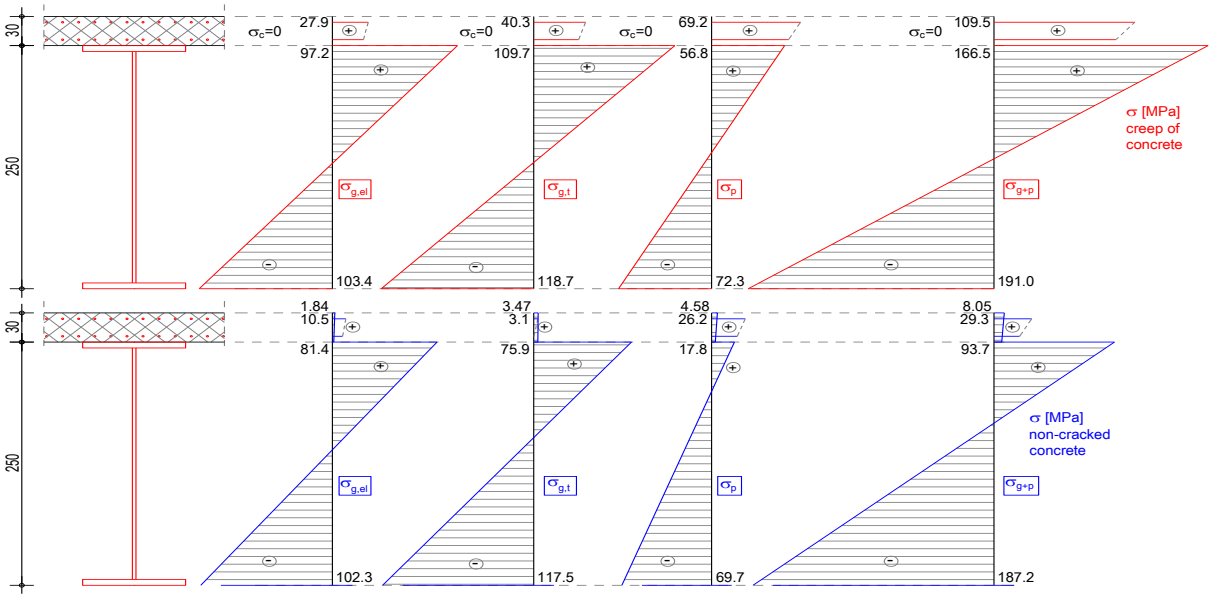

Figure 8. Stresses in the cross-section of the composite beam support

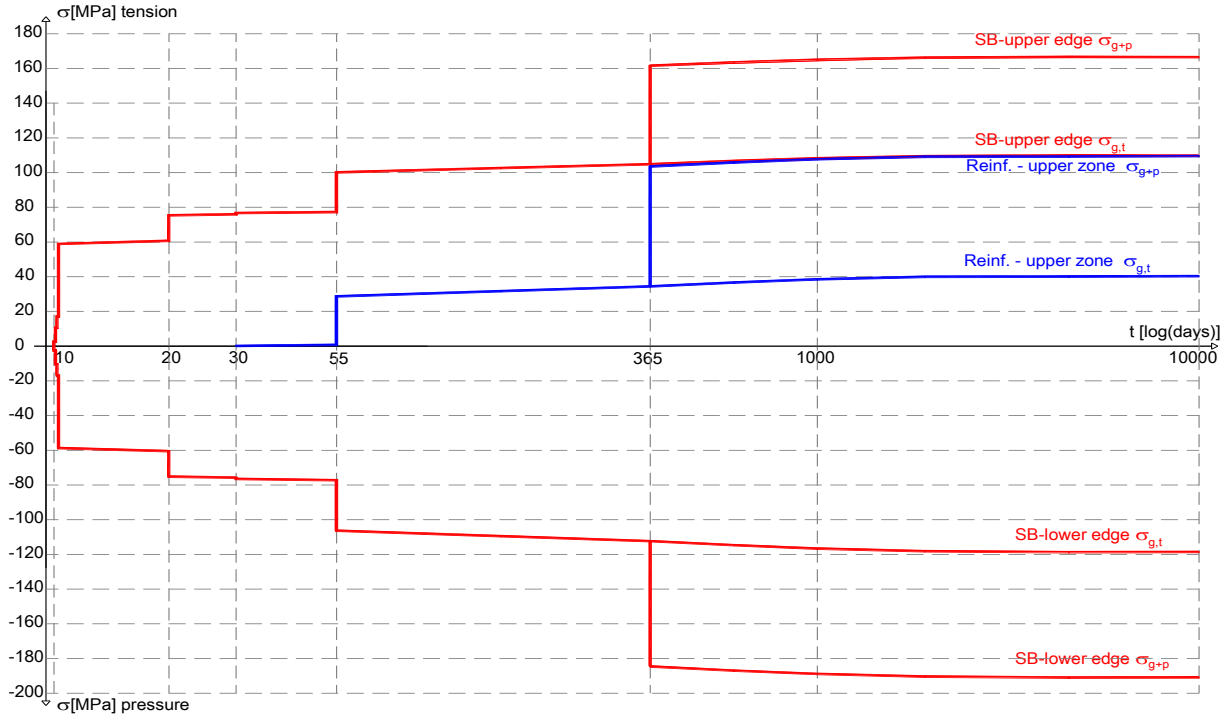

Figure 9. Stresses in the cross-section above the support over time, cracked tensioned concrete

In general, the presented calculation analysis results show that the viscous properties of the concrete slab caused a considerable redistribution of stress between the composite layers along the span of the bridge beam. At the same time, this redistribution takes place in the form of unloading of concrete and additional stress of the steel parts.

CLOSING REMARKS AND CONCLUSION

The additional analysis of the spanning structure of the bridge, which considers the rheological properties, i.e., shrinkage and creep of concrete included the period from the start of the construction to the age of 27.4 years. The stiffness of the concrete slab is analysed for the cross-section without cracks (according to EN 1994-1-1 [39]) and for the cross-section with cracks in the zone of tensioned concrete.

In concrete without cracks, the stresses in all layers are lower compared to the condition with cracks in the tensioned zone. It is shown that the redistribution of the stress, mid-span, is more intensive over time for the less aged concrete. However, even the stresses obtained in this way are within the permissible limits, and at the same time, they were conservative in terms of safety, in the procedure of beam designing.

Based on the analysis results of the coupled bridge in question, it can be concluded that the designed structure meets all safety, economic, and aesthetic requirements. Yet, it was shown that, in order to obtain a more realistic understanding of the behaviour of the composite spanning beam over time, it is necessary to include the creep and shrinkage of concrete in the design. The time-dependent of stresses and deformations considerably contribute to their redistribution, which is necessary to take into consideration when designing the structure. It is also demonstrated that it is not justified to introduce the full stiffness of tensioned concrete in the analysis, because one may obtain results that considerably depart from the actual status.

The design mode according to FEM (developed by the author) employed in the case study, in the framework of the introduced assumptions, makes it possible to analyse different cases in engineering practice when it comes to the control of the limit states of serviceability. The model is generalized and includes statically indeterminate structures with the rigidly composed layer elements. In the process, the real procedures during construction and operation are introduced, in the form of the change of the static system, load, geometry, and rheological properties of the beam.

Received September 2023, accepted October 2023)

REFERENCES

[1] Ranzi, G., Leoni, G., Zandonini, R.: State of the art on the time-dependent behaviour of composite steel-concrete structure, Journal of constructional steel research, 80, 2013, 252-263.
[2] Ding, M., Jiang, X., Lin, Z:, Ju, J.: Long-term stress of simply supported steel-concrete compozite beams, The Open Construction and Building Technology J., 2011, 5, pp. 1-7.
[3] AASHTO LRFD Bridge design specifications, SI Units, 4th Edition, 2007.
[4] Eurocode 2: 2004. Design of Concrete Structures – part 1-1: General rules and rules for buildings – EN 1992-1-1:2004, European Committee for Standardization, Brussels.
[5] Eurocodes 3 and 4 – Application to steel-concrete composite road bridges, Guidance book, Sétra, Department of the French Ministry of transport, France, 2007.
[6] El Sarraf, R., Iles, D., Montahan, A., Easey, D., Hicks, S.: Steel-concrete composite bridge design guide, NZ Transport Agency research report 525, September 2013.
[7] CEB-FIP: Model Code 1990, T. Telford, London, 1993.
[8] FIB Model Code 2010, Paris, 2013.
[9] ACI 209R-02: Prediction of creep, shrinkage, and temperature effects in concrete structures. ACI Committee, 2002.
[10] Mathematical Modeling of Creep and Shrinkage of Concrete, Ed. Z. Bažant, A. A Wiley- Int.. Public. 1988.
[11] Partov, D., Kantchev,V.: Eurocode 2 provision against standards (ACI 209R-92 and Gardner&Lockman models) in creep analysis of composite steel-concrete section, Engineering Mechanics, Vol. 22, 2015, No. 2, pp. 109-127.
[12] Vayas, I., Iliopoulos, A.: Design of steel-concrete comosite bridges to eurocodes, CRC Press, 2014.
[13] Hendy,C.R., Johnson, R:P.: Designers guide to EN 1994-2 Eurocodes 4: Design of steel and comosite structures, Part 2: General rules and rules for bridges, 2004.

[14] Al-Darzi, S.Y., Chen, A.: Conceptual design and analysis of steel-concrete comosite bridges: State of the Art, Steel Strustures, 2006, pp. 393-407. www.kssc.or.kr
[15] Folić R., Radonjanin, V., Malešev, M.: „Design and Analysis of Steel-Concrete Composite Structure“, Introductinary - Invited paper on 6th Greek National Conference on Metal Structures, Athens: Greek Association for Metal Structures, 2008, pp. 72 – 87.
[16] Sassone, M., Casalegno, C.: Evaluation of the structural response to the time-dependent behaviour of concrete: Part 2 – A general computational approach, ICJ The Indian Concrete Journal, 86, 2012. 12, 39-51.
[17] Wang, G-M., Zhu, L., Zou, G-P., Han, B., Ji, W-Y.: Experimental research of the time-dependent effects of steel-concrete composite girder bridges during construction and operation periods, MDPI Materials, 2020, 13, 2123, doi:10.3390/ma13092123
[18] Cardoso, R. A: Design of comosite steel and concrete bridges, Univeridade de Aveiro Dep. de Eng. Civil, Arno 2015.
[19] Kim, S.: Creep and shrinkage effects on steel-concrete composite beams, Master Thesis.
[20] Kostić, S., Deretić-Stojanović, B., Stošić, S.: „Redistribution effects in linear elastic analyses of continuous composite steel-concrete beams according to Eurocode 4“, Facta Universitatis, Series: Architecture and Civil Engineering,Vol. 9, No 1, 2011, pp. 133-145.
[21] Nguyen, Q-H. Hjiaj, M.: Nonlinear time-dependent behaviour of composite steel-concrete beams, Hal, April 13, 2015.
[22] Chiorino, M.A., Carreira, D.J.: Factors affecting creep and shrinkage os hardened concrete and guide for modelling, ICJ The Indian Concrete Journal, vol.86, No.12, Theme: Creep and Shrinkage, A state-of-the-art report on international recommendations and scientific debate, Maharashtra, India, 2012, pp. 11-24.
[23] Collin, P., Nilsson, M., Häggström, J.: International Workshop on Eurocode 4-2, Composite Bridges, Technical report, Stockholm, 2011.
[24] Macorini, L., Fragiacomo, M., Amadio, C., Izzuddin, B.A.: Long-term analysis of steel-concrete composite beams; FE modelling for effective with evaluation, Engineering Structures,, 28, 2006, pp. 1110-1131.
[25] Gara, F., Leoni, G. Dezi, L.: A beam finite elerment including shear lag effect for the time-dependent analysis of steel-concrete composite decks, Eng. Struct., 31, 2009, pp. 1888-1902.
[26] Reginato, L.H., Tamoyo, J. L., Morsch, I. B.: Finite element study of effective width in steel-concrete composite beams under long-term service load, Latin Amer. J. of Solid and Structures, 2018,15(8), 15 p.
[27] Bradford, M.A., Gilbert,R.I.: Time-dependent behaviour of simply supported steel-composite beams, The University of New South Wales, SCE, UNICIV Report No. R-286 July 1991.
[28] Dezi, L., Leoni, G., Tarantino, A.M.: Creep and shrinkage analysis of composite beams, Composite construction, Constr. Research Communications Limited, 1998, pp. 170-177.
[29] Souici, A., Tehrani, M., Rahal, N., Bekkouche,M.S. Berehet: Creep effect on composite beam with perfect steel-concrete connection, Steel structures, 15, 2, 2015, pp. 433-445.
[30] Fragiacomo,M., Amadio, C., Macorini, L.: Finite-element model for collapse and long-term analysis of steel-concrete composite beams, ASCE, Journal of structural engineering, March, 2004, pp. 489-497.
[31] Chen, F., Ai, Z., Wang, C., Hou, S.: Research on simulation method of steel-concrete composite beam with finite element, IOP Conf. Series: Earth and Enviromental Science, 719, 2012, 022035; doi:10.1088/1755-1315/719/2/022035
[32] Gholamhoseini, A., Gilbert, R.I., Bradford, M.A.: A simplified method for calculation of long-term deflections in composite slabs, Steel Innovationa, 2015, Auckland, N. Zealand, 3-4 September 2015.
[33] Yao, K., Zhou, D. He, Y., Wu, S.: The simplified algorithm to the simple-supported steel and concrete comosite beam, Hindawi, Computational Inteligence and Neuroscience, Vol. 2022, Article ID 4951080, 10 p.
[34] Zhang, C., Shao, C. Su, Q. Changyuan, D.: An experimental study on negative banding behaviour of composite bridge decks with steel-fiber-reinforced concrete and longitunal buld-flat ribs, I. J. of steel structures, 16 March 2023.
[35] Niu, Y., Tang, Y.: Effect of shear creep on long-term deforoamtion analysis of long span concrete girder bridge, Hindawi, Advances in Materils Science aand Engineering, Vol. 2019, Article ID 4382904, 10 p. https://doi.org/10.1155/2019/4382904
[36] Morano, S. G., Mannini, C.: PreflexBeams: A method of calculation of creep and shrinkage effects, ASCE, Journal of Bridge Engineering, January/february 2006, pp. 48-58.
[37] Cumbo, A., Folić, R.: Layered finite elements in the analysis of composite structures exposed to long-term effect, Građevinar, 69, 2017, No. 11, Zagreb, 2017, pp. 991-1005.
[38] Cumbo, A.: Analisis rheollogical properties influences of composite structures by layered finite elements, Ph Thesis, Faculty of Civil Engineering and Architecture, Niš, 2017. (in Serbian).
[39] Johnson, R:P. Composite structures of steel and concrete, Blackwall P., Therd Edition, Oxford, 2004.

Professional work
http://dx.doi.org/10.59456/afts.2023.1529.035P

ANALYSIS, COST ESTIMATION AND OPTIMIZATION OF REINFORCED CONCRETE SLAB STRENGTHENING BY STEEL AND CFRP STRIPS

Petrov Ramona[1], Goleš Danica[1]

[1]*Faculty of Civil Engineering Subotica, University of Novi Sad, Serbia,*
e. mail: ramona.petrov@gf.uns.ac.rs

ABSTRACT

As a result of the planned change of use, the imposed load on the existing reinforced concrete mezzanine slab will be significantly increased, wherefore a diagnostics and assessment of the current state of the structure has been carried out. The control calculation showed that the slab does not have sufficient bearing capacity for the increased load. After qualitative analysis of possible strengthening methods, two methods were selected for detailed analysis: strengthening with steel strips and strengthening with carbon fiber-reinforced polimer (CFRP) plates.

The criterion for choosing the optimal solution was the total cost of the material. It has been shown that the total price of materials for strengthening with steel strips is almost 40% lower than the price of strengthening with CFRP plates. It has also been observed that, when using steel strips, the contribution of the price of adhesive in the total cost of material is extremely high. When varying the level of strengthening, for imposed loads from 3 to 7.5 kN/m^2, the ratio of the total costs of materials for steel and CFRP strips ranges between 60 and 73% and shows a slight tendency to increase with the increasment of loads.

Keyword: *cost estimation, optimization, strengthening of reinforced concrete slab, CFRP strip, steel strip*

INTRODUCTION

The one storey residential building with atic was designed and built in the sixties of the last century in Subotica, Republic of Serbia. The current owner of the building intends to repurpose the ground floor and first floor from residential to office area, while the purpose of the attic, for housing, would remain unchanged. The change of purpose will significantly increase the imposed load, wherefore it is necessary to carry out an assessment of the bearing capacity of the existing structure and the possible need for its strengthening.

The design and technical documentation of the building was lost, so the condition of the structure was assessed based on information received from the owner, visual inspection, results of measurements and testings performed on site and results of laboratory testings on samples taken from the mezzanine slab. The bearing capacity of the existing mezzanine slab, calculated in accordance with current regulations, proved to be insufficient to sustain the increased imposed load, which is why the planning of its strengthening was started.

Three methods were considered: addition of a new steel reinforcement and a new layer of concrete, strengthening with externally bonded steel strips, and strengthening with externally bonded fiber-

reinforced polymer (FRP) plates. Bearing in mind the requirements and limitations set by the investor, two methods were chosen that were analyzed in detail to find the optimal solution, which will provide the required bearing capacity at the minimum cost. Due to large fluctuations in the price of labor, the analysis was carried out only from the aspect of the price of materials, based on the market state on March 20, 2023. The price in euros is given according to the official middle exchange rate of the NBS (National Bank of Serbia) on April 7, 2023, according to which 1 EUR = 117.28 RSD.

A significant difference in the cost of materials was observed when strengthening with steel and CFRP strips. Since the required level of strengthening in this specific example was minimal, the authors wanted to investigate whether the price ratio for these two methods will change with the increasement of the level of strengthening. Therefore, the calculations of the strengthening and the cost of materials were carried out for imposed loads of 4, 5, 6 and 7.5 kN/m^2, for both considered methods. The results of the analysis are presented in this paper.

ASSESSMENT OF THE CONDITION AND BEARING CAPACITY OF THE EXISTING SLAB

Considering the time when it was built, it is assumed that the building meets the requirements of the Provisional Technical Regulations for Loads for Buildings from 1948 and the Provisional Technical Regulations for Concrete and Reinforced Concrete from 1947 [1], which means that the mezzanine slab is designed for the imposed load of 1.5 kN/m^2. After the change of purpose, the facility should meet the requirements of the SRPS EN 1990 [2,3], SRPS EN 1991**Greška! Nije pronađen izvor reference.** i SRPS EN 1992-1-1 [5,6]. The design value of the imposed load for the office area, which is classified as an area of category B [4], is 3.0 kN/m^2, which is an increase of 100% in relation to the load for which the existing slab was designed, so it is necessary to carry out an assessment of the condition of the existing structure and, if necessary, strengthen it.

Following the procedure presented in [7], an assesment plan was prepaired, and a detailed visual inspection of the building, with the necessary measurements, was carried out. A report was drawn up, after which field and laboratory testing was performed. The mezzanine slab under consideration is located inside the building and was not exposed to the actions of external environment or chemical agresion, so chemical analyzes of the embedded concrete and steel reinforcement were not carried out. Locating the reinforcement in the concrete was done using the magnetic method.

The compressive strength of concrete was determined by laboratory testing of the concrete cores drilled from the structure. A non-destructive ultrasonic method was used for confirmation of the compressive strength of concrete, for checking the uniformity of quality of concrete and to determine the slab thickness. In order to reveal possible concrete defects and the condition of the reinforcement, the mortar was removed from the lower surface of the slab. The results obtained by the conducted testings are presented in the following text.

The structure of the building is consisted of 38 cm thick brick load-bearing walls, placed around the perimeter of the building, with the clear distance of 5.2x12.0 m, supporting a solid rectangular reinforced concrete (RC) slab. The clear height of the ground floor and the first floor is 2.80 m.

The simply supported 20 cm thick RC slab is made of concrete whose strength corresponds to the class C16/20. The main steel reinforcement of class Č37 consists of 12 mm diameter bars at 10 cm spacing. The average thickness of the concrete cover is 1 cm. The floor consists of 5 cm thick cement screed and 2 cm of covering. The bottom surface of the slab is covered with a 2 cm thick mortar layer.

The calculated permanent load on the existing slab is 6.54 kN/m². Due to the repurpose, the imposed load increases from 1.50 kN/m² to 3.0 kN/m². The effective span of l_{eff} = 5.5 m was adopted.

The analysis of the slab using the above data, carried out in accordance with the Rulebook for Building Structures [8], showed that the moment capacity M_{Rd} of the unstrengthtened slab is smaller than the maximum bending moment M_{Ed} that occures under the increased load (figure 1):

$$M_{Rd} = 40.27 \text{ kNm/m} < M_{Ed} = 50.40 \text{ kNm/m},$$

wherefore the strengthening of the slab is necesery.

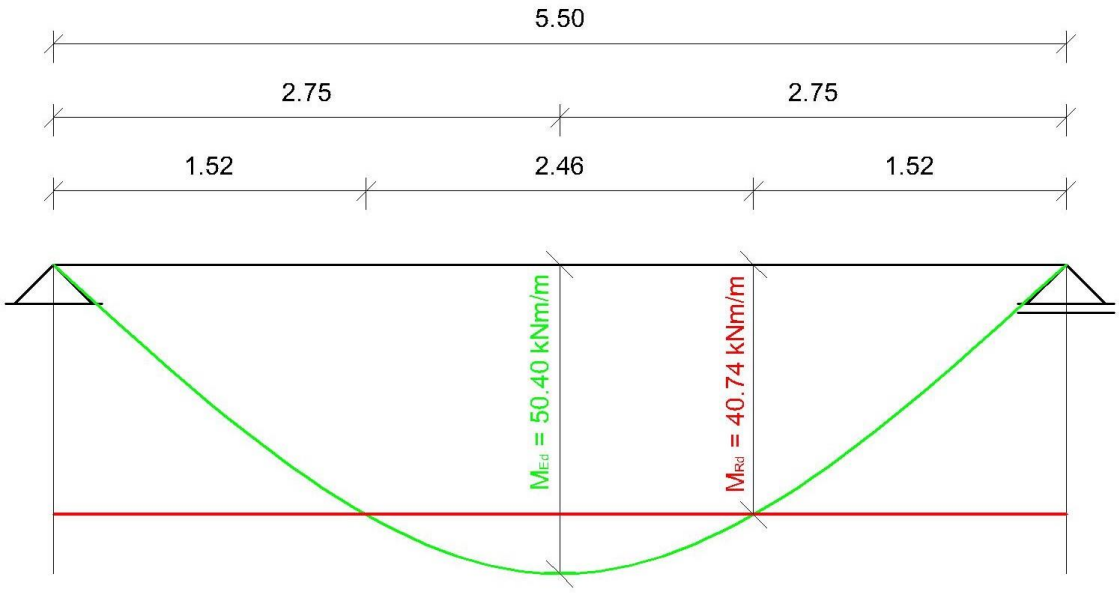

Figure 1. Moment capacity M_{Rd} of the existing slab and the bending moment M_{Ed} diagram after the change of purpose

CONSIDERATION OF POSSIBLE STRENGTHENING METHODS

The following requirements and limitations were considered when choosing a suitable method of strengthening of the existing reinforced concrete slab:

- Available space. The clear height of the rooms is currently 2.8 m. The investor requires that, after strengthening, the clear height should be at least 2.7 m, which leaves a space of 10 cm for the total height of the strengthening;
- Increasment of the load on the existing structure. It has been assessed that the existing walls and foundations have a sufficient capacity to bear the increased imposed load. Still the strengthening should not significantly increase the permanent load;
- Impact of construction works on the surrounding area. Strengthening should be carried out in such a way that the subsequent work on the surfaces of the surrounding walls and floors is reduced to the minimum possible extent;
- The impact of the works on the unhindered use of the facility. During the strengthening works, it is desirable to enable unhindered use of the atic, so the generation of noise, debris and dust should be reduced to a minimum;
- Availability of adequate labor and materials. The locally available materials and local labor should be preferred;
- Duration of works. The investor requires the works be completed in the shortest possible time;
- Price.

Based on these requirements and limitations, from all the possible solutions for strengthening the slab [9], strengthening by applying a new RC layer to the bottom surface of the slab, strengthening using steel strips and strengthening using FRP plates were taken into the further consideration.

Strengthening by applying a new RC layer to the bottom surface of the slab

Strengthening by addition of a new RC layer includes the local "exposing" of the existing tensile reinforcement and its connection with the new reinforcement by welding, after which a 3 cm thick layer of shotcrete is sprayed in a dry-mix process. This traditional method allows the hiring of local labor and the use of locally available materials, but at the same time it significantly increases the dead load on the structure and produces a lot of waste material, noise and dust, due to which it is necessary

to suspend the use of the building during the works. The increase of the mezzanine structure's mass also affects the change in its behavior under seismic actions.

Strengthening by externally bonded steel strips

The slab strengthening with steel strips is performed by bonding the steel strips to the previously prepared concrete surface using epoxy adhesive. If planned, supporting the structure during execution must last at least 24 hours, depending on the type of adhesive used. The advantage of this strengthening method is its price, which is lower than the price of the most other RC slab strengthening methods. Also, the works can be carried out regardless of weather conditions, and the execution itself is relatively simple. When applying this type of strengthening, the cross-section dimensions remain almost unchanged, with minimal impact on other structural elements.

The method is used at temperatures no higher than 60 ^{o}C and relative humidity below 70%, without chemical aggression, which makes it applicable for strengthening mezzanine slabs of residential and commercial buildings. Since a layer of mortar was removed from the lower surface of the slab for the purposes of testing, it must be leveled with repair mortar before the strengthening. Steel strips are installed to a cleaned surface. It is necessary to ensure the optimal room temperature for bonding, which depends on the type of adhesive used, and most often ranges from +8 ^{o}C to +35 ^{o}C.

Strengthening by externally bonded FRP plates

By strengthening with polymer plates (strips) reinforced with carbon fibers, an increase in the load-bearing capacity of the structure is achieved without significan reduction of the clear volume of the building, since the thickness of the carbon fiber reinforced polymer strips is usually only 1 to 5 mm. The slab is strengthened by placing the CFRP strips in the zone of highest tensile stress, in the load-carrying direction. This strengthening system simultaneously increases the bearing capacity and stiffness of the structural member, limits deformations (deflection) and cracks, and increases fatigue resistance.

Compared to conventional strengthening systems, such as placement of steel strips, CFRP plates have the following advantages: they are lighter than steel strips, they are supplied in rolls and can be easily cut on site, the installation is simple and fast, they are durable and resistant to fatigue and corrosion, they are thin, easily covered with paint, have higher tensile strength and high stiffness of fibers. The bond between the existing slab and FRP strip depends on the quality of the preparation of the substrate. Installation of CFRP plates can only be performed on concrete substrates that will ensure a satisfactory degree of adhesion between concrete and adhesive during the exploitation of the building. Therefore, before installation, the substrate must be completely cleaned and dry. Surface humidity of concrete must not be higher than 4%.

The effective concrete pull-off strength after surface preparation must be verified by testing and should not be less than 1.5 MPa. To monitor the effectiveness of the strengthening, it is suggested to place one or two additional plates that will be tested by the pull-off method immediately after hardening. High temperatures, in case of fire, can seriously impair the effectiveness of the strengthening, so it is necessary to protect the CFRP plates externally with special coatings, gypsum panels, etc. Strengthening systems with CFRP plates must be protected from permanent exposure to direct sunlight, moisture and/or water. Maximum permissible continuous service temperature is approximately +50 °C. [10,11,12]

Selection of two methods for detailed analysis and their qualitative comparison

Strengthening the structure by placing a new layer of reinforced concrete, due to its disadvantages - a large amount of waste material, an increase in the weight of the structure and a decrease in the clear height of the room, will not be further analyzed. A detailed analysis and calculation will be carried out for the remaining two methods - strengthening of the RC slab by externally bonded steel strips and by externally bonded CFRP plates. Table 1 shows a qualitative comparison of the two selected strengthening methods, according to [13].

Table 1. Comparative analysis of steel and CFRP strips [13]

Criterion	Steel strips	CFRP strips
Self-weight	High	Low
Tensile strength	High	Very high
Thickness	Small	Very small
Corrosion	Possible	Not possible
Length	Limited	Practically unlimited
Processing	Complex	Easy
Behavior	Stiff	Flexible
Fatigue resistance	Significant	Sufficient
Price	Low	High
Installation cost	High	Low
Specific equipment for the installation	Supporting equipment	Not needed
Qualified labor needed	Yes	Yes

CALCULATION AND OPTIMIZATION OF STRENGTHENING WITH STEEL STRIPS

Steel strips made of construction sheet S 235 JR, installed to the bottom side of the slab in the load-carrying direction, were selected to strengthen the slab. Since the existing slab is able to carry the full permanent load, the strengthening can be done without supporting, and the steel strips are "activated" only when the imposed load is applied. By the ultimate limit state analysis of the cross-section with the maximum design bending moment, it was established that the required steel strips cross-section area is 2.90 cm^2/m. The analysis was carried out for steel strips with thicknesses of 1.5, 2.0 and 2.5 mm, and widths of 50, 100, 150, 200, 250 and 300 mm. The length of the individual strip of 3.5 m was determined by adding the anchoring length to both sides of the strengthening length (the length of 2.46 m in figure 1). The calculation results are shown in table 2. The axle distance of the strips is limited to 1 m, which is why some solutions are oversized (shaded fields in table 2).

Table 2. Geometric characteristics and arrangement of steel strips, and moment capacity of the strengthened slab

Serial number	Strip thickness [mm]	Strip width [mm]	Strip cross-section area [cm^2]	Required axle distance [cm]	Adopted axle distance [cm]	Total number of strips [kom]	Length of individual strip [m]	Total length of strips [m]	Moment capacity M_{Rd} [kNm/m]
1	1.5	50	0.75	25.86	25	48	3.50	168.00	50.70
2	1.5	100	1.50	51.72	51	24	3.50	82.35	50.50
3	1.5	150	2.25	77.59	77	16	3.50	54.55	50.43
4	1.5	200	3.00	103.45	100	12	3.50	42.00	50.70
5	1.5	250	3.75	129.31	100	12	3.50	42.00	53.25
6	1.5	300	4.50	155.17	100	12	3.50	42.00	55.77
7	2.0	50	1.00	34.48	34	35	3.50	123.53	50.51
8	2.0	100	2.00	68.97	68	18	3.50	61.76	50.51
9	2.0	150	3.00	103.45	100	12	3.50	42.00	50.71
10	2.0	200	4.00	137.93	100	12	3.50	42.00	54.11
11	2.0	250	5.00	172.41	100	12	3.50	42.00	57.46
12	2.0	300	6.00	206.90	100	12	3.50	42.00	60.76
13	2.5	50	1.25	43.10	43	28	3.50	97.67	50.41
14	**2.5**	**100**	**2.50**	**86.21**	**86**	**14**	**3.50**	**48.84**	**50.41**
15	2.5	150	3.75	129.31	100	12	3.50	42.00	53.28
16	2.5	200	5.00	172.41	100	12	3.50	42.00	57.48
17	2.5	250	6.25	215.52	100	12	3.50	42.00	61.61
18	2.5	300	7.50	258.62	100	12	3.50	42.00	65.66

For the calculation of the consumption and cost of the material, the use of "*Eporip Mapei*" adhesive is assumed, the consumption of which (from the technical sheet [14]) is 1.35 kg/m² for 1 mm of layer thickness. For a smooth substrate surface the consumption of 1.00 kg/m² can be adopted. The cost calculation also includes anti-corrosion protection of the strips by applying a one-component anticorrosive coating for steel sheets - "*Wash Primer*", whose consumption is 80-90 gr/m^2, before finishing the ceiling.

Based on a detailed analysis of the material cost for the selected steel strips, shown in table 3, the conclusion is that the optimal solution of strengthening can be accomplished with strips 2.5 mm thick, 100 mm wide, at a mutual axle distance of 86 cm (serial number 14 in tables 2 and 3). The total cost of material for this type of strengthening is 138.47 EUR, i.e. 16239.56 RSD.

Table 3. Analysis of cost of materials for strengthening with steel strips

Serial number	Total area of strips [m²]	Unit price of adhesive [rsd/m²]	Unit price of strips [rsd/m]	Total cost of adhesive [rsd]	Total cost of strips [rsd]	Unit price of coating [rsd/ m²]	Total cost of coating [rsd]	Total cost of material [rsd]	Total cost of material [EUR]
1	8.40	1868.35	37.00	21187.09	6216.00	142.97	1200.95	28604.04	243.90
2	8.24	1868.35	40.00	20771.66	3294.12	142.97	1177.40	25243.17	215.24
3	8.18	1868.35	43.00	20636.78	2345.45	142.97	1169.75	24151.98	205.93
4	8.40	1868.35	46.00	21187.09	1932.00	142.97	1200.95	24320.04	207.37
5	10.50	1868.35	48.00	26483.86	2016.00	142.97	1501.19	30001.05	255.81
6	12.60	1868.35	50.00	31780.63	2100.00	142.97	1801.42	35682.06	304.25
7	6.18	1868.35	52.00	15578.74	6423.53	142.97	883.05	22885.32	195.13
8	6.18	1868.35	54.00	15578.74	3335.29	142.97	883.05	19797.09	168.80
9	6.30	1868.35	56.00	15890.32	2352.00	142.97	900.71	19143.03	163.22
10	8.40	1868.35	58.00	21187.09	2436.00	142.97	1200.95	24824.04	211.66
11	10.50	1868.35	60.00	26483.86	2520.00	142.97	1501.19	30505.05	260.10
12	12.60	1868.35	62.00	31780.63	2604.00	142.97	1801.42	36186.06	308.54
13	4.88	1868.35	64.00	12318.08	6251.16	142.97	698.23	19267.46	164.29
14	**4.88**	**1868.35**	**66.00**	**12318.08**	**3223.26**	**142.97**	**698.23**	**16239.56**	**138.47**
15	6.30	1868.35	68.00	15890.32	2856.00	142.97	900.71	19647.03	167.52
16	8.40	1868.35	70.00	21187.09	2940.00	142.97	1200.95	25328.04	215.96
17	10.50	1868.35	72.00	26483.86	3024.00	142.97	1501.19	31009.05	264.40
18	12.60	1868.35	74.00	31780.63	3108.00	142.97	1801.42	36690.06	312.84

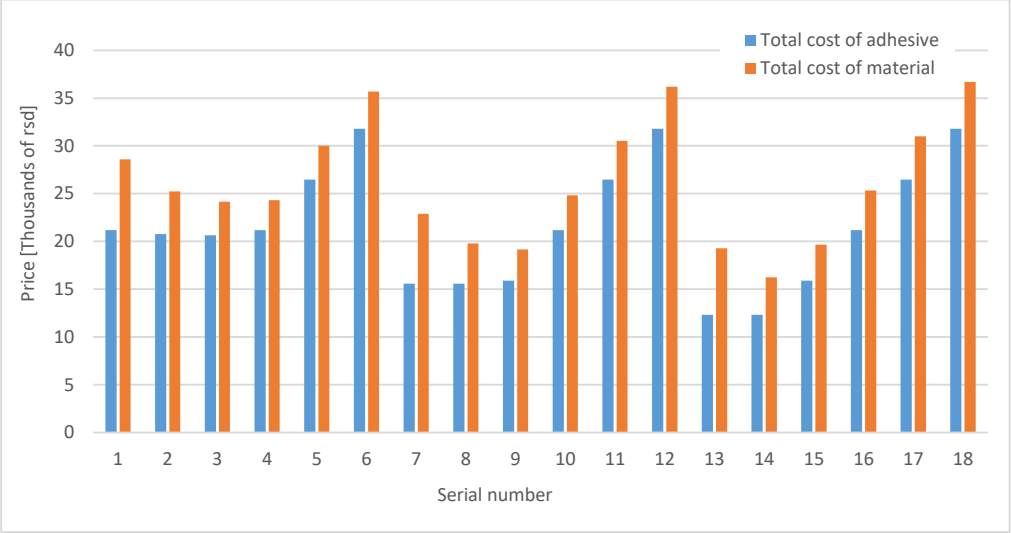

Figure 2. Total cost of material and total cost of adhesive for strengthening with steel strips

It should be noted that the contribution of the price of adhesive in the total cost of material is extremely high, in some cases even exceeding 80% (figures 2 and 3). The non-monotonic function of the total cost of material in figure 2 ("wavy" shape of the diagram) is a consequence of the fact that, due to the spacing limitation to 100 cm, in some cases was adopted a significantly larger area of steel than is necessary to achieve the design moment capacity (shaded fields in table 2). As will be shown later, this phenomenon is lost when strengthening is designed for higher imposed loads (figure 3).

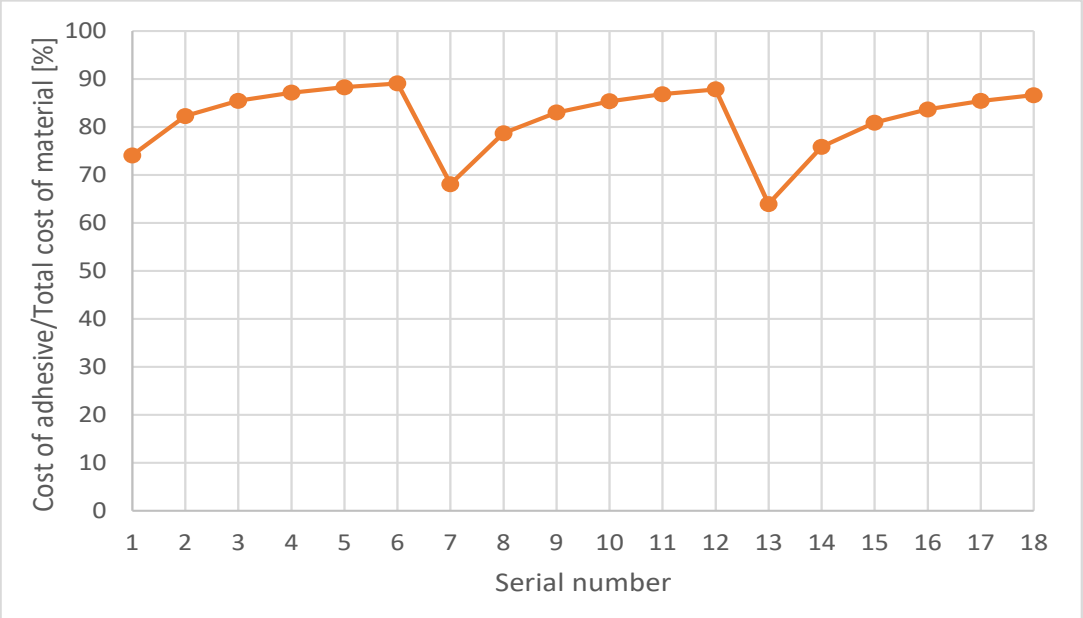

Figure 3. The ratio of the cost of adhesive and the total cost of material for strengthening with steel strips

CALCULATION AND OPTIMIZATION OF STRENGTHENING WITH CFRP PLATES

The Sika® CarboDur® system was chosen for the calculation and optimization of RC slab strengthening by FRP plates. The analysis was performed using Sika® CarboDur® FRP Design Software [15,16]. Three categories of CFRP lamellae were considered - S, M and E series [10,11], [12], which differ from each other in tensile strength (from 2300 to 3500 MPa) and elastic modulus (between 170 and 210 GPa).

Like in the strengthening by steel strips, FRP plates are applied to the bottom surface of the slab in the load-carrying direction, without supporting. The results of dimensioning according to the ultimate limit state are shown in table 4. The spacing of the strips is limited to 1 m, which is why some solutions are oversized (shaded fields in Table 4).

For the calculation of consumption and cost of materials, the use of *Sikadur®-30* adhesive [17] is assumed, whose consumption was adopted from the manufacturer's technical sheets [10,11,12], as a function of the type and width of CFRP plates.

Based on a detailed analysis of the material cost for the considered CFRP plates, shown in table 5, the conclusion is that the optimal solution is the strengthening with Sika® CarboDur® S 214 plates, placed at a mutual axle distance of 52 cm (row number 2 in tables 4 and 5). The total cost of material for this type of strengthening is 227.64 EUR, i.e. 26697.13 rsd, which is almost 65% higher than the cost of the material needed for the strengthening by steel strips.

The share of the price of adhesive in the total cost of material when strengthening with CFRP plates is much lower than in the case of strengthening by steel strips, and ranges between 27 and 51% (figures 4 and 5).

Table 4. Geometric characteristics and arrangement of Sika® CarboDur® FRP plates, and the moment capacity of the strengthened slab

Serial number	**Type of plate**	Plate width [mm]	Plate thickness [mm]	Required axle distance [m]	Length of individual plate [m]	Total length of plates [m]	Moment capacity M_{Rd} [kNm/m]
1	S 212	20	1.2	0.45	3.50	94.50	50.42
2	**S 214**	**20**	**1.4**	**0.52**	**3.50**	**84.00**	**50.53**
3	S 512	50	1.2	1.00	3.50	42.00	51.69
4	S 514	50	1.4	1.00	3.50	42.00	53.60
5	S 612	60	1.2	1.00	3.50	42.00	53.97
6	S 614	60	1.4	1.00	3.50	42.00	56.23
7	S 626	60	2.6	1.00	3.50	42.00	69.44
8	S 812	80	1.2	1.00	3.50	42.00	58.46
9	S 814	80	1.4	1.00	3.50	42.00	61.42
10	S 914	90	1.4	1.00	3.50	42.00	63.97
11	S 1012	100	1.2	1.00	3.50	42.00	62.86
12	S 1014	100	1.4	1.00	3.50	42.00	66.49
13	S 1212	120	1.2	1.00	3.50	42.00	67.19
14	S 1213	120	1.3	1.00	3.50	42.00	69.33
15	S 1214	120	1.4	1.00	3.50	42.00	70.90
16	S 1512	150	1.2	1.00	3.50	42.00	72.05
17	M 614	60	1.4	1.00	3.50	42.00	60.01
18	M 814	80	1.4	1.00	3.50	42.00	66.33
19	M 914	90	1.4	1.00	3.50	42.00	69.43
20	M 1014	100	1.4	1.00	3.50	42.00	71.49
21	M 1214	120	1.4	1.00	3.50	42.00	74.71
22	E 512	50	1.2	1.00	3.50	42.00	52.04
23	E 514	50	1.4	1.00	3.50	42.00	54.00
24	E 812	80	1.2	1.00	3.50	42.00	59.00
25	E 1014	100	1.4	1.00	3.50	42.00	67.25
26	E 1214	120	1.4	1.00	3.50	42.00	71.41

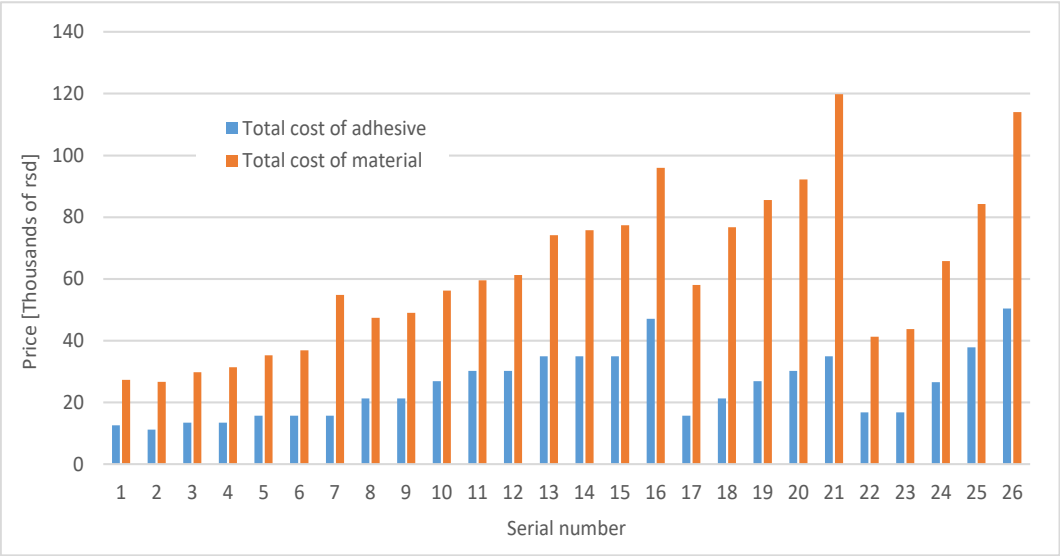

Figure 4. Total cost of material and total cost of adhesive for strengthening with CFRP plates

Table 5. Analysis of cost of materials for strengthening with CFRP plates

Serial number	**Type of plate**	Consumption of adhesive [kg/m]	Unit price of adhesive [rsd/kg]	Total cost of adhesive [rsd]	Unit price of plates [rsd/m]	Total cost of plates [rsd]	Total cost of material [rsd]	Total cost of material [EUR]
1	S 212	0.1	1333.33	12599.97	155.36	14681.52	27281.49	232.62
2	**S 214**	**0.1**	**1333.33**	**11199.97**	**184.49**	**15497.16**	**26697.13**	**227.64**
3	S 512	0.24	1333.33	13439.97	388.40	16312.80	29752.77	253.69
4	S 514	0.24	1333.33	13439.97	427.24	17944.08	31384.05	267.60
5	S 612	0.28	1333.33	15679.96	466.08	19575.36	35255.32	300.61
6	S 614	0.28	1333.33	15679.96	504.92	21206.64	36886.60	314.52
7	S 626	0.28	1333.33	15679.96	932.16	39150.72	54830.68	467.52
8	S 812	0.38	1333.33	21279.95	621.44	26100.48	47380.43	403.99
9	S 814	0.38	1333.33	21279.95	660.28	27731.76	49011.71	417.90
10	S 914	0.48	1333.33	26879.93	699.12	29363.04	56242.97	479.56
11	S 1012	0.54	1333.33	30239.92	699.12	29363.04	59602.96	508.21
12	S 1014	0.54	1333.33	30239.92	737.96	30994.32	61234.24	522.12
13	S 1212	0.625	1333.33	34999.91	932.16	39150.72	74150.63	632.25
14	S 1213	0.625	1333.33	34999.91	971.00	40782.00	75781.91	646.16
15	S 1214	0.625	1333.33	34999.91	1009.84	42413.28	77413.19	660.07
16	S 1512	0.84	1333.33	47039.88	1165.20	48938.40	95978.28	818.37
17	M 614	0.28	1333.33	15679.96	1009.84	42413.28	58093.24	495.34
18	M 814	0.38	1333.33	21279.95	1320.56	55463.52	76743.47	654.36
19	M 914	0.48	1333.33	26879.93	1398.24	58726.08	85606.01	729.93
20	M 1014	0.54	1333.33	30239.92	1475.92	61988.64	92228.56	786.40
21	M 1214	0.625	1333.33	34999.91	2019.68	84826.56	119826.47	1021.71
22	E 512	0.3	1333.33	16799.96	582.60	24469.20	41269.16	351.89
23	E 514	0.3	1333.33	16799.96	640.86	26916.12	43716.08	372.75
24	E 812	0.475	1333.33	26599.93	932.16	39150.72	65750.65	560.63
25	E 1014	0.675	1333.33	37799.91	1106.94	46491.48	84291.39	718.72
26	E 1214	0.9	1333.33	50399.87	1514.76	63619.92	114019.79	972.20

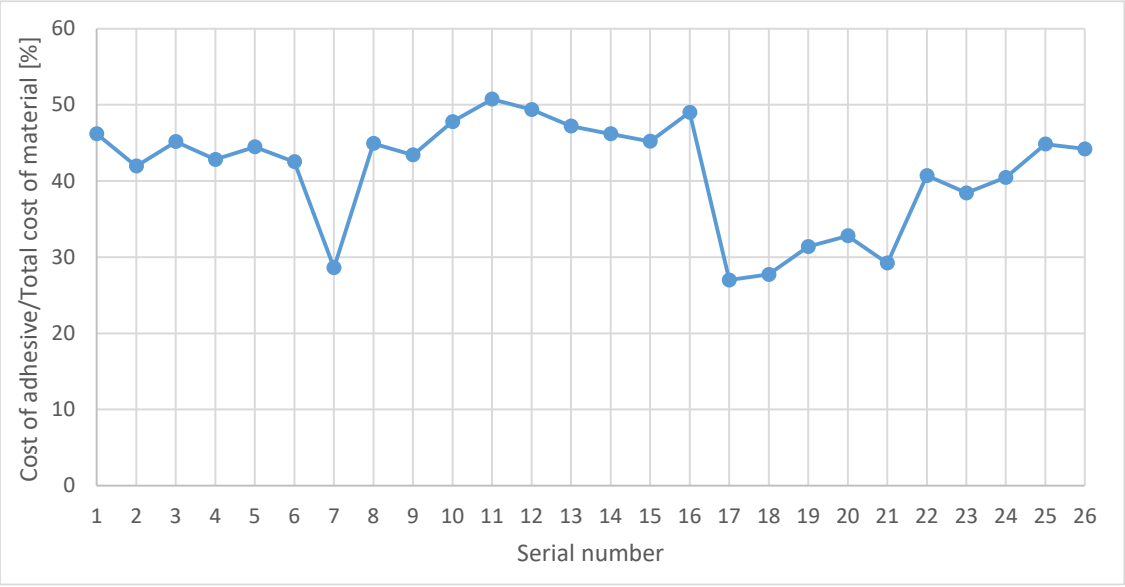

Figure 5. The ratio of the cost of adhesive and the total cost of material for strengthening with CFRP plates

COMPARATIVE ANALYSIS OF STRENGTHENING METHODS AND SELECTION OF THE MOST ECONOMICAL SOLUTION

The strengthening of the existing mezzanine slab includes the following activities:

- Visual inspection of the structure, measurement, registration of all visible defects and marking of places for further testings,
- Mechanical removal of mortar from the lower part of the slab for the purpose of assessing the condition of the reinforcement and possible defects and cracks in the concrete,
- Extraction of concrete cores by drilling and the laboratory testings of samples,
- Confirmation of concrete strength and slab thickness determination by ultrasonic method and locating the reinforcement using the magnetic method,
- Renovation of the lower part of the slab at the places of cores extraction and mortar removal,
- Installation of strips in places as provided by the design (steel strips/FRP plates),
- Plastering of the ceiling with lime plaster in two layers,
- Smoothing of finely plastered ceilings with dispersive putty,
- Painting walls and ceilings with a brush, with dissolved aged slaked lime and
- Cleaning the construction site after the completion of all works.

All listed activities are identical for both considered methods of strengthening, except for the execution of the strengthening itself. For this reason, the total cost of strengthening materials - adhesive, strips and, in the case of steel strips - anticorrosive coating, were used as the basis for comparison of the two methods.

As shown in the previous chapters, after analyzing the strengthening with steel and FRP strips of different geometric characteristics, for both methods was selected the solution with the lowest total material cost. When strengthening with steel strips, the lowest cost of EUR 138.47 is achieved by using strips 2.5 mm thick, 100 mm wide, placed at an axle distance of 86 cm. The lowest total material cost of 227.64 EUR for strengthening with CFRP plates is achieved by using strips S 214, on a mutual axle distance of 52 cm. Considering the criterion of the lowest cost of materials, the most economical solution for strengthening the existing RC slab is the installation of the above-mentioned steel strips.

It is interesting to note that the contribution of the cost of adhesive in the total cost of material when strengthening with steel strips ranges between 64 and 90%, while with the application of CFRP plates this share is significantly lower - between 27 and 51% (figure 6), depending on the plate type.

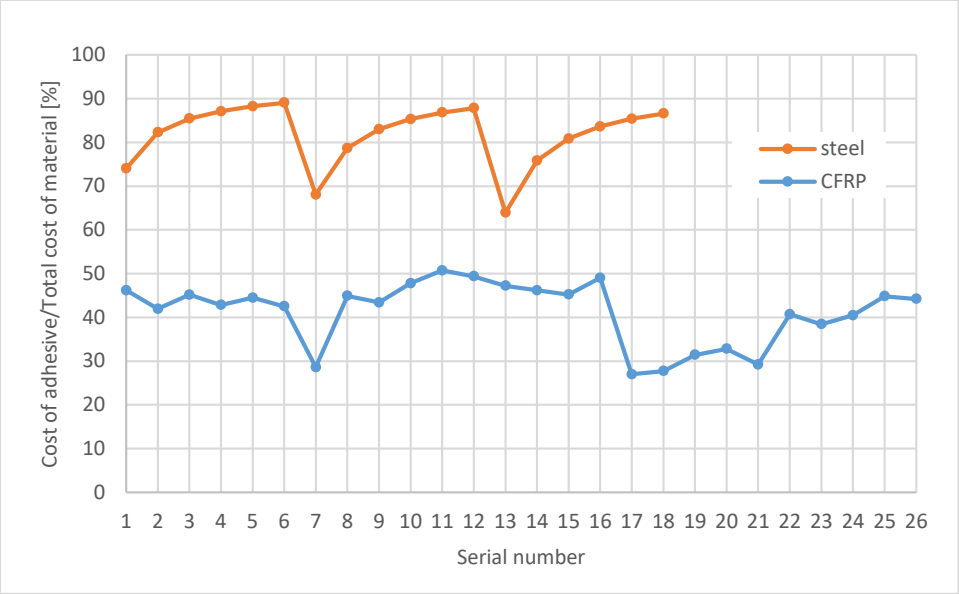

Figure 6. The ratio of the cost of adhesive and the total cost of material

ANALYSIS OF STRENGTHENING WITH STEEL AND CFRP STRIPS FOR VARIOUS INTENSITIES OF IMPOSED LOAD

In accordance with the task, the bending moment capacity of the existing RC slab had to be increased by only about 25%, which is achieved with minimal strengthening. In this specific example, the total cost of material for strengthening with steel strips was about 40% lower than the cost of material for strengthening with CFRP plates. The question is whether this price ratio remains unchanged in case that the strengthening is carried out for greater imposed loads.

To answer this question, an analysis was carried out for strengthening with steel and CFRP strips of the same types as in tables 2 to 5, but for imposed loads of 4, 5, 6 i 7.5 kN/m^2. The maximum value of the imposed load meets the criterion that the moment capacity of the strengthened section $M_{Rd,str}$ does not exceed twice the value of the moment capacity $M_{Rd,unstr}$ of the unstrengthened section, that is

$$M_{Rd,str} \leq 2 \cdot M_{Rd,unstr} = 2 \cdot 40.27 = 80.54 \text{ kNm/m}.$$

For each level of the imposed load, the same analysis was carried out as for q = 3.0 kN/m^2, both for steel and CFRP strips. The solution with the lowest material cost was selected for both methods. The total cost of materials and the cost of adhesive for the imposed load q = 6.0 kN/m^2, for different types of steel strips, is shown in figure 7, and for CFRP plates in figure 8.

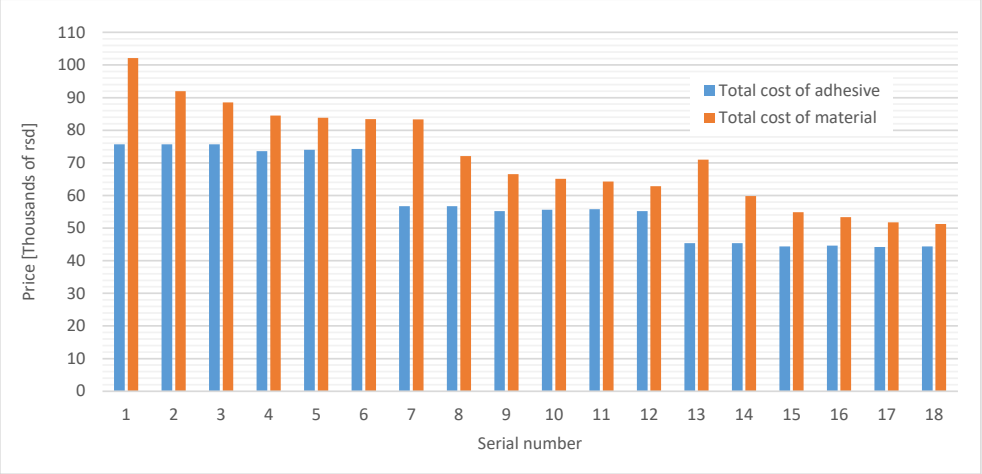

Figure 7. Total cost of material and total cost of adhesive for strengthening with steel strips, for imposed load of 6.0 kN/m^2

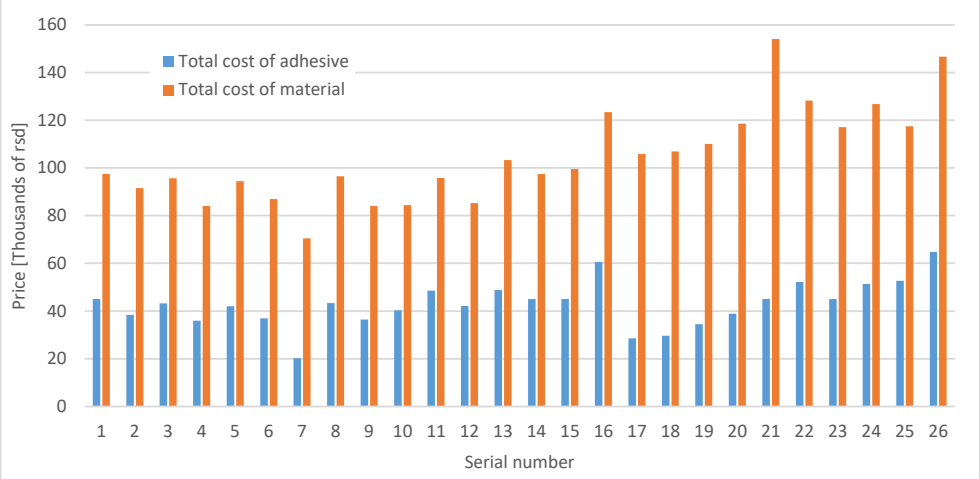

Figure 8. Total cost of material and total cost of adhesive for strengthening with CFRP strips, for imposed load of 6.0 kN/m^2

During the analysis, it was observed that when using steel strips, for all levels of imposed load, the lowest total material cost is achieved by using the thickest strips (2.5 mm). This is probably a consequence of the large share of the price of adhesive in the total price of material, because the consumption of adhesive depends only on the area covered by the strips, which is the smallest when the thickest strips are used.

When using CFRP plates, for all analyzed levels of imposed load, the most economical solutions were achieved with strips 60 mm wide. An exception is the imposed load of 3.0 kN/m^2, for which the lowest total cost of materials was obtained by using 20 mm wide strips. The most economical thickness of the plates up to the imposed load of 5.0 kN/m^2 is 1.4 mm, and for loads of 6.0 and 7.5 kN/m^2 the economical plate thickness is 2.6 mm.

Considering only the solutions that achieve the lowest material cost for each load level, figure 9 shows the total material cost and adhesive cost for steel and CFRP strips as a function of the intensity of imposed load.

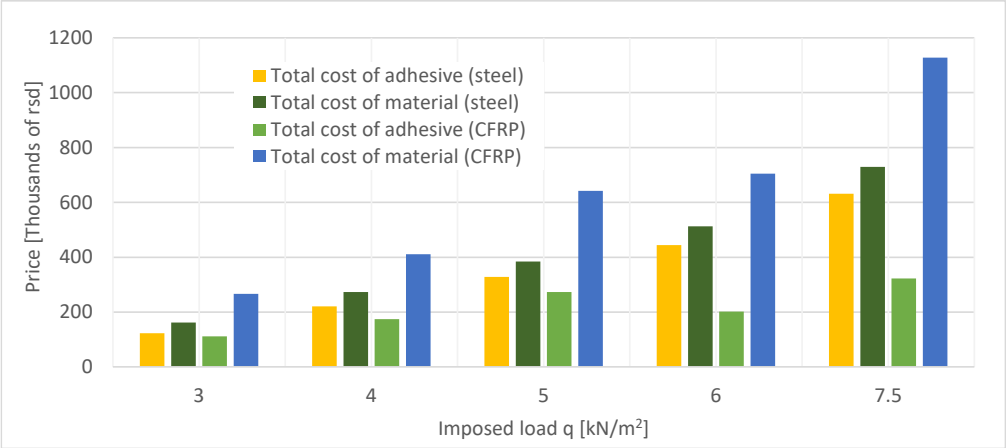

Figure 9. Total cost of material and total cost of adhesive for strengthening with steel and CFRP strips, for various intensities of imposed load

The increase of the total cost of materials with the increase of the imposed load for steel and CFRP strips, with their trendlines is shown in figure 10.

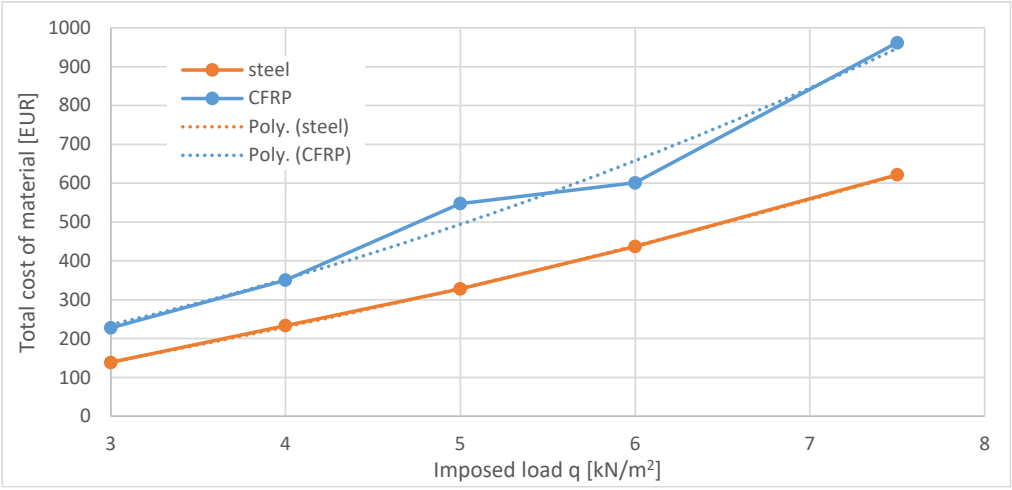

Figure 10. Total cost of material for various values of imposed load

The ratio of the total costs of materials for strengthening with steel and CFRP strips, for various values of the imposed load, is given in figure 11. Observing the trendline in figure 11, it can be concluded that the total cost of strengthening materials using steel strips is always lower than the cost of strengthening with CFRP plates. This price ratio is in a fairly narrow range between 60 and 73% and shows a slight

increase with the increase of load. This practically means that, with the increase in the intensity of strengthening, the economy of the application of steel strips slightly decreases.

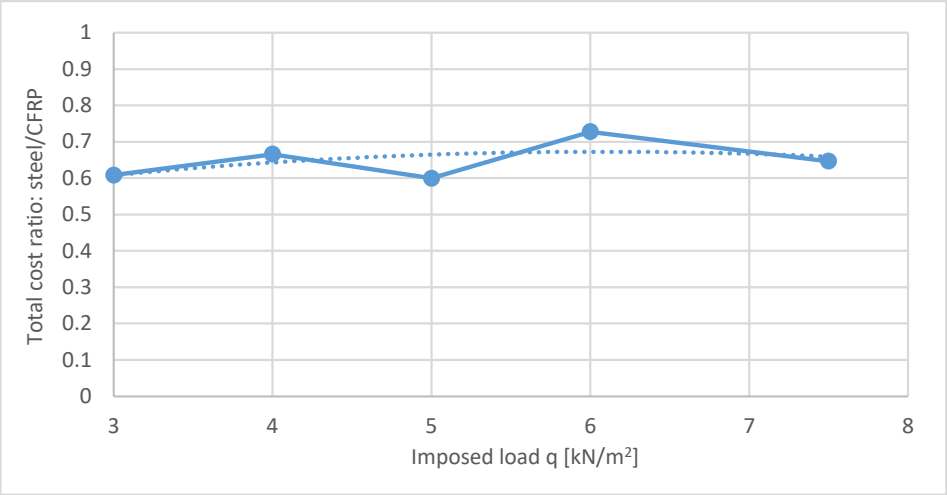

Figure 11. The ratio of the total costs of materials for steel and CFRP strips for various values of imposed load

CONCLUSION

When planning the strengthening of existing structural members, from many available methods, the one that optimally meets the set requirements and limitations is chosen. Universal requirements are contained in the technical regulations, but each project also contains a number of specific requirements set by the investor himself (e.g. maximum price, duration of works, overall dimensions, etc.) or imposed by the environment conditions, market conditions, etc. However, one of the most important criteria for choosing a strengthening method is its price, which has also been used as the final criterion for choosing a strengthening method for the existing solid RC slab with a span of 5.5 m.

After a qualitative analysis of three strengthening methods that potentially met the set requirements, two were selected for detailed analysis - strengthening by steel strips and by FRP plates installed to the underside of the slab. Further comparison of these two methods was carried out solely according to the criterion of cost of material. For each method, the types of strips were varied, and the one with the lowest total material cost was adopted. In this way, the most economical solution of strengthening was chosen - the use of steel strips S 235 JR, 2.5 mm thick, 100 mm wide, at a mutual axle distance of 86 cm, with a total cost of materials of 138.47 EUR.

The lowest material price of EUR 227.64 for strengthening with CFRP plates was obtained by using strips S 214 at a spacing of 52 cm, which is almost 65% higher than the price of strengthening with steel strips. A significant contribution of the cost of adhesive in the total cost of materials was observed when using steel strips (from 64 to 90%), while this share was between 27 and 51% when using CFRP plates.

The ratio of the total costs of material for strengthening with steel and CFRP strips did not change significantly even for higher strengthening levels, i.e. for imposed loads of 4, 5, 6 and 7.5 kN/m^2. The cost of material for strengthening with steel strips, for various levels of strengthening, ranges from 60 to 73% of the cost of material for strengthening with CFRP plates. A slight tendency of increasing of this ratio with the increase of load was observed.

Due to the large share of the cost of adhesive in the total cost of materials when strengthening with steel strips, the most economical solution for all levels of strengthening is obtained with strips of the largest considered thickness. The lowest cost of strengthening with CFRP plates for all load levels was achieved with strips of smaller width (20 mm for imposed load of 3.0 kN/m^2, i.e. 60 mm for all other load levels).

This research is based solely on the comparison of material prices for the two strengthening methods. In order to reach the optimal solution, all other advantages and disadvantages of the considered methods should be also taken into account.

Received August 2023, accepted September 2023)

REFERENCES

[1] Temporary Technical Regulations (1960). Construction book, Belgrade *[Serbian language]*.
[2] SRPS EN 1990 Eurocode - Basis of structural design, (2012). Institute for Standardization of Serbia, Belgrade.
[3] SRPS EN 1990/NA Eurocode - Basis of structural design - National Annex (2012). Institute for Standardization of Serbia, Belgrade.
[4] SRPS EN 1991-1-1 Eurocode 1: Actions on structures - Part 1-1: General actions - Densities, self-weight, imposed loads for buildings (2012). Institute for Standardization of Serbia, Belgrade.
[5] SRPS EN 1992-1-1 Eurocode 2: Design of concrete structures - Part 1-1: General rules and rules for buildings (2015). Institute for Standardization of Serbia, Belgrade.
[6] SRPS EN 1992-1-1/NA Eurocode 2: Design of concrete structures - Part 1-1: General rules and rules for buildings - National Annex (2015). Institute for Standardization of Serbia, Belgrade.
[7] Radic, J. (2010). Concrete structures 4, Rehabilitation, Croatian university press, Faculty of Civil Engineering, University of Zagreb, Zagreb *[Croatian language]*.
[8] Rulebook for building structures, Official Gazette of the RS, no. 89/2019, 52/2020 i 122/2020. *[Serbian language]*.
[9] Goleš, D. (2022). Lectures of the course "Maintenance, protection and rehabilitation of structures", Master academic studies. Faculty of Civil Engineering Subotica.
[10] Technical sheet Sika® CarboDur® S, [On the network]. [The last approach September 2023]. Available: https://srb.sika.com/dms/getdocument.get/ed9180a4-88f5-452a-bae3-1c0640641222/sika_carbodur_s.pdf.
[11] Technical sheet Sika® CarboDur® M, [On the network]. [The last approach September 2023]. Available: https://srb.sika.com/dms/getdocument.get/792f3f60-f1fa-4cf2-8348-11186f81cc2d/sika-carbodur-m.pdf.
[12] Technical sheet Sika® CarboDur® E, [On the network]. [The last approach September 2023]. Available: https://srb.sika.com/dms/getdocument.get/f25e0d71-f63d-470c-99a5-6fcde513174b/sika_carbodur_e.pdf.
[13] Najdanovic, D. (2023). [On the network]. [The last approach September 2023]. Available: https://www.grf.bg.ac.rs/p/learning/4_ojacanja_karbonskim_trakama_1387902496292.pdf.
[14] MAPEI, [On the network] [The last approach September 2023]. Available: https://cdnmedia.mapei.com/docs/librariesprovider51/products-documents/tl-eporip-(web).pdf?sfvrsn=9c7a5322_0.
[15] SIKA, „SIKA® CARBODUR® FRP CALCULATION SOFTWARE" [On the network]. [The last approach September 2023]. Available: https://srb.sika.com/sr/sadrzaj-za-preuzimanje/sika-carbodur-frp-design-software.html.
[16] USER GUIDE, Sika® CarboDur® calculation software (2017). BASED ON TR55 (2012) AND EUROCODE 2. Sika®
[17] Technical sheet Sikadur®-30, [On the network]. [The last approach September 2023]. Available: https://srb.sika.com/dms/getdocument.get/04122d86-03e5-4582-aede-2376715ff155/sikadur_-30.pdf.

AGRIKULTURE

Yield quality

Editors

Acad. Prof. Ph.D. Novo Pržulj
Prof. Ph.D. Svetlana Radmanović (Cupać)

Original scientific article
http://dx.doi.org/10.59456/afts.2023.1529.049M

INFLUENCE OF DIFFERENT NUTRIENT SOURCES AND GENOTYPES ON THE CHEMICAL QUALITY AND YIELD OF LETTUCE

Malešević Zoranka[1], Govedarica-Lučić Aleksandra[1], Bošković Ivana[1], Petković Marko[2], Đukić Dragutin[2], Đurović Vesna[2]

[1]*University of East Sarajevo, Faculty of Agriculture, East Sarajevo, Bosnia and Herzegovina, e-mail: zorankamalesevic@msn.com*
[2]*Faculty of Agronomy Čačak, University of Kragujevac, Serbia*

ABSTRACT

The aim of this study was to examine the effect of different fertilizers on the yield and antioxidant capacity of two lettuce genotypes "Santoro RZ" and "Kiribati RZ".

Lettuce genotypes are fertilized with organic fertilizer (Slavol) and organic-inorganic NPK fertilizer (Fitofert hemisuper plus) during the vegetation. The analyzed parameters were root length and head weight of lettuce, total phenols, and flavonoids, as well as antioxidant capacity. Lettuce genotypes "Santoro RZ" and "Kiribati RZ" fertilized with organic fertilization showed the highest content of total phenols (358.13 ± 1.30 mg RU/100 g of fresh sample), the total content of flavonoids (114.22 ± 0.3 mg RE/100 g of fresh sample) and antioxidant capacity (neutralization of DPHH radicals 58.72 ± 1.88%).

The results revealed that the yield and antioxidant capacity of lettuce can be improved by using organic fertilizers.

Keywords: *lettuce, genotype, fertilizer, total phenols, antioxidant capacity*.

INTRODUCTION

Lettuce (*Lactuca sativa* L.) is a very important and widespread vegetable plant. The largest producers of lettuce in Europe are Spain, Italy, and Germany (FAO, http:// www.fao.org/faostat/en/#data/QC). Lettuce is consumed as a fresh vegetable, mostly as a salad or as a minimally processed vegetable. It is important in the human diet because of its content of vitamins, minerals, and antioxidants. The advantage of lettuce, eaten raw, is that it maintains more nutrients than thermally processed food [1].

The biological characteristics of lettuce and its specific growth and development are the basis for establishing the optimal method of cultivation. Fertilization of lettuce with various organic, mineral, and microbiological fertilizers is performed to achieve higher yields. Different fertilization systems can affect the high and good yield of vegetables in greenhouse production [2,3]. Organic fertilizers are of primary importance in plant growth and development. This fertilizer has all the necessary macro and microelements, and during mineralization, they improve the physical and chemical properties of the soil [4]. Various types of organic fertilizers should be applied in combination with mineral fertilizers, to achieve the best yields [5,6].

Manipulation of mineral fertilizers is much easier because nutrients are introduced into the soil in a directly accessible form. Overdressing of mineral fertilizers can cause various problems, such as soil contamination and underground water after harvesting crops [7]. Mineral fertilizers can have a detrimental effect on plant quality, declining dry matter content, increasing soil acidity, degeneration of physical characteristics, and increased erosion, and instability of soil aggregates [8,9].

Biostimulators are popular in sustainable agriculture because they activate several physiological processes that improve food efficiency, stimulate plant growth, and reduce fertilizer consumption [10]. The use of biofertilizers has ecological and economic justifications. These fertilizers occupy a special place in organic, sustainable agricultural production. Biostimulators help the plant to resist the effects of biotic and abiotic stresses, increasing the quality and yield of the plant [11].

The aim of our study was to determine the effect of different fertilization methods on the yield, nutritional value, and antioxidant capacity of lettuce.

MATERIAL AND METHOD OF WORK

Plant material

Two genotypes of lettuce "Santoro RZ" and "Kiribati RZ" were used during the study. The experiment was set up at the Lukavica site, in the area of the city of East Sarajevo (43.8269 0N 18.3832 0E) from spring 2021. in greenhouse conditions.

Experimental design

The test plants were planted by block method in three replicates with the size of the experimental plot $2m^2$ (1 x 2 m). Lettuce was grown by planting seed 530 x 310 x 60 mm. One month of seedlings with well-formed 4–5 true leaves was transplanted at a distance of 30x20cm. Dripping irrigation was used during the experiment.

Fertilizers

We applied different types of fertilization in the experiment. One part of the plants were fertilized with a biostimulator-Slavol. Slavol is a preparation that contains nitrogen-fixing bacteria and phosphorus mineralizer, growth stimulators that produce auxins (indole-3 acetic acid) in the fermentation process in the range from 0.01 to 0.1 mg/L. It was used in the amount of 200 mL/10 L of water.The other part of the plants was fertilized with organic-inorganic NPK fertilizer-Fitofert hemisuper plus. In addition to organically active components, this fertilizer contains humic and fulvic acid, carbohydrates, betaine, and lignosulfonates. It is used in the amount of 100 mL/10 L of water.A third of the experimental plants were not treated with fertilizer. These were control plants.

Fertilization was performed in the following stages of lettuce development: rooting phase, rosette leaf formation phase, and head formation phase.

Harvesting and handling after harvest

Lettuce samples were harvested at the stage of technological value. After harvest, the fresh weight of the rosette (head) (FW) was measured using a digital scale to two decimal places and the results are shown in grams (g) as the mean value for three replicates.

Applied methods:

Determination of total phenols and flavonoids

The plant material (50 g) was extracted with 75% ethanol, and the extraction with the same plant material was repeated three times with five times the volume of solvent relative to the weight of the

crushing plant, for 24 h. The resulting extracts were filtered, combined, and concentrated in a vacuum.The content of total phenolic compounds was determined by the Folin-Ciocalte spectrophotometric method [12] and was expressed as gallic acid equivalent (mg GAE/100 g fresh sample).The total amount of flavonoids was determined by the method with $AlCl_3$, described by [13], and the results are presented as equivalently rutin (mg RE/100 g fresh sample). All results are expressed as the mean of the three measurements of the analyzed samples (± standard deviation).

Determination of antioxidation activity

DPPH „scavenger" activity was determined by the method which spectrophotometrically monitored the reaction between a stable DPPH radical (1,1-diphenyl-2 picrylhydrazyl radical) and a sample whose antioxidant activity was examined [14]. A modified method was used to determine the antioxidant activity by the ABTS test (Total Equivalent Capacity assay). Antioxidant activity is expressed in % inhibition.

Statistical analysis

All samples were analyzed in triplicates. The results are expressed as mean values ± standard deviation (SD). Differences were considered significant if *P*-values were under 0.05. Statistical analysis of experimental data was performed using the Statistica (Tukey HSD Test) (StatSoft Inc. "STATISTICA Data Analysis Software System, (Version 10).

PCA

Principal component analysis (PCA) is a statistical technique applied to a set of variables when the researcher is interested in which variables of the set form coherent subsets that are relatively independent of each other [15].

RESULTS AND DISCUSSIONS

Root length and rosette weight were measured from growth parameters, and the results are given in Figure 1.

The highest root length was recorded in the genotype "Kiribati RZ" treated with the fertilizer Slavol (11.21 cm), while the lowest value was recorded in the genotype „Santoro RZ" in the control variant (8.44 cm). Use of biostimulators actively helps the development of the root system [16,17].

The weight of the rosette varied depending on the genotype and the type of fertilizer. The highest weight was in the genotype „Kiribati RZ" treated with Slavol fertilizer (249.48 g), followed by the genotype „Santoro RZ" treated with the same fertilizer (222.99 g). In their research, a group of authors concluded that the use of biostimulators stimulates the growth of the aboveground part of the plant by an average of 29% compared to the control variant [4,18,19].

Chemical characterization of lettuce leaves

Total phenolic content and antioxidant activity

In the extracts of lettuce, the content of total phenols, flavonoids, and antioxidant capacities was determined, the results are shown in Figure 2. All samples contain total phenols and flavonoids. The content of total phenols and flavonoids depends on the genotype and the type of fertilizer. The highest concentration of total phenols was measured in genotype "Kiribati RZ" fertilized with Slavol (358.13 ± 1.30 mg RE/ 100 g fresh sample).

The lowest concentration was in the genotype "Kiribati RZ" which treated with Fitofert hemisuper plus (from 115.35 ± 1.64^a mg GAE / 100 g fresh sample). All samples treated with fertilizer showed higher phenol content compared to the control sample. Application of fertilizers affects the yield,

physiological characteristics, and content of phenolic compounds in wheat grain *(Triticum aestivum L. ssp. aestivum)* [20,21,22].

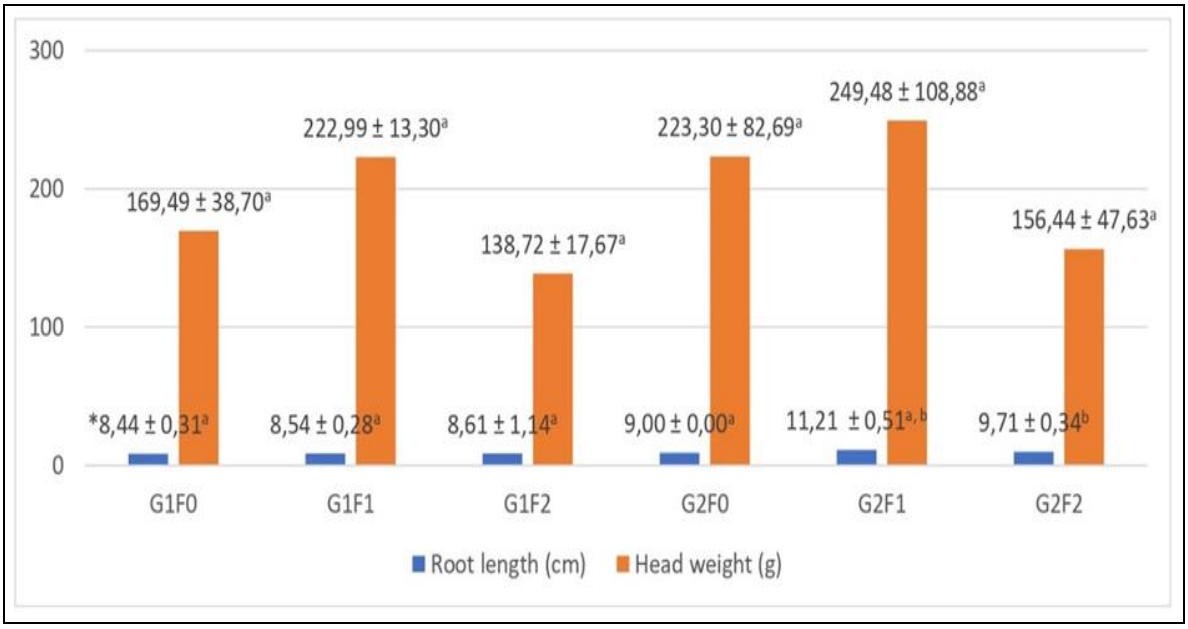

Figure 1. Effect of different fertilization methods on root length and head weight in lettuce

G – genotypes (G_1 – Santoro RZ, G_2 – Kiribati RZ); F – Fertilizers (F_0 – control, F_1 – Slavol, F_2 – Fitofert hemisuper plus)
* = Mean value ± standard deviation (n = 3)
[a-b] Different letters in superscript indicate the statistically significant difference between values, at a significance level of $p<0.05$ (based on Tukey's HSD test)

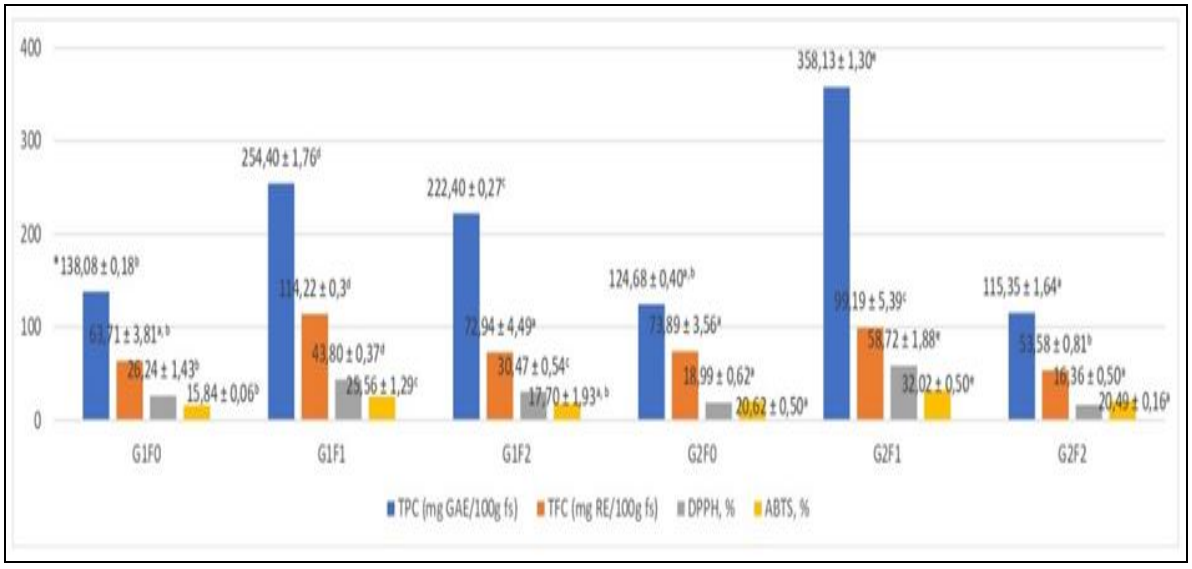

Figure 2**.** Total phenols, flavonoids and antioxidant capacity of lettuce leaves

G – genotypes (G_1 – Santoro RZ, G_2 – Kiribati RZ); F – Fertilizers (F_0 – control,F_1 – Slavol,F_2 – Fitofert hemisuper plus)
* = Mean value ± standard deviation (n = 3)
[a-b] Different letters in superscript indicate the statistically significant difference between values, at a significance level of $p<0.05$ (based on Tukey's HSD test)

The flavonoid content is dominated by genotype „Santoro RZ" treated with Slavol fertilizer (114.22 ± 0.3^d mg RE/100 g fresh sample). The lowest content of flavonoids (53.58 ± 0.81^b mg RE/100 g of fresh sample) was in genotype "Kiribati RZ" treated with Fitofert hemisuper plus fertilizer. It can be concluded that the type of fertilizer affects the phenolic and flavonoid content [2,6].

In our study, values for total phenolic content and flavonoids were higher for plants treated with organic fertilizers. The effect of organic fertilizers, fish pellets and manure mixtures affect the phenol content, and the overall fruit quality of tomato varieties [23]. Also the influence of fertilizers during the growth and development of the plant, shows an increased content of phenols and flavonoids compared to the control soil [24].

The antioxidant activity of lettuce was determined by DPHH and ABTS tests. All samples showed antioxidant capacity. The percentage of neutralization of DPHH radicals ranges from 58.72 ± 1.88 e% for genotype "Kiribati RZ", treated with Slavol fertilizer, to 16.36 ± 0.50% for "Kiribati RZ" sample treated with Fitofert hemisuper plus fertilizer (Figure 2).

The examined samples also show a high degree of $ABTS^+$ „scavenging" activity. Both methods confirmed that fertilizer-treated lettuce samples had a much higher antioxidant potential compared to the control sample. The results are in agreement with previous research that different ways of fertilizing vegetables adding biostimulants, significantly affect the antioxidant capacity [25, 26].

A similar observation for an increase in total phenols content and antioxidant capacity was reported after treatment with organic fertilizers in peppers ,cucumbers, watermelons and melon fruits [27].

Thus, the results revealed that the quality and nutritional value of lettuce leaves could be improved by applying organic fertilization for the production of foods for human healthy nutrition.

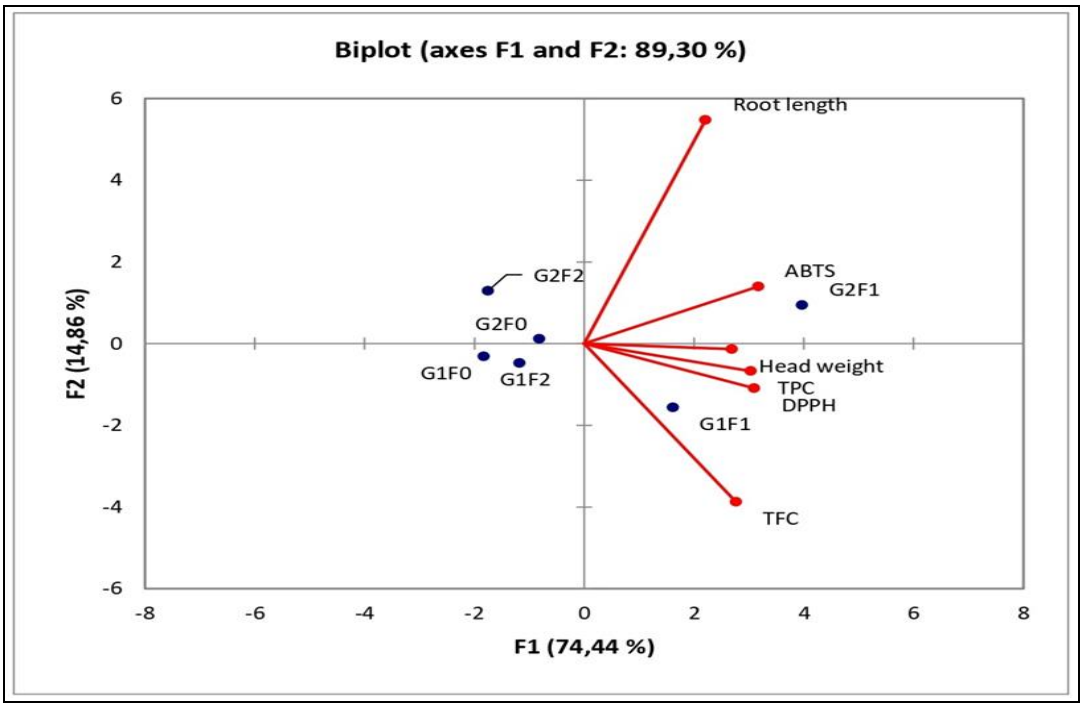

Figure 3. PCA of independent variables and responses of root length/rosette weight and bioactive components

The results of the PCA are shown in Figure 3. A scatter plot was created with the first two principal components from PCA of the data matrix, with the first principal component at the x-axis and the second at the y-axis, to visualize trends in the displayed data and demonstrate the discriminating effectiveness of the descriptors used. The contribution of the variables (%) showed that ABTS (20.69%), DPPH (19.94 %), TPC (18.95%) and head weight (14.87%) most participated in F_1, and root length (61.63%), and TFC (30.92%) in F_2.

The position of the samples in Figure 3 was primarily influenced by the type of fertilizer than the genotype of the values of the first principal component. Samples G_2F_1 and G_1F_1 were characterized by higher values of all analyzed parameters (oriented on the positive side of the x-axis by the positive value of the F_1 component), compared to other samples G_1F_0, G_2F_0, G_1F_2, and G_2F_2 oriented on the

negative side of the x-axis (by the negative value of the F_1 component). Therefore, sample G_2F_1 was characterized by the high values of the following parameters: root length and ABTS, and sample G_1F_1 was characterized by the high values of the following parameters: head weight, DPPH, TPC, and TFC.

The high concentrations of flavonoids contribute to the higher antioxidant activity of lettuce as well. Various studies have shown cohesion between total phenol content and antioxidant activity of fruits, plants, and vegetables.

A comparative study, of antioxidant properties, and phenolic profile [28] shows the cohesion of antioxidant properties and phenolic profile of the most consumption of berry species. Different investigations have shown a relationship between the total phenolic contents and the antioxidative activity of fruits, plants and vegetables [29,30].

CONCLUSION

The application of biostimulants gave statistically significant effects on the components of the growth and development of lettuce. It strongly influenced the development of the root system and aboveground mass.

The application of biostimulants had the greatest impact on the accumulation of secondary metabolites of phenol and total flavonoids compared to mineral fertilization. These results also support the concept of organic fertilization of lettuce genotypes “Santoro RZ” and “Kiribati RZ” that have strongly increased the antioxidant potential of vegetables.

The application of biostimulants can be an important strategy to increase the quality and yield of lettuce.

Received September 2023, accepted September 2023)

REFERENCES

[1] Aćamović-Đoković, G., Pavlović, R., Mladenović, J., Đurić, M. (2011). Vitamin C content of different types of lettuce varieties. Acta Agriculturae Serbica,vol.16, (32): 83–89.

[2] Bogdanović, D., Ilin, Ž., Čabilovski, R., Marijanušić, K., Adamović, B. (2014).Effect of direct and residual fertilization with organic and mineral fertilizers on tomato yield. Chronicle of Scientific Papers, Faculty of Agriculture Novi Sad,38(1): 59–68. https://doi.org/10.5937/lnrpfns1401059B

[3] Adejero, S.A., Arije, D. N., Adegaye, A. C. (2019). Residual effects of neem Azadirachta indica A. Juss.*(Sapindales: Meliaceae)* seed-based fertilizer and NPK on the performance of Basella alba L.*(Caryophyllales: Basellaceae)* plant. Brazilian Journal of Biological Sciences, 6(12): 141–148. http://dx.doi.org/10.21472/bjbs.061213

[4] Chatterjee, R., Bandhopadhyay, S., Jana, J. C. (2014). Organic amendments influencing growth, head yield and nitrogen use efficiency in cabbage *(Brassica Oleracea var. Capitata L.)*.American International Journal of Research In Formal, Applied & Natural Sciences 5(1): 90–95. http://www.iasir.net/

[5] Fatimah Obaid Saeed Ali Kalbani, Mohammed, A. Salem., Abdul, J. Cheruth,, Shyam, S. Kurup., A, Senthilkumar (2016). Effect of some organic fertilizers on growth, yield and quality of tomato (Solanum lycopersicum). International Letters of Natural Sciences Submitted: ISSN: 2300–9675, 53: 1–9. http://dx.doi.org/10.18052/www.scipress.com/ILNS.53.1

[6] Palia, M., Saravanan, S., Prasad, V.M., Upadhyay, R.G., Kasera, S.(2021). Effect of Different Levels of Organic and Inorganic Fertilizers on Growth, Yield and Quality of Brinjal (*Solanum melongena* L.). Agricultural Science Digest 41 (special issue), 203–206. https://arccjournals.com/journal/agricultural-science-digest/D-5157

[7] Gordon, W. B., Whitney, D. A., Raney, R. J. (1993). Nitrogen Management in Furrow Irrigated, Ridge-Tilled Corn. Journal of production agriculture, 6(2): 213–217. https://doi.org/10.2134/jpa1993.0213

[8] Hammad, H. M., Khaliq, A., Abbas, F., Farhad, W., Fahad, S., Aslam, M., Bakhat, H. F. (2020). Comparative effects of organic and inorganic fertilizers on soil organic carbon and wheat productivity under arid region. Communications in Soil Science and Plant Analysis, 51(10): 1406–1422.

[9] Adeniji, A.A. (2020). Effects of Incorporated Green Manure and Inorganic Fertilizer on Amaranth *(Amaranthus Caudatus.* L.) Vegetable. International Journal of Trend in Scientific Research and Development (IJTSRD),4(6): 1414–1419. http://eprints.federalpolyilaro.edu.ng/id/eprint/1466

[10] Yakhin, O.I., Lubyanov, A.A., Yakhin, I.A., Brown, P.H. (2017). Biostimulants in plant science a global perspective.Frontiersin in Plant Science 7, article 2049, 1–32. https://doi.org/10.3389/fpls.2016.02049

[11] Banaker, S. N., Kumar, M. P. (2020). Foliar application of red seaweed *(Kappaphycus alvarezii)* bioformulations increased the levels of chlorophyll content in rice. Journal of Pharmacognosy and Phytochemistry, vol.9, Issue 1, 408–410.

[12] Singleton, V. L., Orthofer, R., Lamuela-Raventos, R.M. (1999). Analysis of total phenols and other oxidation substrates and antioxidants by means of Folin-Ciocalteu reagent. Methods in Enzymology 299: 152–178. https://doi.org/10.1016/S0076-6879(99)99017-1

[13] Brighete, I.M.C., Dias, M., Verdi, L.G., Pizzalatti, M.G. (2007). Antioxidant activity and total phenolic content of some Brazilian species. Pharmaceutical Biology 45:156–161. https://doi.org/10.1080/13880200601113131

[14] Kumarasamy, Y., Byres, M.,Cox, P.J., Jasapars, M., Nahar, L., Sarker, S.D. (2007): Screening seed of some Scottish plants for free-radical scavenging activity. Phytotherapy Research 21: 615–621. http://dx.doi.org/10.1002/ptr.2129

[15] Rajčić, K. (2015). Comparison of principal component and factor analysis, Master's thesis, University of Zagreb, Faculty of Science.

[16] Zeljković, S., Parađiković, N., Babić, T., Đurić, G., Oljača, R., Vinković, T., Tkalec, M. (2010). Influence of biostimulators on the growth and development of *(Salvia splendens L.)* seedling roots. Journal of Agricultural Sciences, 55: 29–36. http://www.doiserbia.nb.rs/img/doi/1450-8109/2010/1450-810910010029Z

[17] Ergović, L. (2019). Influence of biological preparation on salad seedling adaptation, Doctoral dissertation, Josip Juraj Strossmayer University of Osijek. Faculty of Agrobiotechical Sciences Osijek.Department for agroecology. https://urn.nsk.hr/urn:nbn:hr:151:965440

[18] Cvijanović, G., Petrović, G. B., Marinković, J., Cvijanović, V., Đurić, N., Roljević Nikolić, S. (2017). Microbiological activity of land and productivity of different genotypes of wheat in a sustainable system of production.Knowledge–International Journal,20(5): 2351–2356.

[19] Zeljković, S., Parađiković, N., Tkalec Kojić, M., Mladenović, E. (2021). Effect of biostimulant application on development of pansy *(Viola tricolor var. hortensis dc.)* seedlings. Journal of Central European Agriculture, 22(3): 596–601. https://doi.org/10.5513/JCEA01/22.3.3191

[20] Stumpf, B., Yan, F., Honermeier, B. (2019). Influence of nitrogen fertilization on yield and phenolic compounds in wheat grains *(Triticum aestivum L. ssp. aestivum*). Journal of Plant Nutrition and Soil Science, 182(1): 111–118. http://dx.doi.org/10.1002/jpln.201800342

[21] Khan, M. A., Basir, A., Saeed, B. (2020). Biochar Improves Phenological and Physiological Attributes of Wheat in Soil Amended with Organic and Inorganic Nitrogen Sources. Sarhad Journal of Agriculture, 36(4): 1214–1226. http://dx.doi.org/10.17582/journal.sja/2020/36.4.1214.1226

[22] Tian, W., Wilson, T. L., Chen, G., Guttieri, M. J., Nelson, N. O., Fritz, A., Li, Y. (2021). Effects of environment, nitrogen, and sulfur on total phenolic content and phenolic acid composition of winter wheat grain. Foods10 (11): 2857. https://doi.org/10.3390/foods10112857

[23] Bileva, T., Petkova, N., Babrikov, T.(2020). Influence of Organic Fertilization on Nutritional Characteristics and Antioxidant Capacity of Melon Fruits. Bulletin of University of Agricultural Science and Veterinary Medicine Cluj-Napoca. Food Science and Technology 77(2): 17–25.http://dx.doi.org/10.15835/buasvmcn-fst:2020.0013

[24] Malenčić, Đ., Kiprovski, B., Rajković, M., Miladinović, J., Kljakić, S., Šućur, J. (2019). Changes in polyphenol content in soybeans *(Glycine max L.)* and tatula (*Datura stramonium* L.) after treatment with herbicides and Delfan Plus.Annals of Agronomy,43(1): 26–37. http://fiver.ifvcns.rs/handle/123456789/2187

[25] Chu, Y., Sun, J., Wu, X., Liu, R. (2002). Antioxidant and antiproliferative activities of common vegetables. Journal of Agricultural and Food Chemistry, 50(23): 6910–9616. https://doi.org/10.1021/jf020665f

[26] Emeghara, U., Olukotun, O., Olagunju, O. E., Akanni-John, R., Oni, B.O., Ganiyu, L., Rasheed, F. M. (2020). Effect of Different Organic Manures on the Growth and Yield of Water melon *(Citrullus lanatus)*.Asian Soil Research Journal, 37–43. https://doi.org/10.9734/asrj/2020/v4i230091

[27] Babrikov, T., Bileva, T., Tzvetkov, P., Petkova, N., Ivanov, I., Denev, P. (2016). Influence of biofertilizers and biopesticides on the growth, development and production quality of some vegetable crops, Agricultural University – Plovdiv, Scientific Works, LX (2), 61–70. https://mc04.manuscriptcentral.com/agriculture

[28] Okatan, V. (2020). Antioxidant properties and phenolic profile of the most widely appreciated cultivated berry species: A comparative study. Folia Horticulturae, 32(1): 79–85. https://doi.org/10.2478/fhort-2020-0008

[29] Gao, Y., Guo, X., Liu, Y., Zhang, M., Zhang, R., Abbasi, A. M., You, L., Liu, R.H. (2018). Comparative assessment of phytochemical profile, antioxidant capacity and anti-proliferative activity in different varieties of brown rice (*Oryza sativa* L.).Food Science and Technology 96:19–25. https://doi.org/10.1016/j.lwt.2018.05.002

[30] Fitriana, A. S., Royani, S. (2020). Identifying Antioxidant Activities of Guava Fruit Using DPPH Method. Proceedings of the 1st International Conference on Community Health (ICCH 2019) https://doi.org/10.2991/ahsr.k.200204.027

ENVIRONMENT

Renewable resources,
thermal comfort, use of public space

Editors

Prof. Ph.D. Jovan Đuković,
Prof. Ph.D. Svjetlana Radmanović (Cupać)

Original scientific article
http://dx.doi.org/10.59456/afts.2023.1529.057S

ENVIRONMENTAL, SOCIAL AND OTHER NON-PROFIT IMPACTS OF MOUNTAIN STREAMS USAGE AS RENEWABLE ENERGY RESOURCES

Stevović Ivan[1], Hadrović Sabahudin[2], Jovanović Jovana[3]

[1]*Innovation Center, Faculty of Mechanical Engineering in Belgrade, Republic of Serbia, e.mail: istevovic@mas.bg.ac.rs*
[2]*Institute of forestry, Belgrade, Republic of Serbia*
[3]*Faculty of Civil Engineering and Management, University Union Nikola Tesla, Belgrade, Republic of Serbia*

ABSTRACT

The main subject of this manuscript is mountain streams used by construction of small hydro power plants. The motivation for this research stemmed from a number of conflicting opinions about the justification of the construction of small hydropower plants and their facilities. This research encompasses different methods for the analysis of the justification of the construction of a small hydropower plant, starting from tradition in correlation with water mills, through a techno-economic approach to a complex multi-criteria research model. All methods are represented by objective formulas.

World experiences are also presented, through the level of potential utilization, compared to the degree of development. The possible positive and negative impacts of the construction of such facilities for the exploitation of the potential of small watercourses were analyzed. After the conducted research, and with respect to the principle of minimum energy, which has become the paradigm of modern civilization, it can be concluded that using the potential of small watercourses by building small hydropower plants belongs to the domain of using renewable energy sources and that it is a function of sustainable development.

Decision makers are recommended to exclusively apply a multi-criteria methodology, which can holistically include all technical, economic, environmental, social and other non-profitable but important impacts.

Key words: *streams, renewable energy, resources, environmental impacts, social impact*

INTRODUCTION

Analysis of coal reserves and coal quality show decreasing function [1] and that is why the transition to renewable energy sources is imperative and the paradigm of the new age. The potential of small streams and small hydropower plants (SHPP) is one of the possible resources and means of using renewable energy sources (RES). The recent negative practices in some countries that SHPP couldn't be constructed due to public hearing; although the design fulfilled every legal step, are a motive for the research carried out in this paper. The goal is to examine the issues of conflicting interests on a holistic way, to quantify and rank certain negative environmental impacts and seek synergistic sustainable solutions with less negative environmental, social and other non-profit impacts.

The obtaining of a permit for the construction of SHPPs, in accordance with the law, necessarily follows the preparation and adoption of the Environmental and Social Impact Assessment Study. The study is reviewed by the competent authorities, but since the public hearing becomes one of the most important steps in a decision making process, the study has to be accepted by the interested local community and the wider public. Rejecting a study, and consequently rejecting a project at a public hearing, regardless of whether the investment is private or social, results in the devaluation of previously invested funds in the project. At the same time, if the Study is accepted and if the project is approved and implemented, the question arises whether the prescribed biological minimum and environmental and social protection measures, such as monitoring and sanctions for offenses, will be respected in practice.

The implementation of renewable energy sources is an imperative of the modern age and obligations under the Kyoto Protocol, the Paris Agreement and other binding international agreements signed so far [2]. Although RES are far more favorable for the environment, it happens more and more often that environmental movements in public debates shoot down hydropower projects, including SHPP projects. That is why this manuscript represents a tradition, techno economy and multi-criteria holistic assessment of relevant aspects of synergic incorporation of SHPPs.

In order to manage resources efficiently, so that they can be used by future generations, and in order to avoid any abuse, it is necessary to include all relevant stakeholders in the decision-making process at the very beginning of the optimal construction concept. Also, it is important to have access to adequate methodologies. The goal of this paper is to analyze all potential impacts, all conditions and constraints, and then to align the criteria by degree of importance as positive or negative, in order to help in compromise decisions. Comprehensive and long term consideration of the problem is required, and that is why the methodology starts from the traditional approach. In this paper, after tradition and techno economy approach, for the selection of an optimal SHPP concept, whether it will be a multipurpose, accumulative, flow or derivative type of plants, it proposes a methodology with multicriteria approach with respect to all conflicting interests and the search for synergistic compromise solutions. Examples of different practices in the field of hydropower in EU are given too. Main positive and negative environmental and social impacts are analyzed. The multicriteria methodology is offered as a support for decision makers, with the goal to reach the optimal holistic solution for optimal streams exploitation.

METHODOLOGY

Although the carbon dioxide level is very high and SHPP are RES, in some countries, SHPP can't be constructed due to negative public hearing. Recently, in some cases, consideration of environmental protection has appeared as absolute conservation of everything in the stage "as it is". That idea is to remain small rivers intact. A series of random events is possible to happen on public hearing. This introduces entropy in decision making process of big strategic projects. On the same time, elimination of some profitable strategic energy structure by giving such a big importance to public hearing in local community is under risk sometimes, although this construction can present big benefit for wider social community. Science try to develop a different multicriteria holistic approaches in order to prevent mistakes in strategic decisions, such as the construction of hydro technical structures, HPPs or SHPPs are. The methodology in this manuscript encompasses holistic approach which respects tradition and develops multicriteria analyze of all relevant input variables, i.e. influencing factors for decision-making.

Methodology based on tradition

Carter d'Kinsey said that in order to reach the original principles in the contemporary construction and building creativity of different countries, there were several paths [3]. The main ones, which lead to the goal the fastest, rely on the tradition and nature of the given area, on concepts and phenomena proven throughout history, as well as on the cultural monuments already built. One of the cultural monuments is certainly the water mill, as a forerunner of SHPP.

Starting from the traditional principles of construction and the selection of the location of the existing, old mills, optimal solutions for the construction of SHPP are arrived at [4]. The researches on the locations of old water mills have confirmed that the locations of old water mills are most often the optimal disposal solution for small, mini, or micro hydropower plants. With relatively small additional investments, it is possible to reconstruct and revitalize the mill building, install equipment for a small hydroelectric power plant, implement "feed in" tariffs, or be part of the program of co-financed CDM (clean development mechanism) projects, with green certificates, reap benefits on the CER market (certified emission reduction), and yet preserve the quality of the environment and have a positive social impact on the local community.

The reconstruction of old mills into small hydroelectric plants, while retaining the authentic architectural and cultural values of the buildings, is one of the possible ways of efficient use of renewable hydro energy, in the function of sustainable development.

If the region of Serbia is analyzed as a case study, it can be said that throughout history, from the time of the Nemanjic dynasty until today, significant constructions that use renewable energy sources have been recorded. Regardless of the history and literary works related to the mills, it is evident that they were built in the locations where the flows are relatively stable, where the watercourse rarely dries up and where, definitely, there is technically usable potential, so notes from history can still be purposeful used today. The hydro potential at the site of an old water mill is not large, but it is significant through the mathematics of a series of small numbers and in the context of preventing global warming and the difference related to the impact on the environment, when renewable, instead of non-renewable energy sources are used.

In a long-term analysis, Serbia does not have enough energy resources to meet the needs of its own consumption in the future and that in this case it would have the right to ignore the potential of small watercourses.

Techno economy approach

Profitability can be examined by the cost-benefit method of economic analysis. Comparison and evaluation of all advantages and shortcomings of different models of small hydro power plant, as a business operation, is to be performed. Also, costs and benefits are analyzed. This method is important for making right decisions and project corrections, but this method doesn't include environmental and social impact factor.

Techno economy approach relly on calculation of correlation between all benefits (measured by money income) and real construction cost of all necessary feacilities. When calculating the profitability coefficient, as basic techno-economic indicator of profitability, following formula (1) is to be applied:

$$r = \frac{B}{C} \tag{1}$$

with following values:

- r_i – profitability coefficient for small hydro power plant
- B_i – financially quantified benefits (gains) of small hydro power plant
- C_i – costs (investment, maintenance and operational costs) of small hydro power plant

Multicriteria approach

Small-scale hydropower is a promising area and at the same time has its theoretically proven justification [5]. Sometimes one comes across various abuses of the water resources of small streams, as a common good, on blocked fishing paths, on situations with non-observance of the specified guaranteed ecological flow, which unfairly casts a shadow on the entire area of small hydropower and forces scientists and engineers to look for more adequate methodological approaches to testing and

proving the justification for the construction of such facilities. When a wider area is chosen for the construction of the SHPP, the methodology offered in the following text enables the selection of an optimal synergistic solution, which holistically respecting all relevant decision-makers at the very beginning of the process, would reconcile conflicting interests in the function of environmental protection, positive social impacts, as well as other components of sustainable development.

New methodologies must inevitably have a holistic approach. To solve a series of problems, a synergistic solution can be sought by forming a multi-criteria system with n relevant input variables that should holistically include, but not be limited to:

- Technical
- Economic
- Financial
- Energy
- Environmental
- Cultural and historical
- Political
- Regulatory influencing factors

For each individual situation in practice, the relevant input variables are specifically formed, ie. influencing factors for decision-making. In the light of today's sharpened conflicting interests, for the solution of the optimal concept of the SHPP construction, for the selection of, whether it will be a multi-purpose, accumulation, flow or derivation plant, a methodology is proposed that respects all opposing actors and seeks compromise synergistic solutions, using multi-criteria optimization, supplemented with Delphi method and survey method.

In order to understand all possible developing strategies for construction of small hydro power plant, not only from the angle of technical, economic and financial parameters, but also from the angle of environmental, social and other impacts, a multi-criteria analysis can be applied. *n* alternative solutions for electricity supply from small hydro power plant a_i are analyzed:

a_1 – Supply from small hydro power plant technical solution 1
a_2 – Supply from small hydro power plant technical solution 2
a_3 – Supply from small hydro power plant technical solution 3
...
a_n – Supply from small hydro power plant technical solution n

Alternative supply solutions can be scaled by one of multicriteria method: Analytic Hierarchy Process (AHP) [6], ELECTRE [7], PROMETHEE [8], VIKOR [9], Simple Additive Weighting (SAW) [10] and their variations. It is considered that for the decision maker following criterion functions f_j are crucial:

f_1 - investment (€),
f_2 - maintenance and other costs (€/day),
f_3 - price of 1 kWh in the energy market (€c/kWh)
f_4 - environmental impact (objective note, scaled from 1 to 5, gained by Delphi method)
f_5 - social impact (objective note, for instance scaled from 1 to 5, gained by Delphi method or survey method)
...
f_j - other impacts not numerically quantified.

i = 1, 2, 3, ..., n
j = 1, 2, 3, ..., m

The matrix with criteria values k_{ij} for each variant can be constructed as presented in Table 1.

Table 1: Matrix of alternatives a_i and relevant criteria f_j

	f_1	f_2	f_3	...	f_j
a_1	k_{11}	k_{12}	k_{13}	...	k_{1m}
a_2	k_{21}	k_{22}	k_{23}	...	k_{2m}
a_3	k_{31}	k_{32}	k_{33}	...	k_{3m}
...	...	...	...	...	...
a_n	k_{n1}	k_{n2}	k_{n3}	...	k_{nm}

Investment (€) represents the criteria f_1 for each variant. Criteria f_2 means maintenance and other costs (€) on daily bases. Criteria f_3 represents the price of 1 kWh in the energy market. For instance criteria f_4 or f_5 can be calculated as objective notes (scaled from 1 to 5), obtained by Delphi method or questioner method.

Every community strives to minimize investment, maintenance and other costs (criteria f_1 and f_2). At the same time, the goal is to maximize the selling price of electricity on energy market (criteria f_3) and positive impact on the environment (criteria f_4) and social impact (criteria f_5). In this case the function of criteria f_1 and f_2 are to be minimized, and the function of criteria f_3, f_4 and f_5 are to be maximized, as per equations:

$$\lim (f_1, f_2) \rightarrow \min \quad (2)$$

$$\lim (f_3, f_4, f_5) \rightarrow \max \quad (3)$$

In order to test results stability and conclusions, an analysis of sensitivity of the result changes to input variables change has to be made by criteria weight. Matrix of different combinations of criteria weight f_j is to be done. The results of the multi-criteria ranking by any method can have a graphic and/or table representation.

Delphi method

Experts from the field were interviewed, all of them in long-term business contact with the small hydro power plants, among which were: main investor, chief manager, marketing manager, main supply manager, main engineer for construction, main engineer for the design of small hydro power plant, environmental expert, social expert, economy expert, low expert, energy expert, etc. Experts have been asked a set of the most important questions, for which it is considered, after the experts' response, to be able to reach conclusions on the best solution [11].

Answers of individual experts, their probability and statistical analysis of expert team survey results using the Delphi method can be presented graphically for each of the selected questions. The expert team is to be composed of renowned experts in the field, which ensured objectivity and competence. The experts answered the same questions in four rounds. Arithmetic mid, variant and standard deviation are statistical indicators can be calculated for each question.

Based on answers obtained in the first round of the Delphi method, average forecasts are calculated that represent the mid value of individual forecasts, as well as variations of forecasts around the mid value, which represent a corresponding degree of forecast precision. The second round of the Delphi method, sent to the experts, contained a calculated average forecast, a corresponding degree of forecast precision and extreme forecasts with their explanations. Experts were asked to review their original forecasts, make possible corrections, and deliver an opinion on extreme forecasts along with appropriate argumentation.

The final forecast was obtained as the mid value of the forecasts from the last round of the Delphi method. In the next phase of the Delphi method, testing of time dimension of achieved and set target functions was carried out, as well as the level of compliance of the experts' responses with respect to all issues and realization period of targeted events with high probability.

RESULTS AND DISCUSSION

EU experiences

The utilization of water potential is on average around 65% in Europe [12], while for example in Africa it is 1,2% [13]. Some European countries have a very high level of hydropower utilization:

- Norway – 100%
- France and Italy - 87%
- Spain and Switzerland – 86%
- Sweden – 65%

In many underdeveloped countries, the percentage of technically and economically utilized hydro potential is relatively low. As a renewable form of energy, the most environmentally acceptable and cheapest form of energy, hydro potential certainly represents a natural source, i.e. good of public interest and significant economic potential in the development strategy of each country. It also plays an important role in the country's electricity balances, in the present and the future, which is characterized by a large lack of electricity in relation to the increase in the number of inhabitants and the increase in consumption on the one hand and the imperative to switch to RES on the other. Over 4,000 small hydroelectric power plants operate in Austria. The short-term plan is to build several hundred more MHE. Austria's national goal is to produce 100% of energy from RES by 2030 [14]. More than 70,000 SHPPs operate in Germany [15]. In Norway, for example, it produces more than 6000 GWh/year at small hydroelectric plants [16].

Positive and negative results in practice

By building a large number of SHPPs, the problem of increasing consumption and demand for energy cannot be solved entirely, but water can be used for multiple purposes and much more efficiently. Water flows in any case, it is a cheap and renewable resource, always available. After passing through the turbine, that resource is available to other users with unchanged quality. In addition, the implementation of SHPP reduces proportionally the use of non-renewable, environmentally much less clean type of resources, such as e.g. fossil fuel.

Various protective measures are being used to speed up the use of hydro potential at small hydro power plants in both developed and underdeveloped countries. Their positive impacts are numerous: SHPPs use water, which is a renewable natural resource, they have almost no negative impact on the environment, and there are feasible protection measures for eventualities, they have a favorable impact on the development of the domestic electrical and mechanical industry, the entire water management and small economies of underdeveloped regions, participate in the electrification of terrain and areas far from roads and main traffic routes, contribute to savings in the construction of the general distribution network, regulate and establish the biological minimum of mountain streams, help in the regulation of sediment transport of torrential watercourses.

Given the numerous advantages, many countries are introducing various forms of incentive norms, as well as hybrid models [17]. For example, the Norwegian government, which has almost 100% utilized hydro potential, provides non-refundable financial assistance for the construction of small hydropower plants, providing up to 80% of the total construction costs. Such large subsidies have their own strategic and economic justification, because they primarily refer to small hydropower plants, which are usually built outside the distribution network, as an independent energy facility, intended to supply and meet the energy needs of a small number of remote consumers.

If the natural conditions are analyzed, it can be concluded that in many countries there are prerequisites for the construction of small hydropower plants, but there is still not enough attention and necessary activities directed to this area. Today, bearing in mind the number of small hydroelectic

power plants that have already been built and the need to consider the mass construction of such facilities, the construction possibilities are still increasing. In the field of construction of small hydropower plants, the following activities can be carried out:

- reconstruction and revitalization of existing small hydropower plants,
- automation of small hydropower plants that are in operation,
- adaptation of existing mills into small hydropower plants,
- additional installation of new aggregates with an installed power of up to 10 MW, within the existing dams and hydroelectric power stations, with the aim of fully utilizing the existing hydro potential and
- construction of new small hydroelectric power plants as independent facilities, at previously unused locations

With the goal of converting the existing hydro potential into used at small hydro power plants as soon as possible, standardization of projects and equipment for small hydro power plants should be done. The execution of typical construction works and facilities is the first step, which precedes the necessary standardization of electro-mechanical equipment, which enables faster and easier installation of the automatic system of control and management of small hydropower plants, without a crew. At the same time, this standardization represents the right move that makes the production of equipment for small hydropower plants financially attractive and profitable for the entire industrial production of a country. Another possibility lies in the research of all abandoned buildings and mills where the production of electricity could be ensured, in a short period of time and with relatively low investments and minimal construction work, which could be very necessary and important for the local consumers. It is necessary to analyze all possibilities of construction and reconstruction of small hydropower plants in order to solve the issue of supplying various small consumers, who are sometimes far from the power grid.

CONCLUSION

Today, when the principle of minimum energy is becoming a paradigm of civilization, using the potential of small watercourses by building small hydropower plants belongs to the domain of using renewable energy sources and is a function of sustainable development. The topic of this manuscript was research into the use of the hydro potential of small watercourses as synergistic solutions, analyzed multi-criteria, through tradition, time and space and in function of today's many conflicting interests. Current examples of world experiences are also given. Just as watermills once had a great sociological and cultural importance and role in the social life of the village, so today MHE, designed and built as a result of a multi-criteria holistic approach, can become a center of events and a feature of the development of the local community. Science can solve any engineering, environmental and social problem. Related to that, synergy with the monitoring function is needed in practice, as well as with the education and adequate information.

Small hydropower plants with the most modern standardized solutions for construction and equipment are very quick and easy to construct, operate and maintain. With standard electromechanical equipment and typical construction works, small hydropower plants require minimal technical and organizational conditions for management, have reduced construction and maintenance costs, and therefore a quick return on invested capital. Today, small hydropower plants play a significant role in the strategy of increasing the production of electricity from RES [18], in the context of reducing global warming and the humanitarian policy "Energy for all".

The construction of small hydropower plants relies on the natural wealth in the streams of mountainous regions. Positive legal regulations and stimulating forms of financing play a major role in accelerating development and giving due importance to small hydropower plants. The production of electromechanical and hydromechanical equipment at the local level could have the same effect. The existence of as many as possible of adequate solutions of small hydropower plants can alleviate the energy crisis, help stabilization and economic development, and most importantly, practically do not

endanger the environment, and contribute to the general development of both local communities and the entire society.

ACKNOWLEDGEMENT

The results presented in this manuscript are obtained from the research supported by the Ministry of Science, Technological Development and Innovation of the Republic of Serbia under Contract no 451-03-47/2023-01/ 200213 dated 02/03/2023 year.

Received September 2023, accepted September 2023)

LITERATURE

[1] Ivković, Z., Tošić, D., & Dramlić, D. (2022). Analysis of coal reserves with the potential for underground exploitation in the Republic of Serbia. Archives for Technical Sciences, (26-1), 43-48.

[2] Mahabadi, D. (2023). Enhancing fairness in the Paris Agreement: lessons from the Montreal and Kyoto protocols and the path ahead. International Journal of Environment and Sustainable Development, 22(3), 329-348.

[3] Schneider, M., Golan, G., Yang, S., & Kinsey, D. (2015). US public diplomacy since 9/11: The challenges of integration. International public relations and public diplomacy, 15-36.

[4] Punys, P., Kvaraciejus, A., Dumbrauskas, A., Šilinis, L., & Popa, B. (2019). An assessment of micro-hydropower potential at historic watermill, weir, and non-powered dam sites in selected EU countries. Renewable energy, 133, 1108-1123.

[5] Stević, S., Milošević, H., Stević, I., & Hadrovic, S. (2014). Sustainable management of water resources in Prokletije region. Industrija, 42(1), 47-61.

[6] Ali, S., Stewart, R. A., Sahin, O., & Vieira, A. S. (2023). Integrated GIS-AHP-based approach for off-[]river pumped hydro energy storage site selection. Applied Energy, 337, 120914.

[7] Stević, I. (2017). Strategic orientation to solar energy production and long term financial benefits. Archives for Technical Sciences, (17), 1-12.

[8] Urošević, B. G., & Marinović, B. (2021). Ranking construction of small hydro power plants using multi-criteria decision analysis. Renewable Energy, 172, 1174-1183.

[9] Pan, Y., & Hashemizadeh, A. (2023). Circular economy-based assessment framework for enhancing sustainability in renewable energy development with life cycle considerations. Environmental Impact Assessment Review, 103, 107289.

[10] Taherdoost, H. (2023). Analysis of simple additive weighting method (SAW) as a multiattribute decision-making technique: A step-by-step guide. Journal of Management Science & Engineering Research, 6(1), 21-24.

[11] Yang, X., Xu, Z., & Xu, J. (2023). Large-scale group Delphi method with heterogeneous decision information and dynamic weights. Expert Systems with Applications, 213, 118782.c

[12] Wagner, B., Hauer, C., & Habersack, H. (2019). Current hydropower developments in Europe. Current Opinion in Environmental Sustainability, 37, 41-49.

[13] Bogaart, P. (2023). The potential for sustainable hydropower. Nature Water, 1(1), 22-23.

[14] Gaugl, R., Sommer, M., Kettner, C., Bachhiesl, U., Klatzer, T., Gruber, L., ... & Wogrin, S. (2023). Integrated Power and Economic Analysis of Austria's Renewable Electricity Transformation. Energies, 16(5), 2229.

[15] Couto, T. B., & Olden, J. D. (2018). Global proliferation of small hydropower plants–science and policy. Frontiers in Ecology and the Environment, 16(2), 91-100.

[16] Engen, S., Hausner, V. H., Fauchald, P., Ruud, A., & Broderstad, E. G. (2023). Small hydropower, large obstacle? Exploring land use conflict, Indigenous opposition and acceptance in the Norwegian Arctic. Energy Research & Social Science, 95, 102888.

[17] Kakoulaki, G., Sanchez, R. G., Amillo, A. G., Szabó, S., De Felice, M., Farinosi, F., ... & Jaeger-Waldau, A. (2023). Benefits of pairing floating solar photovoltaics with hydropower reservoirs in Europe. Renewable and Sustainable Energy Reviews, 171, 112989.

[18] Gebara, C. H., & Laurent, A. (2023). National SDG-7 performance assessment to support achieving sustainable energy for all within planetary limits. Renewable and Sustainable Energy Reviews, 173, 112934.

Original scientific article
http://dx.doi.org/10.59456/afts.2023.1529.065Dj

WBGT ANALYSIS OF THERMAL COMFORT OF THE AREA OF SEMBERIJA

Đurić Dijana[1]

[1]*Faculty of Civil Engineering Subotica, University of Novi Sad, Serbia,*
e mail: dijana.djuric.gf@gmail.com

ABSTRACT

Thermal comfort of urban areas is a highly researched field of science, which is gaining more and more importance in the field of ecology. The research of the area from the aspect of the convenience of physical activities and outdoor life provides data that is also useful in the health sector. This research included the area of Semberija in Bosnia and Herzegovina, which is characterized by unfavorable conditions during summer, due to high temperatures, swampy land and increased artificial presence of construction and industries.

Not all areas have the same weather conditions, therefore other factors such as relief and presence of forests are important in the overall state of the area. Therefore, data from two meteorological stations, at a short distance from each other, but in a different natural and artificial environment, were analyzed. These are the station in the town of Bijeljina and the station within the Mine and Thermal Power Plant in Ugljevik.

Within this research, the WBGT bioclimatic model was used, which is widely used in the world for the purposes of calculating the time that the human body can spend in direct sunlight during work or exercise, without rest. Given that the same time period is not covered, an average of 14 years (period 2005 - 2018) was analyzed for the area of Bijeljina, and an average of 8 years (period 2015 - 2022) for Ugljevik. The period from 2015 to 2018, which covers both locations, was also analyzed in order to make a comparison and notice the differences and determine the factors that affect the thermal comfort of the space.

Keyword: *thermal comfort, WBGT, bioclimatic indices, urban environment, land use*

INTRODUCTION

Thermal comfort represents an interesting field of research from the aspect of people's comfort and their functioning in the area they live in, but also from the aspect of spatial planning in terms of the layout and intensity of construction. The uneven population of the area, the growth of the cities and the extinction of villages, leads to different microclimatic characteristics of several areas at close distances.

As a consequence of increasing development of the cities, appear many problems such as overcrowding of certain areas, which further leads to changes in space that affect the growth of temperature in urban environments, such as concrete and asphalt surfaces, lack of green areas, increasing number of cars, etc. Many cities have higher temperatures than the environment due to the level of urbanization that modifies land use, creating a specific phenomenon, urban heat islands [1, 2].

According to the audit of the world perspective of urbanization from 2018, 68% of the population will live in urban areas by 2050 [2, 3]. The quality of urban living conditions often depends on the thermal comfort of the open urban spaces, which are used on a daily basis [4]. In order to understand the conditions of certain area, especially conditions that are affecting everyday human life, thermal comfort is used.

Human thermal comfort is defined as a condition of mind which expresses satisfaction with the surrounding environment, according to ANSI/ASHRAE Standard 55 [5]. High temperatures and humidity provide discomfort sensations and sometimes heat stress. People react differently to environmental elements, depending on their physical and mental health and their adaptation to certain conditions. Common for everyone is that they are not immune to meteorological conditions, especially air temperature and humidity [6].

Due to the influence of external factors, a person is in constant danger of accumulating heat in the body. Heat is constantly produced in the human body due to metabolic reactions, which is also constantly lost in the immediate environment. When the degree of heat in the body is equal to the degree of heat loss, thermal equilibrium occurs, also known as Human heat balance [7].

The amount of heat produced and delivered by a person depends on physical activity, clothing, gender, age, body weight, diet, mental and health status, external conditions, etc. Heat generated by metabolic processes is given off by humans using basic heat transfer mechanisms. These are: radiation, conduction, convection and evaporation. All these processes, that are shown on figure 1, depend on atmospheric conditions [7,8].

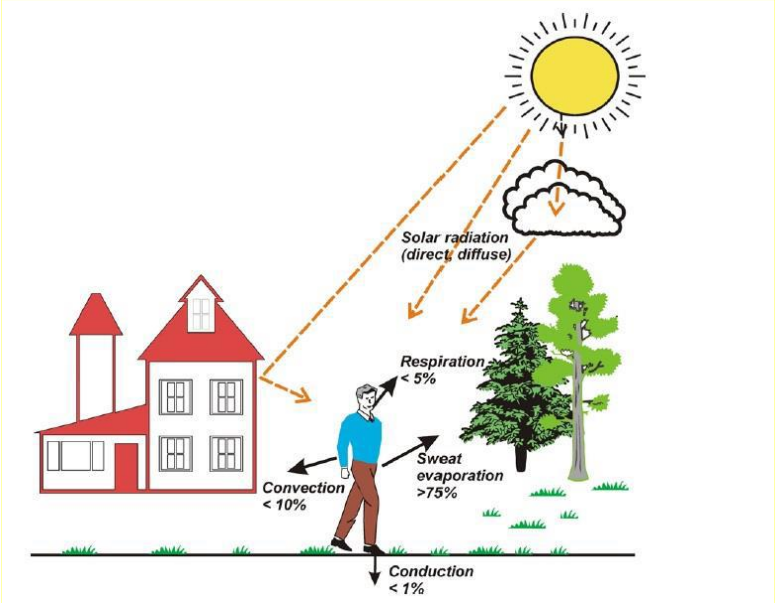

Figure 1. Ways of heat release in the environment

LOCATION

The area of Semberija is located on the northeast part of Bosnia and Herzegovina, in the entity of Republic of Srpska. The location is at the crossroads between Serbia, Croatia and internal Bosnia and Herzegovina, which has enabled this area accelerated development and increase of the population since the beginning of the 21st century.

Total researched area is 904.43 km^2 [9]. It consists of two municipalities: The City of Bijeljina and municipality Ugljevik. Total number of inhabitants is 123 425 [9]. Population density varies within the area, with lowland parts being more populated than the mountainous. For the purposes of this research, data from two meteorological stations were used, one in the city of Bijeljina named Station 1 and one in the area of Mine and Thermal Power Plant in Ugljevik town named Station 2 (figure 2). Air distance between the stations is around 20 km [10].

Figure 2. Location of weaher stations on the researched area

Bijeljina is a characteristic example of heat island in Bosnia and Herzegovina. Construction of facilities since the beginning of the 21st century made a complete transformation of the space and created from small town an urban environment [11,12]. According to the last Census in 2013, the city of Bijeljina has 42 278 inhabitants, which is 16 1 % more than in the year 1991 [13]. According to the previous research, the city of Bijeljina shows unfavorable characteristics of thermal comfort, which are pronounced during the warmer part of the year (especially months Jun, July and August) [6,12,14,15]. The weather station from which the data were obtained is located about 1.5 km by air from the city center, at the altitude of around 90 meters [10].

The second station is located at the location within the Ugljevik Mine and Thermal Power Plant, in the Ugljevik settlement. The characteristics of this station are that it is located within the industrial complex, in the immediate vicinity of the forest cover. Despite its small population, the municipality of Ugljevik is considered a more developed municipality in Bosnia and Herzegovina. The reason for this is the exploitation of coal. Station is at altitude of around 170 meters [10]. Previous research that used data from this weather station are scarce and do not give a concrete picture of the state of thermal comfort in the narrow area of the Ugljevik settlement [16].

METHODOLOGY

There are a lot of different bioclimatic models and indices that are used today for the analysis of thermal comfort of certain areas. For the purpose of this paper was used bioclimatic model, Wet bulb globe temperature (hereinafter referred to as WBGT). It has a total of five thermal stress categories. Those are: Unlimited, Possible heat stress, Heat stress at unacclimated, Heat stress at acclimated and All activity should be stopped.

According to National weather service [17] WBGT is a measure of heat stress in direct sunlight, which takes into account: temperature, humidity, wind speed, sun angle and cloud cover (solar radiation). WBGT was developed by Yaglou and Minard in 1957 and is regarded as one of the main experimental indices for measuring heat stress [18]. It was first used during the 1950s as a component of a successful campaign to reduce heat-related illnesses in the training camps of the US Army and Marine Corps [19].

WBGT is commonly used index of heat stress today, especially by military, universities and sports organizations. One of its purposes is to keep people safe while performing outdoor activities at high temperatures. For these reasons, athlete organizations are using this bioclimatic index, so the athletes could reach a full potential without being put in health danger. WBGT addresses the physical activities that human body can stand in different climatic conditions regarding different seasons in the area of Semberija on two researched locations in this paper. In table 1 are presented values of WBGT and recommendations for involvement in outdoor activities for every value of the index [20].

Table 1 Recommendations for outdoor activities for wet bulb globe temperature (WBGT) values

	VALUE	DESCRIPTION
Unlimited	< 18	Unlimited
Possible heat stress	18 – 23	Keep alert for possible increases in the index and for symptoms of heat stress
Heat stroke at unacclimated	23 – 28	Active exercise for unacclimatized persons should be limited
Heat stroke at acclimated	28 – 30	Active exercise for all but the well-acclimated should be limited
Activity should be stopped	≥30	All training should be stopped

Data from two meteorological stations were used for calculation of thermal comfort of the two location within the area. Values, obtained from the meteorological station in the city, are calculated in software program Bioklima 2.6 [21]. This study included data for a period of 18 years in total, 14 years from the station in Bijeljina (2005 – 2018) [22] and 8 years from the station in Ugljevik (2015 – 2022) [23]. Only summer months were observed, June, July and August, because they have the least favorable conditions that affect human comfort. Years that overlap were compared in order to obtain more effective understanding of differences and similarities between these two observed locations on a small researched area.

According to Köppen's climate classification, Semberija belongs to the Cfb type – where the climate is moderate continental, with moderately cold winters and warm summers [22]. Heat waves appear every few years. 2019 was one of the warmest in the last 100 years on the research area. August had an average of 2° C higher mean air temperature [24], November was one of the 5 warmest in the last 150 years, with an average monthly temperature of 11.3°C [25] and December was the tenth warmest since the year 1861 [26]. Higher parts of Semberija have lower temperatures during the summer months, therefore are more pleasant.

WGBT is widely used for the presentation of possible heat stress for workers whose activities are carried out outside. The International Standard for heat stress uses WBGT to recommend work – rest limits for work in hot environments in order to ensure that average core body temperatures of worker populations do not exceed 38°C. Chapter 8.1.2 of the standard states that workers should be allowed sufficient time to acclimatize to an extremely hot or cold environment, including major changes in climatic conditions [27]. Many countries have national standards based on this international standard for WBGT limit values [28].

If the value of WBGT is within Heat stroke at unacclimated level, body is stressed after 45 minutes of working out. It is necessary to take breaks of 15 minutes. If the value of WBGT is within Heat stroke at acclimated level, body is stressed after 20 – 30 minutes of working out. It is necessary to take breaks of 30 – 40 minutes. Finally, if the value of WBGT is within Activity should be stopped level, body is stressed after 15 minutes of working out and should have at least 45 minutes breaks [17]. These recommendations should be followed in order to preserve health and obtain comfort of human body while carrying out outdoor activities (table 2).

Table 2. Suggested actions and Impact Prevention

EFFECTS	PRECAUTIONARY ACTIONS
None	None
Working or exercising in direct sunlight will stress your body after 45 minutes	Take at least 15 minutes of breaks each hour if working or exercising in direct sunlight
Working or exercising in direct sunlight will stress your body after 30 minutes	Take at least 30 minutes of breaks each hour if working or exercising in direct sunlight
Working or exercising in direct sunlight will stress your body after 20 minutes	Take at least 40 minutes of breaks each hour if working or exercising in direct sunlight
Working or exercising in direct sunlight will stress your body after 15 minutes	Take at least 45 minutes of breaks each hour if working or exercising in direct sunlight

Increased heat exposure raises the core body temperature of the human body. While some increase in core temperature above 37°C is acceptable, an increase beyond 39°C creates health risks, which vary from person to person, depending on ethnic group, age, gender, the duration of high heat exposure, and the degree of acclimatization. The core body temperature of all humans is maintained close to 37°C. The main mechanism of internal heat gain is the heat generated by muscles that work at approximately 20% efficiency [17,29].

Physical readiness is different for people of certain groups, but everyone is affected by meteorological factors, especially those that are new and that human organism of certain area is not used to them [14]. All categories of people are considered while researching and analyzing the results of WGBT. Some however, are more prone to experience heat stress. Discomfort and heat stress reduce productivity of workers and may lead to more serious health problems, especially for aged persons.

RESULTS

In this research all five categories are present on both locations, during the summer months. However, the number of each category varies between the locations. The categories show an uneven presence, with the largest number of days within the categories belonging to categories Possible heat stress and Heat stress at unacclimated.

For the human body, the most favorable days are within the category Unlimited, with values lower than 18. During those days human organism can have as the name says it, unlimited period of exercise and work without feeling exhausted in direct sunlight. This category has the least number of days on both location during observed period, with location Ugljevik showing higher numbers for every month and year (figure 3).

Category Possible heat stress, with values between 18 and 23, has the biggest presence of all categories during the summer months on location Ugljevik. This category represents the first warning towards the hot summer days that are characterized with unfavorable thermal comfort for human organism. On both locations this category counts between 10 to 15 days a month, with the least number of days in July (figure 4).

Category Heat stress at unacclimated, with values between 23 and 28, has the biggest number of all categories during summer months on Bijeljina location. It counts between 10 to 15 days on both locations, although it frequently goes up to 20, especially during the month of August, on location Bijeljina (figure 5).

Category Heat stress at acclimated, with values between 28 and 30, and category All activity should be stopped, with values higher than 30, has bigger presence at the Bijeljina location (figures 6 and 7). These two categories present the biggest threat for human organism and thermal comfort of the area.

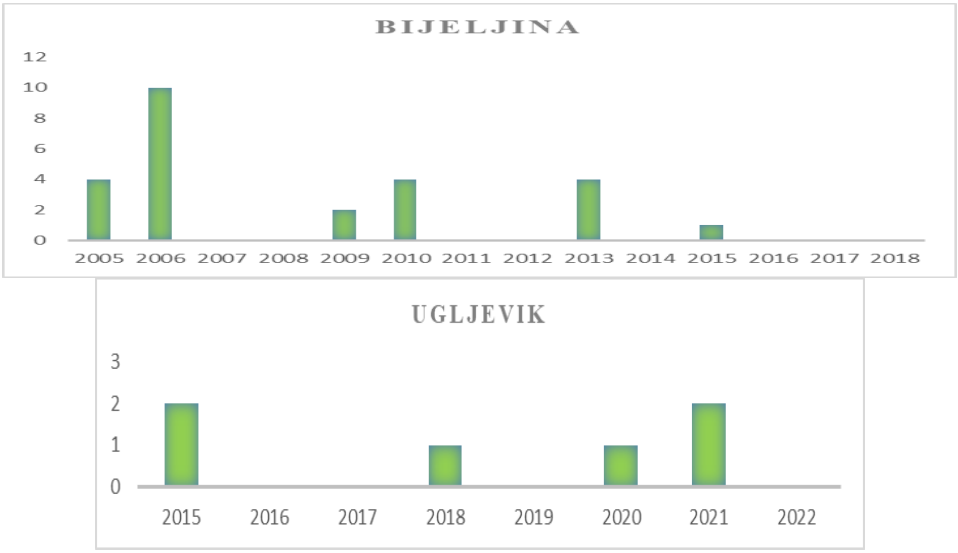

Figure 3. Number of days in the category Unlimited on both locations

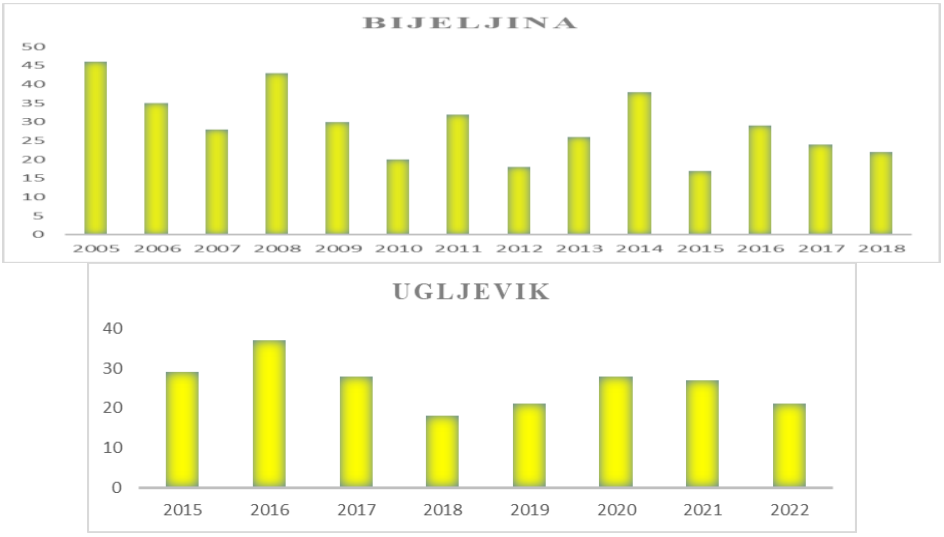

Figure 4. Number of days in the category Possible heat stress on both locations

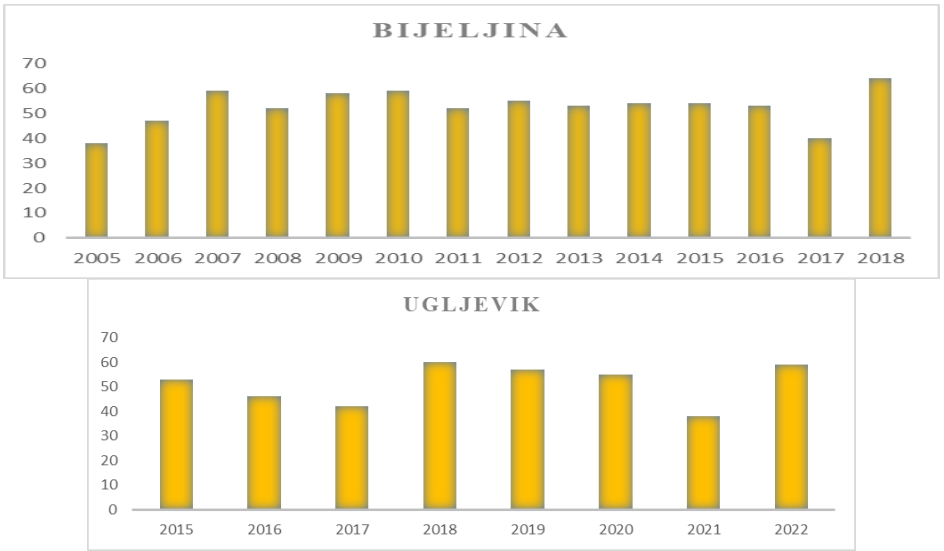

Figure 5. Number of days in the category Heat stress at unacclimated on both locations

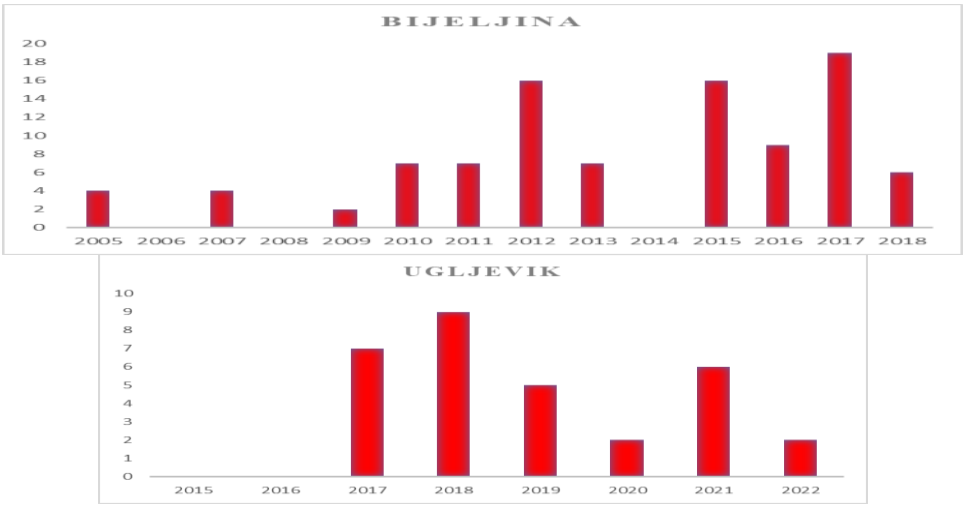

Figure 6. Number of days in the category Heat stress at acclimated on both locations

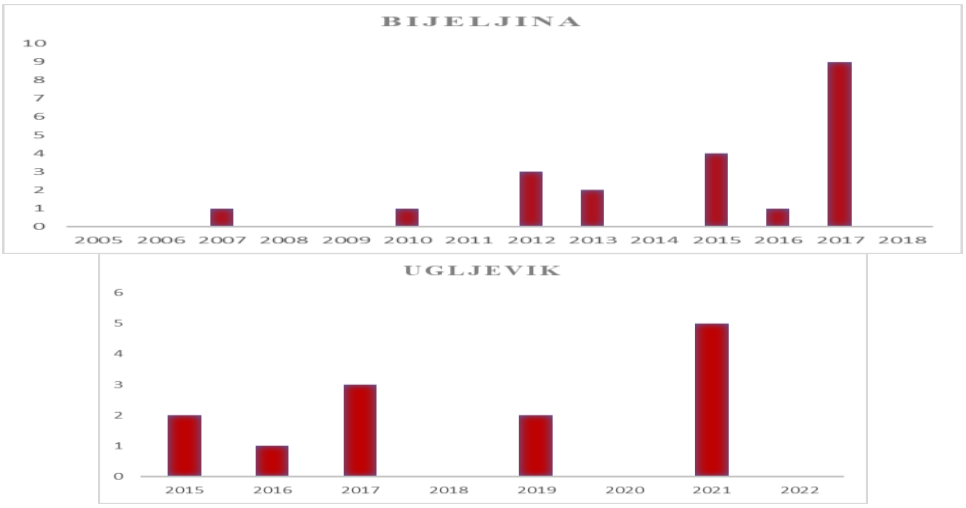

Figure 7. Number of days in the category All activity should be stopped on both locations

From the above data it is obvious that the location Bijeljina has more days that belong to the unfavorable categories regarding thermal comfort. However, since the years observed and the longevity of the research do not match on these two location, in the following chart are shown the ratios of all categories, but only for the years that overlap for both locations, from 2015 to 2018, four years in total (figures 8 and 9).

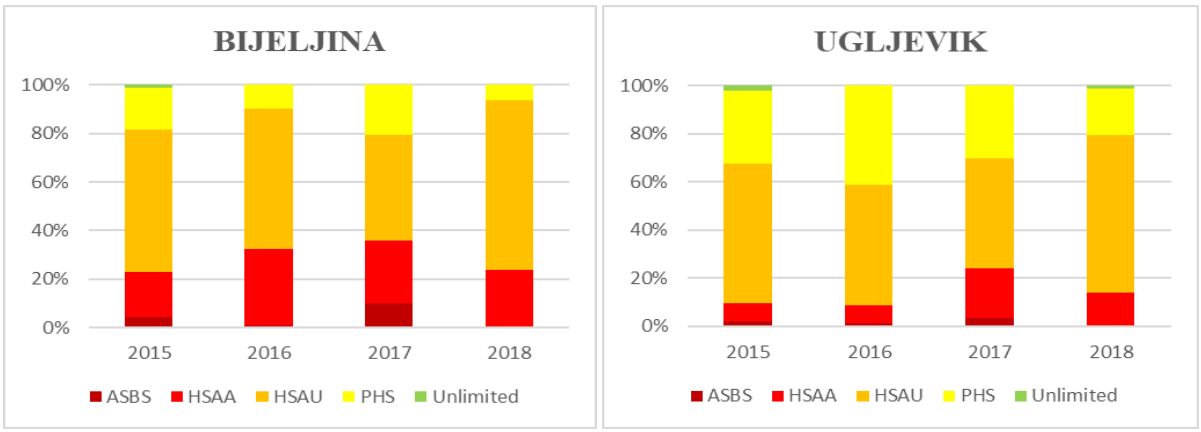

Figures 8 and 9. Ratio of all WBGT categories on both locations for the period 2015 – 2018

The ratio of categories within the summer months goes in favor of categories with pronounced thermal stress, especially on the location Bijeljina. As such, summer months have adverse thermal comfort which is poorly reflected on the state and health of the human body and it is necessary to take care of the activities of that place during such days.

DISCUSSION

Two observed locations gave similar, yet different results. In general, location Bijeljina has less days with favorable conditions for outdoor activities during summer months. On contrary, location Ugljevik, even though it has the presence of days in Activity should be stopped category, has overall better days suitable for pleasant thermal comfort for human organism, ie suitable for work and excercise in direct sunlight during the day.

Bijeljina, as a developing center of Republic of Srpska has an increase in construction, lack of green areas and a high influx of inhabitants. All this, plus the geographical conditions, such as swampy ground, lack of wind and trees has led to very unpleasant summers on this location. Thermal comfort during summer months is very harsh and it represents difficulties for people with heart and lung conditions, as it is very hard to breath. If we include work and exercise in this equation, it can be said with certainty that summer months are very unfavorable for outdoor activities during the day.

The second location, Ugljevik, has better conditions regarding thermal comfort, and allows people to work and exercise longer during summer days. The station from which meteorological data were used is places inside Mine and Thermal Power Plant Ugljevik complex which is a location prone to infrastructural works, transport and mining and as such is not favorable for human comfort. However, observing only WBGT values, it has the presence of more favorable days than the location Bijeljina. This is mostly due to forest cover that is present around the industrial complex and higher altitude in which the station is placed (figure 10) [31].

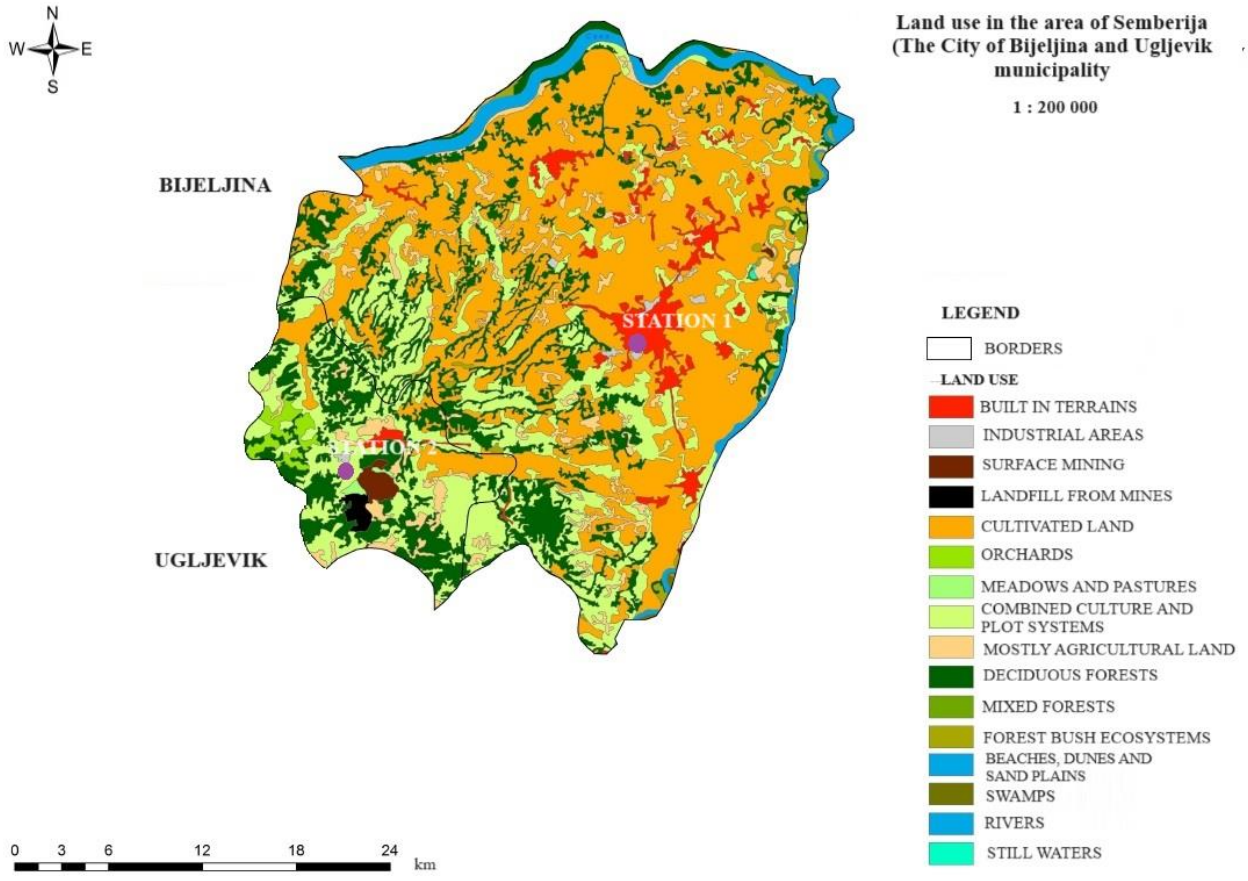

Figure 10. Location of stations in relation to land use of the area of Semberija

Observed in general, Semberija area has unfavorable days regarding thermal comfort that reflect negatively on people's health and wellbeing. Summer months in this area are characterized with high temperature and a lack of wind. The most uncomfortable conditions during summer are present in the area of the city of Bijeljina due to artificial factor that supplement natural negative elements. Going towards higher altitude, forest cover thickens and therefore gives the pleasant felling to human organism, that helps reduce poor thermal comfort.

All positive effects of calculated data can be attributed to the fact that area of Ugljevik, even though it has poor artificial elements, has better natural ones, that contribute to better thermal comfort and the state of human organism during summer months, than in Bijeljina and as such are suitable for work and exercise more than location Bijeljina. Different use of land has an impact on thermal comfort in general and contributes to overall feeling of human organism in space.

CONCLUSION

This research included the analysis of data of two meteorological stations in the area of Semberija. Data used were calculated through program BioKlima, where bioclimatic model WBGT was obtained for two locations, Bijeljina city and Mine and Thermal power plant Ugljevik.

Semberija is the area that has the highest population influx, since the civil war in Bosnia and Herzegovina in the 90s. This has led to intense infrastructural building, pollution, noise and lack of green areas, faster way of life which all have an effect on thermal comfort of people. In combination with unfavorable meteorological elements, it can have dangerous effect on human organism [6]. This is particularly expressed in the area of the city of Bijeljina.

The location within Mine and Thermal power plant Ugljevik showed more favorable days suitable for outdoor work and exercise in direct sunlight during the day. This is mostly due to its surroundings that are covered with forests, and are at a higher altitude.

In general, the area has unfavorable days during summer months that are not suitable for outdoor activities and represent days with poor thermal comfort that has negative effect on human organism and can lead to different health problems. It is necessary to apply proposed measures in order to protect the wellbeing of health and obtain heat balance in the organism.

Received September 2023, accepted October 2023)

REFERENCES

[1] Pigliautile, I., Pisello, A. L., Bou – Zeid, E. (2020). Humans in the city: Representing outdoor thermal comfort in urban canopy models. Renewable and Sustainable Energy Reviews, 133, 1 – 10. https://doi.org/10.1016/j.rser.2020.110103

[2] Stewart, I. D., Tim, R. O. (2012). Local climate zones for urban temperature studies. Bulletin of the American Meteorological Society, 93(12), 1879-1900. http://dx.doi.org/10.1175/BAMS-D-11-00019.1

[3] UN DESA (2018). Revision of world urbanization prospects

[4] Dunjić, J. (2019). Outdoor Thermal Comfort Research in Urban Areas of Central and Southeast Europe: A Review. Geographica Pannonica, 23(4), 359-373. https://doi.org/10.5937/gp23-24458

[5] ANSI/ASHARE Standard 55, Thermal Environmental Conditions for Human Occupancy (2017)

[6] Đurić, D., Topalić-Marković, J. (2019). Thermal comfort in the City of Bijeljina, for the period 2009 – 2018 defined by WGBT. Archives for Technical Sciences, 21(1), 69-74. https://doi.org/10.7251/afts.2019.1121.069Dj

[7] Pecelj, M.R, Pecelj – Purković, J., Pecelj, M. (2015). Geoecology. Faculty of geography, University of Belgrade, Serbia *[in Serbian language]*

[8] Blazejczyk, K., Baranowski, J. and Blazejczyk, A. (2014). Heat stress and ocupational health and safety – spatial and temporal differentiation. Miscellanea geographica – Regional studies on development, 18 (1), 61 – 67.doi: https://doi.org/10.2478/mgrsd-2014-0011

[9] Census of population, households and apartments in Bosnia and Herzegovina. Agency for Statistics of Bosnia and Herzegovina, Sarajevo (2019)

[10] https://earth.google.com/
[11] Đurić, D. (2021). The impact of urbanization of the city of Bijeljina on the thermal comfort of the population. Journal of Faculty of Civil engineering, 39, 45 – 53. doi: https://doi.org/10.14415/zbornikGFS39.04
[12] Đurić, D., Đurić, N., Stević, S. (2021). The importance of thermal comfort of the urban environment during spatial planning and construction. 14th International Scientific Conference "Contemporary Materials". Academy of Sciences and Arts of the Republic of Srpska, Banja Luka, Bosnia and Herzegovina. doi: https://doi.org/10.7251/COMEN2201120D *[in Serbian language]*
[13] http://www.statistika.ba/
[14] Đurić, D. (2021). Comparison of bioclimatic indices WBGT and UTCI in the analysis of thermal comfort in the city of Bijeljina. IX International congress Biomedicine and Geosciences – influence of environment on human health. Book of papers, 101 – 109. Kopaonik, Serbia
[15] Lukić, M., Đurić, D. (2020). Comparative analysis of the outdoor thermal comfort in urban environments – case study of Bijeljina and Loznica. 5th meeting of geographers "Innovative approach and perspectives of applied geography". University of Novi Sad, Novi Sad. Serbia
[16] Đurić, D., Jakšić, V., Šelić, A. and Vlajić, I. (2022). Thermal comfort of Ugljevik town for the year 2021 observed through the bioclimatic index WBGT. Archives for technical sciences, 26, 71 – 78. doi: https://doi.org/10.7251/afts.2022.1426.071Dj
[17] National weather sevice, Tulsa OK. Wet Bulbe Globe temperature. https://www.weather.gov
[18] Yaglou, C.P., and Minaed, D. (1957): Control of heat casualties at military training centers. Archives for Industrial Health, 16, 302–316
[19] Budd, G.M. (2008). Wet-bulb globe temperature (WBGT) - its history and its limitations. Journal of Science and Medicine in Sport, 11, 20–32. doi: https://doi.org/10.1016/j.jsams.2007.07.003
[20] Blazejczyk, K., Epstein, Y., Jendritzky, G., Staiger, H. and Tinz, B. (2012). Comparison of UTCI to selected thermal indices. International Journal of Biometeorology 56, 515–535. doi: https://doi.org/10.1007/s00484-011-0453-2
[21] https://www.igipz.pan.pl/Bioklima-zgik.html/
[22] Hydro meteorological Service of Republic of Srpska (https://rhmzrs.com/)
[23] Mine and Thermal Power Plant Ugljevik (https://www.riteugljevik.com/)
[24] Republic Hydro meteorological Service of Republic of Srpska. Synoptic analysis for August 2019. (2019)
[25] Republic Hydro meteorological Service of Republic of Srpska. Synoptic analysis for November 2019 (2019)
[26] hhh Republic Hydro meteorological Service of Republic of Srpska. Synoptic analysis for December 2019 (2019)
[27] ISO Hot environments – Estimation of the heat stress on working man, based on the WBGT index (wet bulb globe temperature). ISO Standard 7243. International Standards Organization, Geneva (1989)
[28] ILO ambient factors in the workplace. International Labour Organization (ILO) codes of practice. International Labour Office, Geneva (2000)
[29] Wakabayashi, H., Wijayanto, T., Lee, J.Y., Hashiguchi, N., Saat, M., Tochihara,Y. (2011). Comparison of heat dissipation response between Malaysian and Japanese males during exercise in humid heat stress. Int. J Biometeorol 55, 509 – 17. doi: https://doi.org/10.1007/s00484-010-0374-5
[30] Đurić, D. (2021). Geoecological problem of Semberija and Majevica in the Republic of Srpska. Doctoral Dissertation. Faculty of Geography, University of Belgrade *[in Serbian language]*

Original scientific article
http://dx.doi.org/10.59456/afts.2023.1529.075M

THE IMPACT OF PUBLIC EVENTS ON THE USE OF SPACE: ANALYSIS OF THE MANIFESTATIONS IN LIBERTY SQUARE IN NOVI SAD

Mitrović Tanja[1], Vračarić Milica[1]

[1]*Faculty of Technical Sciences, University of Novi Sad, Serbia, E-mail: mitrovict@uns.ac.rs*

ABSTRACT

Urban public spaces play a crucial role in holding various public events. Although events positively enrich the urban environment and encourage real social interactions, there are no guidelines for their spatial organization, posing a challenge in terms of using public spaces. This paper introduces new classifications of public events and temporary structures intended for their maintenance, applied to investigate their role and impact on urban spaces, using Liberty Square in Novi Sad as a case study. This research provides valuable insights for improving urban planning, considering the need for a balance between events and preserving the quality of urban spaces.

Key words: *public event, public space, manifestation, temporary structures, temporary urbanism,*

INTRODUCTION

The number of different events organized in cities in recent years is greater than ever before. Within this overarching trend, there is another less affirmed trend emerging, which is the increasing prevalence of events taking place in public spaces. While some events have always been held in parks, on streets, and in squares, in recent years, a significant number of events have been relocated from traditional venues to prominent urban spaces. This trend is emphasized by organizers seeking unforgettable and spectacular events, as well as by city authorities aiming to engage citizens and visitors and make urban spaces more visible regionally, nationally and especially internationally and globally. Events generally play a positive role in cities, but the transformation of public spaces into event venues can often be challenging. Depending on how they are planned, events can activate public spaces, but they can also lead to overcrowding and congestion.

Throughout history, urban spaces have always been places of encounter. Even today, despite the growing virtual communication, people increasingly desire and value real human interactions, often leading to the organization of events to confirm their virtual connections. People want to meet their virtual friends in person to validate their virtual experiences, but they also want to share recorded digital moments with others as performances of shared presence [1].

Events are no longer just a means to achieve a series of stimuli but have become a new space for socialization in their own right. As Misener et al. observe "new social networks are formed through participation, planning, volunteering, and often consuming events" [2]. Events have become an integral part of modern society, and their significance goes beyond their tourist value. Many authors agree with the assertion that events are used to attract new visitors [3, 4] or, in the case of regular maintenance, to generate repeat visits [5].

The main goal of this research is to understand the role and impact of public events on the use of space in the urban environment. Liberty Square, situated in Novi Sad, holds a distinguished reputation as a primary public space within the city, serving as the prominent host for a multitude of events (Figure 1). Its significance lies in the fact that it attracts and accommodates the largest number of events when compared to other locations in the city. Therefore, an event analysis was performed for this location. The findings are expected to provide valuable insights for event planning and community enhancement in Novi Sad.

Figure 2. Festival of Love in Liberty Square in 2017

METHODOLOGY

The methodology employed in this research is designed to provide a comprehensive understanding of the subject matter. It combines several critical approaches to ensure a robust and multifaceted analysis. These approaches include:

1. Literature Research: The initial step involves an exhaustive review of existing literature. This literature research serves as the foundation for understanding the various aspects of public events and temporary structures in urban settings.
2. Descriptive Analysis: Building on the literature research, a detailed and systematic descriptive analysis is carried out. This process involves categorizing and characterizing different types of public events, temporary objects, and their layouts based on various criteria.
3. Comparative Assessment: The research goes a step further by conducting a comparative assessment. This phase involves comparing and contrasting the categorized manifestations at a chosen location.

Classification of Public Events

The research places significant emphasis on categorizing public events in urban public spaces. This categorization system enables the classification of diverse events occurring at a specific location, employing a uniform set of criteria. The developed classification system encompasses the following categories, each delineated by its program and purpose:

- **Cultural Manifestations** – events that celebrate and promote cultural traditions and artistic expressions,
- **Fair and Festival Manifestations** – gatherings such as fairs and festivals that often revolve around commerce, entertainment, and cultural exhibitions;
- **Sports and Recreational Manifestations** – events centered on physical activities, sports competitions, and recreational pursuits;
- **Artistic Manifestations** – events showcasing various forms of art, including visual arts, performing arts, and creative exhibitions;
- **Musical Manifestations** – events with a primary focus on musical performances;
- **Scientific and Educational Manifestations** – gatherings that aim to educate and promote scientific knowledge, often through exhibitions and seminars;
- **Political and State Manifestations** – events tied to politics, governance, and state affairs, including rallies, conventions, and official ceremonies;
- **Gastronomic Manifestations** – events highlighting culinary traditions and food-related experiences;
- **Entertainment Manifestations** – events designed primarily for entertainment and amusement;
- **Parades and Processions** – events characterized by organized marches and processions that often have cultural, religious, or historical significance;
- **Humanitarian Manifestations** – gatherings focused on raising awareness and support for humanitarian causes and charitable activities;
- **Protests and Initiatives** – events related to public activism and initiatives, including protests, rallies, and advocacy campaigns;
- **Celebrations and Spontaneous Gatherings** – events that arise from spontaneous or celebratory moments, including impromptu street parties and communal gatherings.

Initially based on Getz's work [6], this classification has undergone further refinement and adaptation by the authors of this paper to better suit the complexity of the subject matter. Importantly, it resonates with categorizations proposed by other researchers, such as Kuusik et al. [7] and Bjeljac [8]. These classifications provide a solid framework for understanding and analyzing the wide range of public events in urban settings, taking into account their functions, significance, and impact. In relation to the type of public event that is planned in the public space, different types of temporary structures are used as means of holding the event.

Classification of Temporary Structures

The presence of temporary architectural structures at a designated location is intrinsically linked to time constraints. These structures are designed to be in place for a limited duration, usually aligning with the timeline of a particular event or activity. The temporal nature of these structures plays a crucial role in shaping their design, functionality, and logistics. Structures intended for shorter durations tend to possess higher mobility, making it feasible to relocate them to multiple alternative locations.

This flexibility is essential, especially when events are short-lived, and the need arises to repurpose or reuse the structures for various events, enhancing their efficiency and resource utilization. The classification of the temporary structures can be carried out based on the following criteria:

- **According to their physical configuration:**
  - Temporary structures with dominant volume;
  - Temporary structures with emphasized construction;
  - Temporary structures as landmarks.
- **Based on their formal characteristics:**
  - Temporary structures as elements of cultural and symbolic space;
  - Temporary structures as elements modeling the environment;
  - Temporary structures as elements enhancing emotional and visual characteristics of the environment.

- **By their functional purpose within urban space:**
  - Temporary structures as commercial facilities – kiosks, exhibition stalls, pavilions;
  - Temporary structures as spaces – stages and platforms (covered or uncovered) with accompanying equipment;
  - Temporary structures for visual communication – art installations, sculptures, LED screens, mobile fences, barriers, signaling, and alike;
  - Temporary structures for entertainment of children and adults – ice rinks, carousels, slides, inflatable structures, and alike;
  - Temporary structures for lighting purposes – New Year's decorations, floodlights, and alike.
- **According to their degree of temporality:**
  - Single-use (during the duration of events, festivals),
  - Multiple-use (seasonal, year-round, during specific periods).
- **By the nature of mobility:**
  - Foldable mobile structures,
  - Transformable mobile structures.
- **Based on the construction material used:**
  - Temporary structures with wood and metal as the supporting framework materials;
  - Temporary structures with wood, glass, ice, metal sheets, plastic, awnings, and canvas coverings as cladding and structural elements of enclosures.

The classification is based on the scientific research by Stepanchuk et al. [9], with partial supplementation and revision. In this paper, the emphasis is placed on their functional purpose and their arrangement in space, as an additional established criterion in this classification, which is explained in more detail in the next chapter.

RESULTS

To gather precise data regarding the utilization of public space and the arrangement of temporary structures in connection with the chosen site, a thorough analysis was conducted on the events occurring in Liberty Square between 2017 and 2022.

Table 1 provides a comprehensive list of 17 events held at this venue during the examined timeframe. The categorization of these event was established, along with the identification of the types of temporary structures utilized for its organization, the duration of the event, and the prevalent arrangement of temporary structures specific to that event.

The data in the table about the events held are based on information taken from the website of the Tourism Organization of the City of Novi Sad [10]. Conclusions about the type of temporary structures and the predominant patterns of temporary structure layouts were made based on the firsthand observations, as well as on the analysis of the available video and photo-documentation.

Based on the data from Table 1, it can be inferred that the most prevalent events at Liberty Square are trade fairs and festivals, accounting for 53% of all analyzed events. They are followed by music and entertainment events, each with a share of 17.6%, and sports events with 11.8%.

Table 2: Events that took place in Liberty Square in Novi Sad from 2017 to 2022.

No.	Name of the event	Event type	Type of temporary structures	Duration (days)	Layout of temporary structures
1.	Celebration of the Orthodox New Year	Entertainment	○ Stage ○ Floodlights ○ LED screens ○ Mobile fences ○ NewYear's	1	Dominant stage

			decoration		
2.	Festival of Love	Fair and festival	○ Kiosks ○ Stage ○ Art installations ○ Barriers ○ Carousel ○ Benches	17 - 35	Linear – perimeter
3.	Novi Sad half-marathon	Sports and recreational	○ Stage ○ Mobile fences ○ Signaling ○ Inflatable structures	1	Dominant stage
4.	Colorful square	Fair and festival	○ Kiosks ○ Stage	15	Linear – perimeter
5.	Fair of beekeeping and old crafts	Fair and festival	○ Exhibition stalls ○ Stage	2	Linear – perimeter or corridor
6.	Rhythm of Europe	Musical	○ Stage ○ Floodlights ○ Mobile fences	1	Dominant stage
7.	Taste of Planet (Food Planet)	Fair and festival	○ Stage ○ Kiosks ○ Urban furniture (tables)	6-30	Linear – corridor
8.	International Wine Festival "Interfest"	Fair and festival	○ Stage ○ Pavilions ○ Urban furniture (tables)	3	Linear – corridor
9.	Novi Sad Ultra Challenger	Sports and recreational	○ Stands ○ Pavilions ○ Mobile fences ○ Signaling ○ Floodlights	2	Dominant stands (with linear pavilions)
10.	"Tamburica Fest"	Musical	○ Stage ○ Floodlights ○ Pavilions ○ Mobile fences ○ Parasols	3	Dominant stage
11.	Opens Youth Fair	Entertainment and Fair and festival	○ Exhibition stalls ○ Stage ○ Floodlights ○ LED screens ○ -Mobile fences	2	Linear – perimeter (combined with a central group setting of stalls)
12.	International meeting of old-timer vehicles and rally through Vojvodina and fair of small cars	Fair and festival	○ Exhibition stalls ○ Cars (as exhibits) ○ Mobile fences	1	Linear – perimeter
13.	Festival of honey	Fair and festival	○ Exhibition stalls ○ Stage ○ Floodlights ○ LED screens	3	Linear – corridor
14.	Festival of dance and music "Call of the plain"	Musical	○ Exhibition stalls ○ Stage ○ Mobile fences ○ Floodlights	4	Linear – perimeter

			○ LED screens ○ Pavilions Urban furniture (chairs)		
15.	Day of the young Portugieser	Fair and festival	○ Exhibition stalls ○ Stage	1	Linear – corridor
16.	Novi Sad Winter Fest	Fair and festival	○ Kiosks ○ Stage ○ Barriers ○ Art installations ○ Carousel ○ New Year's decoration	33-49	Linear – corridor
17.	New Year's Eve	Entertainment	○ Stage ○ Floodlights ○ LED screens ○ Mobile fences ○ New Year's decoration	1	Dominant stage

These findings indicate that Liberty Square hosts a significant number of activities related to festivals and trade fairs. While entertainment, music, and sports events also hold a substantial share, trade fairs and festivals are the most prominent, making them the primary focus of events at Liberty Square throughout the year.

However, to assess their impact on space usage, beyond the event type, it's crucial to consider the temporal aspect. This additional criterion provides information about the duration of space occupation by various event types. Events that span several weeks may have a more significant impact on space usage compared to one-day or two-day events. According to the data from Table 1, events at Liberty Square lasting more than 14 days fall into the category of trade fairs and festivals.

It is noticeable that during the events at the analyzed location, the linear layout and the layout with a dominant stage or sports field stand out as predominant. Variations of the linear layout, which include perimeter and corridor layouts, are most prevalent at events where exhibition stands and kiosks are used as primary temporary structures. On the other hand, entertainment and sports events usually have a layout with a dominant stage or sports field.

Perimeter layout involves placing exhibitor stalls or kiosks around the edges or perimeter of the space, typically along walls or in a designated area. This arrangement is often practical in tight spaces and allows for efficient utilization of the available area. Visitors can easily navigate among exhibitors by moving along the walls or within the defined space, facilitating quick and efficient passage through the exhibition area.

Corridor layout refers to arranging exhibitor stalls or kiosks in a line that extends through the space, forming corridors between exhibitors. This type of layout is commonly used when the space is large and when encouragement of the visitors to explore every part of the exhibition is the primary goal. The corridor layout allows for easy access to exhibitors and provides a positive experience for visitors who can freely move through different sections of the event.

A dominant stage (or sports field) layout involves placing the main stage or sports field with bleachers at a central location where the main activities take place. This layout provides better visibility and experience for visitors because the focus of the event is concentrated in one area.

To gain insights into space occupation during multi-day events, it's essential to examine the type of temporary structures, their arrangement, and their quantity. These details shed light on how the space is utilized and how different activities are accommodated and interact within the framework of each event.

CONCLUSION

The findings of this research affirm that Liberty Square is a hub for cultural and commercial gatherings, with trade fairs and festivals taking center stage. Notably, music and entertainment events, as well as sports events, contribute significantly to the diversity of activities hosted at Liberty Square, emphasizing its multifaceted nature. While these event types play a substantial role, it is clear that trade fairs and festivals maintain their prominence throughout the year. Beyond the event type, the temporal aspect of these gatherings is of key importance as it underscores the significance of these longer-lasting events in shaping the use of Liberty Square.

It is crucial to acknowledge that the classifications regarding public events and temporary structures are not rigid and are open to potential alterations and expansions. Furthermore, it should be recognized that certain events, due to their multifaceted nature, may be classified into multiple categories, highlighting the need for flexible and adaptive classification systems.

Moreover, the choice of layout for these events plays a pivotal role in the use of space. Understanding the type, arrangement, and quantity of temporary structures provides valuable insights into how Liberty Square accommodates various activities and how they interact within the framework of each event. These details shed light on the intricate planning and organization involved in ensuring that Liberty Square remains a vibrant and versatile venue for a wide range of events.

When managed with precision and foresight, temporary structures accompanying such events can have a substantial and positive influence. This impact encompasses various dimensions, including bolstering economic development, elevating visitor satisfaction, facilitating the hosting of a wide array of events, stimulating tourism promotion, and fostering robust community engagement within the designated location [11]. However, it's worth noting that temporary structures may not be universally suitable for every location. Careful consideration should be given to their placement and design to prevent any potential disruption to the existing urban landscape, particularly in areas of cultural and historical significance.

Undoubtedly, there is a compelling case for future research on spatial optimization at Liberty Square. The findings emphasize the importance of this aspect in managing and utilizing the space effectively for various events. The multifaceted nature of events hosted at Liberty Square and their consistent prominence throughout the year underscore the importance of prioritizing spatial optimization as a potential area for future research.

Received November 2023, accepted November 2023)

LITERATURE

[1] Richards, G. (2010). Leisure in the network society: From pseudo-events to hyperfestivity. Tilburg University, The Netherlands.
[2] Misener, L., Mason, D. S. (2006). Creating community networks: Can sporting events offer meaningful sources of social capital? Managing Leisure, 11, 39–56.
[3] Getz, D. (2008). Event tourism: Definition, evolution, and research. Tourism Management, 29, 403–428.
[4] McCartney, G. J. (2005). Hosting a recurring mega-event: Visitor raison d'être. Journal of Sport Tourism 10(2), 113–128.
[5] Kaplanidou, K., Vogt, C. A. (2006). A structural analysis of destination travel intentions as a function of web site features. Journal of Travel Research, 45(2), 204-216.
[6] Getz, D. (2007). Event studies. Theory, research and policy for planned events. Butterworth-Heinemann, Oxford.
[7] Kuusik, A., Nilbe, K., Mehine, T., and Ahas, R. (2014). Country as a free sample: The ability of tourism events to generate repeat visits. Case study with mobile positioning data in Estonia. Procedia - Social and Behavioral Sciences, 148, 262 – 270.
[8] Bjeljac, Ž., Ćurčić, N. (2015). Manifestation or event (EVENT) in tourism theory and practice. Hotellink, 23/24. *[Serbian language].*

[9] Stepanchuk, A., Salyakhova, M., and Salyakhova, V. (2021). Preserving identity while reorganizing urban spaces. E3S Web of Conferences, 274 (1).
[10] Tourism organization of the City of Novi Sad. Calendar of events, https://novisad.travel/cp/, approach: May, 2021.
[11] English Heritage. (2010). Temporary structures in historic places: Guidance for local planning authorities, site owners and event organisers. www.historicengland.org.uk